

Structural and Hygrothermal Performance of Light Wood-Frame Walls with
Insulated Sheathing

By

Marko Spasojevic

A thesis submitted in partial fulfillment of the requirements for the degree of

Master of Science

in

Civil (Cross-disciplinary)

Department of Civil and Environmental Engineering

University of Alberta

© Marko Spasojevic, 2019

ABSTRACT

In order to meet a higher standard of building energy efficiency, the thermal insulation of exterior walls is often increased. Adding a layer of continuous thermal insulation exterior to the cavity insulation, insulated sheathing, to reduce thermal bridging is getting more popular in practice. In some cases, the continuous insulation is put outer to the wood sheathing while in other cases the insulation is inserted between the sheathing and framing. The former configuration may limit the air-drying capability of wood sheathing due to the low permeability of commonly selected exterior insulation materials. On the other hand, the latter configuration compromises the racking resistance of the wall due to the soft foam layer inserted between lumber and wood-based panels. Clearly there are contradicting influences on thermal and structural performance of the wall when the insulation thickness changes. This study aims to investigate and compare the hygrothermal and structural performance of two proposed wood-frame exterior wall configurations. The impact of the intermediate insulation on shear wall resistance was investigated and the results show that adding insulation between the sheathing and framing greatly decreases the lateral capacity and stiffness of the wall. Additionally, the lateral capacity of the shear wall with intermediate insulation can be accurately predicted based on nail joint properties. A sensitivity analysis was conducted to investigate the hygrothermal performance of these two wall assemblies considering different air leakage rates and indoor relative humidity levels. The results show that these two wall assemblies show similar drying and wetting potentials when excessive moisture accumulation is prevented by placing enough insulation exterior to the wall cavity.

The minimum ratio of outboard-to-inboard thermal resistance necessary to prevent the mould growth and excessive moisture accumulation within the wall is recommended for eight locations in Canada. Putting insulation between the sheathing and framing, instead of outboard to the sheathing, increases this ratio by approximately 0.07 and 0.04 for 2×4 and 2×6 stud cavity walls, respectively.

PREFACE

This thesis is an original work by Marko Spasojevic. No part of this thesis has been previously published.

ACKNOWLEDGEMENTS

I would like to take this opportunity to express my sincere appreciation to the many wonderful people who have supported me during my studies.

First of all, I would like to express my deepest gratitude to my supervisor, Dr. Ying-Hei Chui, for his extraordinary cooperation, invaluable academic guidance and outstanding supervision.

I would also like to extend my sincere thanks to my co-supervisor, Dr. Yuxiang Chen, for his constant support, motivation, encouragement and guidance.

Besides my supervisors, I would like thank Dr. Meng Gong and Dean McCarthy from the University of New Brunswick, for their support and assistance to conduct the shear wall tests.

Many thanks to my dear colleagues from the ARTS group at the University of Alberta for their wonderful collaboration and great support. I am also grateful to my friends and colleagues Mahmud and Harish for their encouragement and friendship.

I would like to thank my parents Lazar and Gordana, and my sister Jelena for their love and constant moral support which helped me to achieve success in every sphere of life.

Finally, I express my deepest gratitude to my uncle Dragan, aunt Bilja and cousin Stefan for all their love, encouragement and immense support during my studies and life in Edmonton.

Thank you for making me a part of your wonderful family. Without you, none of this would have been possible.

TABLE OF CONTENTS

Abstract..... ii

Preface iv

Acknowledgements v

Table of Contents vi

List of Tables ix

List of Figures..... xi

1 INTRODUCTION 1

 1.1 Background 1

 1.2 Objectives 3

 1.3 Methodology 3

 1.4 Thesis Structure 5

2 LITERATURE REVIEW 6

 2.1 Introduction 6

 2.2 Structural Performance of Wood-Frame Walls 7

 2.2.1 Shear Wall Capacity 7

 2.2.2 Influence of intermediate insulation 14

 2.3 Hygrothermal Performance of Wood-Frame Walls 19

 2.3.1 Influence of exterior insulation, indoor humidity and air leakage 19

 2.3.2 Modeling approaches 22

 2.4 Summary 28

3 STRUCTURAL PERFORMANCE OF LIGHT WOOD-FRAME WALLS WITH INSULATED SHEATHING 30

 3.1 Introduction 30

 3.2 Materials 31

3.2.1	Lumber	31
3.2.2	Sheathing.....	32
3.2.3	Insulation.....	32
3.2.4	Fasteners.....	32
3.3	Properties of Nailed Joints	36
3.3.1	Nail Joint Test Program	36
3.3.2	Nail Joints Test Setup.....	37
3.3.3	Instrumentation and Test Procedure.....	38
3.3.4	Nail Joint Test Results	39
3.3.5	Failure Modes of Nail Joints	42
3.3.6	Shear Wall Strength Predicted Using Nail Joint Properties.....	44
3.4	Shear Wall Performance.....	45
3.4.1	Shear Wall Test Program	45
3.4.2	Shear Walls Test Setup	46
3.4.3	Instrumentation and Test Procedure.....	48
3.4.4	Shear Wall Test Results	48
3.4.5	Failure Modes of Shear Walls.....	52
3.5	Influence of Insulation Layer on Prediction of Shear Wall Strength using Nail Joint Properties.....	53
3.6	Summary	55
4	HYGROTHERMAL PERFORMANCE OF LIGHT WOOD-FRAME WALLS WITH INSULATED SHEATHING	57
4.1	Introduction	57
4.2	Wall Assembly Configurations	58
4.3	Simulation Parameters.....	59
4.3.1	Material Properties	59
4.3.2	Locations and Weather.....	60
4.3.3	Indoor Conditions.....	62
4.3.4	Air Exfiltration	64

4.4	Moisture Accumulation and Thermal Performance of Wood-Frame Walls with Exterior Insulation.....	67
4.4.1	Modeling Approach	67
4.4.2	Influence of exterior insulation on the moisture accumulation.....	69
4.4.3	Influence of exterior insulation on the thermal performance.....	73
4.5	The Effect of Air Leakage Rate and Indoor Relative Humidity on the Hygrothermal Performance.....	75
4.5.1	Modeling Approach and Input Parameters	75
4.5.2	Performance Criteria	77
4.5.3	Results and Discussion.....	79
4.6	Summary	86
5	CONCLUSIONS AND RECOMMENDATIONS	88
5.1	Summary	88
5.2	Conclusions	89
5.3	Recommendations for future research.....	92
	References	93
	APPENDIX A – Density and moisture content of framing members.....	97
	APPENDIX B – Nail joint load-slip response curves.....	100
	APPENDIX C – Nail Joint failure modes.....	105
	APPENDIX D – Shear wall failure modes	106
	APPENDIX E – Nail bending tests.....	110
	APPENDIX F – Hygrothermal material properties.....	112

LIST OF TABLES

Table 2.1: Lateral resistance of nailed connections, (CSA O86-14, Clause 12.9.4.2)..... 11

Table 2.2: Penetration length and member thicknesses for wood-to-wood connections (CSA O86-14, Clause 12.9.2.2)..... 12

Table 2.3: Wood Sheathed Braced Wall Panel Construction Details for Wind or Seismic Loads (Engineering Guide for Wood Frame Construction, 2014) 13

Table 2.4: Framing types specified in Table 2.3 14

Table 2.5: Lateral resistance of nail joints with intermediate insulation (Aune and Patton-Mallory, 1986)..... 15

Table 2.6: Percent reduction in nail joint strength due to presence of foam insulation between wood-based sheathing and lumber (Plesnik et al 2016) 16

Table 2.7: Construction details of braced wall and the results of monotonic loading test (Evaluation Report CCMC 14075-R, 2017)..... 17

Table 2.8: Minimum required ratio of outboard to inboard thermal resistance (1995 NBCC, Table 9.25.1.2)..... 25

Table 2.9: Minimum required thermal resistance ratio when $RH \leq 50\%$ and $RH \leq 60\%$ (Brown et al 2007) 26

Table 3.1: Center-point nail bending test result 35

Table 3.2: Nail Joint Test Program..... 36

Table 3.3: Nail Joint Test Results..... 39

Table 3.4: Shear Wall Strength Predicted Based on Nail Joint Strength 44

Table 3.5: Shear wall Test Program 45

Table 3.6: Shear Wall Test Results	52
Table 3.7: Predicted and Tested Shear Wall Lateral Resistance	54
Table 4.1: Basic Material Properties (Kumaran, et al 2002b and Kumaran 2002c).....	60
Table 4.2: Locations and Climate Zones considered in 1-D analysis	61
Table 4.3: Effective R-Value and Outboard to Inboard Insulation Ratio.....	73
Table 4.4: Winter Average Heat Flux through the Interior Surface.....	74
Table 4.5: Wall Assembly Codes	76
Table 4.6: Mould Index (MI) Description (Ojanen et al, 2010).....	78
Table 4.7: Material sensitivity classes (Ojanen et al, 2010).....	78
Table 4.8: Ratio of Outboard to Inboard Thermal Resistance.....	83
Table 4.9: Minimum Required Outboard to Inboard Ratio of Thermal Resistance	84

LIST OF FIGURES

Figure 2.1: ZIP System® R-Sheathing (Huber, 2012)	17
Figure 2.2: The effect of indoor relative humidity on the amount of moisture accumulated within a wall cavity due to air exfiltration (Ojanen and Kumaran, 1996).....	21
Figure 3.1: Nails used in the study: 10d, 16d, PD (left to right)	33
Figure 3.2: Center-point nail bending test setup.....	34
Figure 3.3: Center-point nail bending test results.....	35
Figure 3.4: Nail Joint Test Setup.....	38
Figure 3.5: Mean Load-Displacement Response of Nail Joints Constructed with: (a) 10d Nails; (b) 16d Nails; (c) PD Nails.....	41
Figure 3.6: Typical failure mode of nail joints constructed with common wire nails.....	43
Figure 3.7: Shear Wall Test Setup.....	47
Figure 3.8: Load-Displacement Responses of Shear Walls Constructed with 10d Nails.....	49
Figure 3.9: Load-Displacement Responses of Shear Walls S3 (10d) and S4 (16d).....	49
Figure 3.10: Load-Displacement Responses of Shear Walls Constructed with 16d Nails...	50
Figure 3.11: Load-Displacement Responses of Shear Walls S5 (16d) and S7 (PD).....	51
Figure 4.1: Wall Assemblies: ISF (left) and SIF (right).....	59
Figure 4.2: Hourly outdoor temperature and relative humidity for Edmonton climate	61
Figure 4.3: Indoor conditions for Edmonton climate: (a) Hourly temperature and relative humidity; (b) Indoor RH dependence on the outdoor temperature.....	63
Figure 4.4: Stack pressure at the top of three-storey building located in Edmonton	65

Figure 4.5: Wind pressure: Average yearly negative wind pressure [Pa] for Edmonton climate	66
Figure 4.6: Hourly wind pressure of wall facing south southwest (Edmonton climate).....	66
Figure 4.7: Air Leakage Path considered in 2-D hygrothermal analysis.....	68
Figure 4.8: Relative humidity distribution during winter (Edmonton)	70
Figure 4.9: Bottom Wood Plate Moisture Content at Sheathing-Batt Interface.....	70
Figure 4.10: OSB Moisture Content: (a) Bottom 15 cm, (b) Average MC for the whole OSB layer.....	71
Figure 4.11: Moisture Content of the Batt Insulation.....	72
Figure 4.12: Heat Flux through the Interior Surface	74
Figure 4.13: Transient Moisture Source (SIF-38.1; 35% indoor RH; Air Leakage rate 0.1 L/(s·m ²) at 75 Pa).....	77
Figure 4.14: OSB Moisture Content (ISF assembly)	80
Figure 4.15: OSB Mould Index (ISF assembly).....	80
Figure 4.16: Cavity Insulation Moisture Content (SIF assembly)	81
Figure 4.17: Mould Index at XPS-Batt Interface (SIF assembly).....	81
Figure 4.18: Total Moisture Content per square meter of a wall	82
Figure 4.19: OSB Moisture Content of ISF-38.1 wall (Edmonton; indoor RH 45%).....	85
Figure 4.20: OSB Moisture Content of ISF-50.8 wall (Edmonton; air leakage 0.02 L/(m ² ·s) at 75Pa).....	85

1 INTRODUCTION

1.1 Background

Wood is the dominant building material in Canada and the light-frame wood construction method is used in most of low-rise and mid-rise residential and commercial structures. Therefore, exterior wood-frame walls are often used as shear walls, providing resistance to lateral loads such as those arising from wind and earthquake. Assembly configurations of these exterior walls are constantly improving to meet higher requirements of building codes and energy efficiency standards. Since these standards demand better energy performance, the development of insulated wall systems with higher performances and longer durability has become a top priority. Increasing thermal performance often means that new assembly configurations of exterior walls, different from current time-tested, have to be proposed. For instance, adding a layer of continuous thermal insulation exterior to the between-stud cavity insulation is getting more popular in practice and has the benefit of removing thermal bridging of the lumber members. In the cases where the continuous insulation is put outer to the wood sheathing, the addition of continuous impermeable thermal insulation may result in trapping of moisture and reduce the drying capacity of a wall system. The wooden materials used in these walls are vulnerable to biological degradation caused by moisture, which typically occurs first at the wall sheathing in the form of mould, fungal growth or rot. Another modified configuration is to insert a layer of foam insulation between wood-based sheathing and lumber. However, the racking resistance of the shear wall is compromised due to the soft foam layer inserted between lumber and wood-based panels. According to the Canadian

Timber Design Standard CSA O86 (CSA 2014), the strength of a shear wall is directly proportional to the strength of its individual nailed connections. The standard prescribes design requirements for timber connections consisting of two or three wood-based members, whereas the connections including a layer of insulation between the sheathing and framing are not included in the standard. Although, the experimental studies on timber connections and shear walls which included a layer of intermediate insulation showed that the lateral capacity decreases significantly as the thickness of insulation increases (Plesnik 2014; Huber 2012), it has not been confirmed if the lateral capacity of a shear wall can be predicted based on the behavior of nail joint properties when insulation is inserted between the sheathing and framing members.

Moisture, on the other hand, is commonly regarded as the greatest threat to the durability and long-term performance of wood-frame assemblies (Newport Partners Raport 2004). Based on a survey presented by (Tsongas G. 2000) of 334 Iowa households, 98% of the residents reported at least one type of moisture problem. The most common types of moisture problems were: condensation on windows (62%), exterior paint peeling (41%), staining of interior windows frames and sills (31%), mildew on walls/ceilings or closets (23%), decay/rotting of interior window frames/sills (20%), moisture/mildew problems in summer (18%), frost/condensation on walls/ceilings (13%), and interior paint peeling (10%).

Clearly, both the structural and hygrothermal performance of wood-frame walls need to be investigated during the wall design. Additionally, Canada is characterized by its climate diversity and different wall assemblies need to be proposed for different locations.

1.2 Objectives

The main objective of this thesis is to improve the understanding on the structural and hygrothermal performance of light wood-frame walls with insulated sheathing. One goal is to evaluate if the shear strength of light wood-frame shear walls, where the insulation is inserted between the sheathing and framing, can be predicted based on the behavior of their individual nailed connections. Another goal is to evaluate the hygrothermal performance of this type of wall construction and compare its performance to the wall where the insulation is placed outboard to the sheathing. The overall intent is to establish a knowledge base about the structural and hygrothermal performance of this relatively new type of wall construction.

This knowledge will help the construction industry meet the increasing requirements for building energy efficiency mandated by building codes while minimizing the risk of moisture-related durability issues. Also, this will help designers to better understand the influence of additional insulation layer placed between the stud and sheathing panel on structural performance of wood-frame shear walls.

1.3 Methodology

One of the project objectives was to investigate if the shear strength of light wood-frame shear walls with intermediate insulation can be predicted based on the behavior of their individual nailed connections. First, a review of the theory and past research on the topic was conducted to set up the research base which was followed by the experimental testing of nailed joints and shear walls. The testing of nailed joints with intermediate insulation, designed to replicate nailed connections in light wood-frame shear walls, included thirty

specimens subjected to monotonic loading. The test matrix included three different nail sizes, and the insulation thickness varied from zero to 50.8 mm. The main intent of this testing was to understand how the intermediate insulation affect the structural performance of nail joints as well as to evaluate the influence of nail diameter, nail length, and insulation thickness on the nail joint load-deformation response. The results from nail joint tests were used for predicting the shear wall strength using the mechanics-based approach addressed in the CSA O86 (2014). This was followed by the testing of seven full-scale shear walls with intermediate insulation constructed using the same materials as the nail joints. The main objective was to compare the test results with the predicted values and investigate if the lateral capacity of shear walls with intermediate insulation can be predicted based on the nail joint properties.

Another goal of the project was to investigate the hygrothermal performance of wood-frame wall assemblies with commonly selected low-permeance exterior insulation. To achieve that, a sensitivity analysis was performed using one- and two-dimensional hygrothermal modeling. The two-dimensional analysis investigated the thermal performance of different wall assemblies comparing their heat flux values and investigated the critical locations within the wall for moisture accumulation. The one-dimensional analysis further investigated the hygrothermal performance of selected wall assemblies considering a range of parameters, such as indoor relative humidity, air exfiltration rate and the position and thickness of exterior insulation. For each simulated scenario, the analysis suggested the amount of exterior insulation required to prevent excessive moisture accumulation and mould growth within the wall assembly.

1.4 Thesis Structure

The thesis begins with a literature review of the previous studies on both the structural and hygrothermal performance of wood-frame wall assemblies. Then, an experimental portion of the study which included testing of nail joints and shear walls is presented. Subsequently, the hygrothermal analysis of wood-frame walls is conducted using a one- and two-dimensional modeling for various climates in Canada. Finally, the thesis ends with conclusions and recommendations for future research. The contents of each chapter are summarized below:

- Chapter 2 reviews the research works that have previously been conducted related to the structural and hygrothermal performance of light wood-frame wall assemblies with insulated sheathing and describes building code requirements relevant to the study.
- Chapter 3 describes the experimental portion of the research which included the testing of nail joints and shear walls with intermediate insulation. Additionally, this chapter includes a description of all the materials used and the procedures followed in the study. The chapter ends with the comparison of the predicted lateral capacity of the shear wall based on its individual nailed connections and the shear wall tested values.
- Chapter 4 describes the hygrothermal modeling of wood-frame assemblies including a low-permeance insulated sheathing. The analysis included one- and two-dimensional modeling and was conducted for different wall assemblies and for various locations in Canada.
- Chapter 5 provides conclusions and recommendations for further research.

2 LITERATURE REVIEW

2.1 Introduction

Rising demands of energy codes and building standards in Canada require higher insulation levels in many new and existing residential buildings. Adding insulation exterior to the wall cavity is a common practice for improving thermal resistance of the wall, however, position and properties of building materials can have a great effect on moisture accumulation, long-term durability, as well as the structural performance of the wall. In the wall assembly, a rigid foam insulation may be installed either exterior to the wood structural sheathing or inserted between the sheathing and framing. If the insulation is placed over the structural sheathing, the wall is expected to perform better under lateral loads compared with the case where the insulation is placed between sheathing and framing. However, this wall assembly may have lower drying potential. On the other hand, insulation inserted between the sheathing and framing will weaken the in-plane shear resistance of the wall assembly.

This chapter presents a review of relevant research on the structural and hygrothermal performance of light wood-frame walls that included an insulated sheathing. First part explains the structural performance of the wall, mechanics of nail joints and design methodology of light wood-frame shear walls according to the Canadian timber design standards. Additionally, this part contains a summary of studies that considered a layer of insulation as an intermediate material and its effect on the structural performance of the wall. Second part gives a review of publications that focused on the hygrothermal performance of light wood-frame walls. This part discusses the significance of the parameters such as

hygrothermal material properties, indoor relative humidity, air exfiltration, and explains different computer modeling approaches that were used in determining the hygrothermal performance of wood-frame walls.

2.2 Structural Performance of Wood-Frame Walls

2.2.1 Shear Wall Capacity

A shear wall is a structural system designed to resist lateral loads such as those arising from winds or earthquakes. A typical light wood-frame shear wall consists of framing members, sheathing panels and fasteners. The framing members are made of nominal 38 mm × 89 mm (2 × 4 in.) or 38 mm × 140 mm (2 × 6 in.) studs and include double top plates, one sill plate, and vertical studs that are usually spaced either 406 mm (16 in.) or 610 mm (24 in.) on centers. The sheathing panels can be applied on one or both sides of the frame and are typically fastened to the framing members with metal fasteners. The main function of fasteners is to connect the sheathing to framing members, framing member to framing member and wall to a foundation so that the wall performs as a system to resist horizontal and vertical loads. When a racking load is applied to a shear wall, fasteners in sheathing-to-framing joints will play a major role to resist the load, whereas fasteners in wall-to-foundation such as hold-down and anchors will work to resist racking and against uplift at a wall end. Shear walls, and particularly the nailed connections are designed to be highly ductile and efficient at energy absorption when subjected to lateral loads.

Previous studies have shown that the lateral resistance of wood shear walls can be accurately predicted based on the nail joint properties and depends on the properties of fasteners and framing members.

Wang (2009) in her study investigated the performance of nail joints and shear walls for the range of parameters: lumber density of 300 - 525 kg/m³, sheathing thickness of 9.5 – 18.5 mm and nail diameter of 2.5 – 4.1 mm. It was observed that nail joint strength has a strong correlation with nail diameter and lumber density whereas the joint strength is not sensitive to changes in sheathing thickness above 15.5 mm. Additionally, the strength of multi-fastener nailed connection with a large size nail (diameter of 4.1 mm) is sensitive to nail spacing when it changes from 50 mm to 25 mm. There is no significant influence of nail spacing on connection strength for small size nail (diameter of 2.5 mm) when nail spacing changes from 50 mm to 25 mm, irrespective of lumber density and sheathing thickness.

Mi (2004) studied sheathing-to-lumber nailed connections constructed with 3.3 mm diameter nails, 11 mm OSB sheathing and SPF lumber. In his study, specimens were subject to lateral loading parallel and perpendicular to the grain of lumber and it was observed that there was a negligible difference between performance of nailed joint loaded parallel and perpendicular to the grain of lumber.

Ni et al (2012) reviewed mechanics-based models for determining lateral load resistances of shear walls and diaphragms, and proposed mechanics-based method for determining the design values of shear walls and diaphragms with commonly accepted construction details in the CSA timber design standard (CSA 2005). Their approach showed that racking strength

of a wood-based shear wall is directly proportional to the strength of the sheathing-to-framing nail connection at the perimeter framing of the shear wall panel.

In the 2014 edition of the Canadian timber design standard CSA O86-14 (CSA 2014), the shear resistance of shear walls and diaphragms sheathed with wood-based panels are determined using the mechanics-based approach. The shear resistance of a shear wall per unit length can be calculated based on the individual nailed joint strength. The factored shear resistance of shear walls constructed with structural wood-based panels is calculated based on Equation (2.1).

$$v_{rs} = \phi \times v_d \times n_s \times J_D \times J_S \times J_{US} \times J_{hd} \quad (2.1)$$

where:

$$\phi = 0.8$$

$$v_d = \frac{N_u}{s} \text{ - specified strength of a shear wall sheathed with plywood or OSB, [kN/m]}$$

$$N_u = n_u K_D K_{SF} K_T \text{ - lateral strength resistance of sheathing-to-framing connection along panel edges, per fastener, [N]}$$

$$n_u \text{ - unit lateral resistance of a nail, [N]}$$

$$K_D \text{ - load duration factor}$$

$$K_{SF} \text{ - service condition factor}$$

$$K_T \text{ - treatment factor}$$

$$s \text{ - fastener spacing along panel edges, [mm]}$$

$$n_s \text{ - number of shear planes in sheathing-to-framing connection for walls sheathed with wood panels}$$

$$J_D \text{ - factor for diaphragm and shearwall construction}$$

$$J_S \text{ - fastener spacing factor}$$

$$J_{US} \text{ - strength adjustment factor for unblocked shear walls}$$

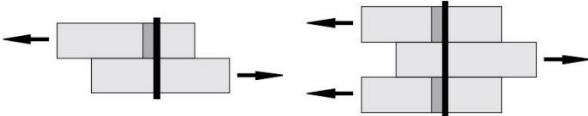

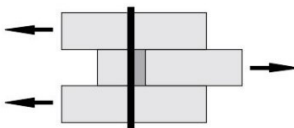
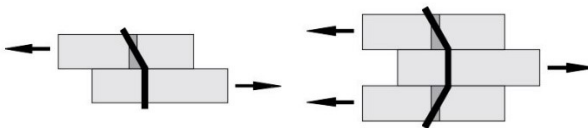
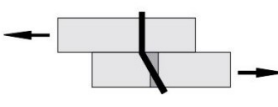
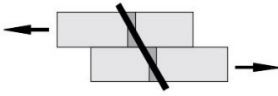
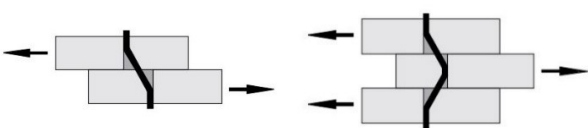
J_{hd} - hold-down effect factor for shear wall segment

The lateral strength resistance of a nailed connections (n_u) in the Canadian timber design standard (CSA 2014) is based on the European Yield Model, which was developed from Johansen's work (Johansen 1949). This timber connection model assumes that both the nail subjected to bending and the wood under embedding stress yield by ideally plastic deformation, whereas the effect of friction is neglected. The factors affecting the lateral strength of the nailed connection are nail diameter, sheathing material and thickness, and lumber relative density. CSA O86-14 Standard gives provisions for calculating the lateral resistance of timber connections composing of two or three wood members considering the following failure modes:

- a) Wood yield (slotting) in side member only
- b) Wood yield (slotting) in main member only
- c) Wood yield (slotting) in both members
- d) Wood yield and one-point nail yield in main member only
- e) Wood yield and one-point nail yield in side member only
- f) Wood yield and two-point nail yield

The capacity of each failure mode is expressed by different equation, as shown in Table 2.1, and the lateral strength resistance (n_u) shall be taken as the smallest of those values.

Table 2.1: Lateral resistance of nailed connections, (CSA O86-14, Clause 12.9.4.2)

Failure Mode	Lateral strength resistance, n_u	Illustration of failure mode
(a)	$f_1 d_f t_1$	
(b)	$f_2 d_f t_2$	
(c)	$\frac{1}{2} f_2 d_f t_2$	
(d)	$f_1 d_f^2 \left(\sqrt{\frac{1}{6} \frac{f_3}{f_1 + f_3} \frac{f_y}{f_1}} + \frac{1}{5} \frac{t_1}{d_f} \right)$	
(e)	$f_1 d_f^2 \left(\sqrt{\frac{1}{6} \frac{f_3}{f_1 + f_3} \frac{f_y}{f_1}} + \frac{1}{5} \frac{t_2}{d_f} \right)$	
(f)	$f_1 d_f^2 \frac{1}{5} \left(\frac{t_1}{d_f} + \frac{f_2 t_2}{f_1 d_f} \right)$	
(g)	$f_1 d_f^2 \sqrt{\frac{2}{3} \frac{f_3}{f_1 + f_3} \frac{f_y}{f_1}}$	

where:

t_1 - head-side member thickness for two-member connections; minimum side plate thickness for three-member connections, [mm]

t_2 - length of penetration into point-side member for two-member connections; centre member thickness for three-member connections, [mm]

f_1 - embedding strength of side plates, [MPa]

f_2 - embedding strength of main member, [MPa]

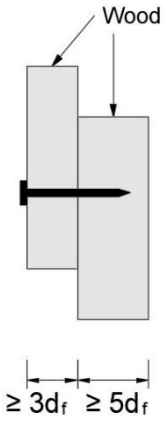
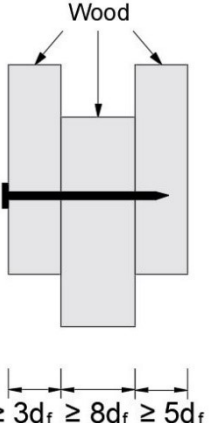
f_3 - embedding strength of main member where failure is fastener yielding, [MPa]

d_F - nail diameter, [mm]

f_y - nail yield strength, [MPa]

For timber connections, CSA O86-14 also specifies a minimum penetration length of nail into the point side member, as well as a minimum member thicknesses, as shown in Table 2.2.


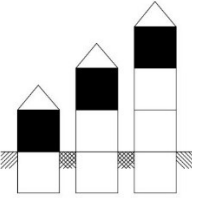
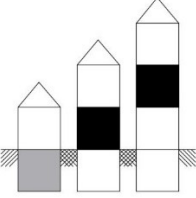
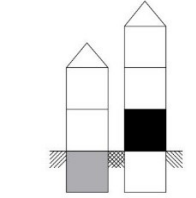
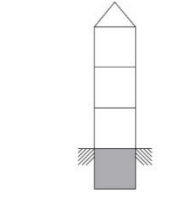

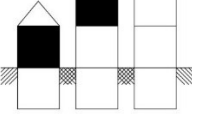
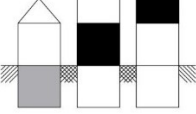
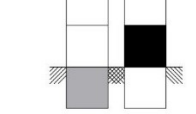
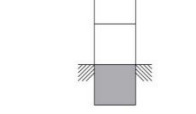
Table 2.2: Penetration length and member thicknesses for wood-to-wood connections (CSA O86-14, Clause 12.9.2.2)

Two-member connection	Three-member connection
 <p>$\geq 3d_f$ $\geq 5d_f$</p>	 <p>$\geq 3d_f$ $\geq 8d_f$ $\geq 5d_f$</p>

Part 9 of the 2015 NBCC (NRC 2015a) in its subsection 9.23.13. gives prescriptive requirements for the lateral resistance of light wood-frame walls due to loads arising from winds and earthquakes. The Standard allows the wall bracing to be designed and constructed in accordance with good engineering practice, such as that provided in Engineering Guide for Wood Frame Construction (CWC 2014). Table 2.3 gives construction requirements for

wood-frame shear walls according to the good engineering practice (Engineering Guide for Wood Frame Construction 2014). The shear wall framing types A-D shown in Table 2.3 are defined in Table 2.3.

Table 2.3: Wood Sheathed Braced Wall Panel Construction Details for Wind or Seismic Loads (Engineering Guide for Wood Frame Construction, 2014)

		Normal Weight Construction			
		Supporting only roof	Supporting roof plus one floor	Supporting roof plus two floors	Supporting roof plus three floors
	Exterior or interior framed wall				
	Interior framed wall only				
1-in-50 Hourly wind pressure or seismic spectral response acceleration [kPa]	Minimum required percentage of length of braced wall band on each storey	25%	25%	40%	75%
$0.8 < q_{1/50} \leq 1.2$	A	A	A	A	
$0.35 < S_a(0.2) \leq 0.50$	A	A	A	A	
$0.50 < S_a(0.2) \leq 0.70$	A	C	C	C	
$0.70 < S_a(0.2) \leq 0.90$	A	C	C	C	
$0.90 < S_a(0.2) \leq 1.20$	B	D	D	D	
$1.20 < S_a(0.2) \leq 1.80$	D	D	D	D	

*Framing types A-D described in Table 2.3

Table 2.4: Framing types specified in Table 2.3

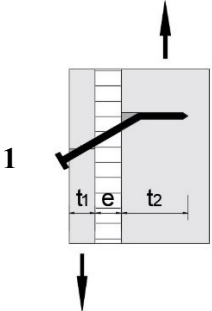
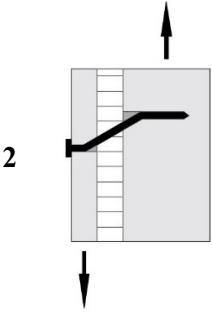
Framing Type	Sheathing thickness for 400 mm o.c. stud [mm]	Fastening along Panel Edges [mm]	Fastening along intermediate supports [mm]	Nail Diameter [mm]	Panel Edges Blocked or Unblocked	Design shear strength [kN/m]
A ⁽¹⁾	9.5	150	300	2.84	Unblocked	2.5
B ⁽²⁾	11	75	300	3.25	Unblocked	5.9
C ⁽³⁾	11	150	300	3.25	Blocked	5.2
D ⁽⁴⁾	11	75	300	3.25	Blocked	9.8

2.2.2 Influence of intermediate insulation

Previous studies that investigated the influence of an intermediate insulation layer on the structural performance of a wall have shown that the insulation thickness has a significant effect on the lateral capacity.

Aune and Patton-Mallory (1986) extended the application of the yield theory to wood connections including a layer of insulation between the sheathing and framing. Embedding strength of the sheathing and framing was considered equal in their model and two possible failure modes were proposed. Table 2.5 summarizes their work on timber connections with the layer of intermediate insulation. The first failure mode included wood and one-point nail yielding in the main member, whereas the second failure mode included wood yielding and two-point nail yielding. Based on their model, the connection yield strength decreases to roughly 60, 40, 30, and 25 percent when the insulation thickness increases from zero to 12.7 mm, 25.4 mm, 38.1 mm, and 50.1 mm, respectively.

Table 2.5: Lateral resistance of nail joints with intermediate insulation (Aune and Patton-Mallory, 1986)

Failure Mode	Lateral strength resistance, N_u [kN]	Failure mode determinants
 <p>1</p>	$\frac{f_e}{3} \left[2\sqrt{t_1^2 + et_1 + e^2 + 3\gamma} - (t_1 + 2e) \right]$	<p>Thickness conditions:</p> $\frac{\sqrt{e^2 + 4\gamma} - e}{2} < t_1 < \frac{\sqrt{e^2 + 8\gamma} - e + 4\sqrt{\gamma}}{2}$ <p>Theoretical length of nail:</p> $l = \frac{2t_1 + e}{3} + \frac{2}{3}\sqrt{t_1^2 + et_1 + e^2 + 3\gamma} - 2\sqrt{\gamma}$
 <p>2</p>	$\frac{f_e}{2} \left[\sqrt{e^2 + 8\gamma} - e \right]$	<p>Thickness conditions:</p> $t_1 \geq \frac{\sqrt{e^2 + 8\gamma} - e + 4\sqrt{\gamma}}{2}$ <p>Theoretical length of nail:</p> $l = \sqrt{e^2 + 8\gamma} + 4\sqrt{\gamma}$

Plesnik et al (2016) undertook a testing program to evaluate the influence of an intermediate insulation layer between wood-based sheathing and lumber on lateral strength of nail joint that consists of oriented strand board (OSB) as sheathing and spruce-pine-fir No. 2 grade lumber as framing member. Two nail sizes were used: 10d (3.66 mm × 76 mm) and 16d (4.06 mm × 89 mm). Selected results from their work for 6.4 mm, 12.7 mm, 25.4 mm and 38.1 mm insulation thicknesses are presented in Table 2.6. It can be seen that the strength of nail joint and therefore shear wall decreases as the insulation thickness increases. For the 4.06 mm nail, a 38.1 mm insulation will cause a strength reduction of 59 percent. The rate of strength reduction appears more significant when a smaller nail of 3.66 mm diameter is used.

Table 2.6: Percent reduction in nail joint strength due to presence of foam insulation between wood-based sheathing and lumber (Plesnik et al 2016)

Insulation thickness [mm]	Nail size (diameter, length)	
	3.66 mm × 76 mm	4.06 mm × 89 mm
0	100%	100%
6.4	59%	95%
12.7	53%	85%
25.4	34%	59%
38.1	-	42%

Huber Engineering Woods LLC (Huber 2012) introduced “ZIP System[®] R-Sheathing”, an exterior wall system that in a single panel incorporates wood structural sheathing, water resisting barrier (WRB), air barrier and exterior insulation layer, as shown in Figure 2.1. This type of wall construction, where four different layers are bonded into one panel, significantly reduces construction time and labour cost, while meeting energy code requirements. Continuous insulation layer inserted between the sheathing and framing increases the overall thermal resistance of the wall reducing the thermal bridging through the studs. Built-in water resistive barrier eliminates the need for housewrap and felt whereas the air barrier markedly reduces unwanted air leakage. However, this proprietary insulating sheathing results in the nail’s head being offset a distance from the lumber stud which leads to the reduction in the lateral resistance of the braced wall.



Figure 2.1: ZIP System® R-Sheathing (Huber, 2012)

The Canadian Construction Materials Centre (NRC 2017) investigated the structural performance of Huber’s “ZIP System® R-Sheathing” and its compliance with the 2015 NBCC. Table 2.7 gives a summary of construction details of braced wall and the results for monotonic loading test. The conclusion was that the “ZIP System® R-Sheathing” product provides a better performance than the NBCC benchmark wall for low seismic zones (Type A – 2.5 kN/m). Additionally, it is suggested that the minimum nail penetration into lumber studs shall be 12.5 times the specified nail diameter for insulating sheathing.

Table 2.7: Construction details of braced wall and the results of monotonic loading test (Evaluation Report CCMC 14075-R, 2017)

ZIP System® R-Sheathing Insulation thickness [mm]	Framing Lumber			Fasteners				Ultimate shear strength [kN/m]
	Stud Material	Stud Size [in.]	Stud Spacing [mm]	Nail Diameter [mm]	Nail Length [mm]	Nail Spacing (Interior Stud) [mm]	Nail Spacing (Edge) [mm]	
12.7	SPF No. 2	2 × 4	600	3.2 mm	76	300	150	4.30
38.1	SPF No. 2	2 × 4	600	3.2 mm	102	300	150	3.74
50.8	SPF No. 2	2 × 4	600	3.2 mm	76	300	150	3.11

APA – The Engineered Wood Association and the USDA Forest Services, Forest Products Laboratory (2014) initiated a research project to investigate the possibility of inserting rigid foam plastic insulation between wood structural panel sheathing and framing in wall applications to satisfy both the structural and energy conservation requirements in the U.S. building codes. Testing of full-scale (2.44 m by 2.44 m) shear walls was conducted to determine the structural performance of this wall configuration and to investigate the feasibility of attaching wood structural sheathing over 25.4 mm expanded polystyrene foam insulation in accordance with the International Residential Code (ICC 2012). Framing members were 38 mm × 89 mm (2 × 4 in.) Douglas-Fir No. 2 spaced 610 mm on centres. The wall assembly included 9.5 mm OSB exterior and 12.5 mm gypsum board interior sheathing and five fastener types were used in attaching the sheathing to framing: 6d common (2.87 mm × 50 mm), 8d cooler (2.87 mm × 60 mm), 8d common (3.33 mm × 64 mm), 10d box (3.25 mm × 76 mm) and 10d common (3.66mm × 76 mm). The acceptable performance was a minimum ultimate test load of 9.5 kN/m in accordance with Performance Standard for Wood-Based Structural-Use Panels PS2 (APA 2010). The results showed that only one out of eight wall configurations tested, constructed with 10d box nails spaced 100 mm on center along the panel edges and 300 mm in the intermediate supports, met the requirements of wall bracing. The study suggested further testing of this wall configuration using different nails or thicker structural sheathing.

Phillips (2015) investigated the behavior of light wood-frame walls constructed using insulated OSB panels. He examined fastener properties that influence the lateral capacity and the possibility to increase insulated OSB shear wall capacity by selecting different types of fasteners. The test results showed that changing the geometry and properties of the fasteners

used for constructing shear walls with insulated OSB sheathing can help to recover some of the shear capacity lost as a result of having an insulation layer between the framing members and exterior sheathing. Using non-traditional fasteners (i.e. longer fasteners, larger diameter fasteners, screws) and closer fastener spacing schedules can yield comparable shear design values for this type of wall system when compared to traditional light-frame wood shear walls.

2.3 Hygrothermal Performance of Wood-Frame Walls

2.3.1 Influence of exterior insulation, indoor humidity and air leakage

Moisture performance is a key consideration in building envelope design. The occurrence of moisture problems resulting from poor design, construction, or unexpected interactions of new building materials can lead to many undesirable consequences, such as mould growth, wood decay, loss of thermal resistance in wet insulation, poor indoor air quality, corrosion of metals, damage to materials and finishes from expansion or contraction, and loss of strength in building materials to the point of structural failure. A detailed overview of failure criteria for building materials is given by Viitanen and Salonvaara (2001).

During the heating season, moisture from the warmer indoor air migrates into and through the building assembly by two processes: vapour diffusion and air convection. Karagiozis and Kumaran (1993) showed that the vapour permeance of interior vapour barrier has a significant effect on the overall hygrothermal performance of the walls in colder climates and that vapour diffusion can be effectively controlled by placing a vapour retarder at the warm

side of the cavity. For instance, buildings in Vancouver required no vapour control, whereas a vapour barrier of a minimum vapour permeance of $60 \text{ ng}/(\text{m}^2 \cdot \text{s} \cdot \text{Pa})$ was necessary for buildings in Winnipeg, in order to prevent excessive water vapour diffusion and consequently condensation. In Canada, it is a code requirement to install a vapour retarder of maximum $60 \text{ ng}/(\text{m}^2 \cdot \text{s} \cdot \text{Pa})$ (Type II) water vapour permeance (WVP) on the warm side of wall assemblies. Such an installation will effectively retard moisture transport through the mechanism of vapour diffusion, but this would not prevent the other mechanism of moisture transport, which in most buildings is the dominating one (Latta 1976). Air convection mostly occurs at joints, holes, and cracks, and even small air fluxes can carry significantly larger volumes of water vapour compared to vapour diffusion (ASHRAE 2009).

Bomberg and Onysko (2002) provided a historic background of the study on heat, air, and moisture control in light wood-frame walls in Canada. Their review shows the studies on the hygrothermal behavior of buildings, augmented by many field and laboratory studies, which formed the basis for requirements and recommendations in building codes in Canada.

Ojanen and Kumaran (1996) investigated the effect of the air exfiltration on the moisture accumulation and heat flow in wood-frame assemblies and found that as the air flow rate increased, the heat flux increased as well. On the other hand, an increase of the air flow rate was not proportionally followed by the moisture accumulation, which increased up to a point beyond which it started decreasing and then abruptly went to zero. An explanation for that was that the air flow rate increase caused the cavity to become warmer which decreased the condensation potential. Figure 2.2 shows their finding for the dependence of the moisture accumulation on the air flow rate and the effect of indoor relative humidity. The authors also

suggested a proper consideration of the indoor relative humidity at the design stage of an air barrier system, and that tolerable air leakage rate should be based on the humidity level of the interior environment. The results also showed that putting an additional thermal resistance exterior to the wall had a significant influence on decreasing the moisture accumulation in the cavity.

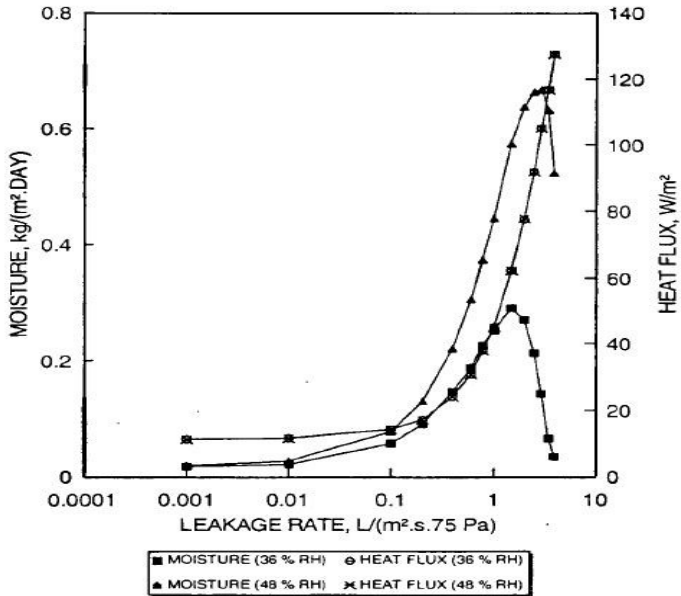


Figure 2.2: The effect of indoor relative humidity on the amount of moisture accumulated within a wall cavity due to air exfiltration (Ojanen and Kumaran, 1996)

Additionally, the study by Ojanen and Kumaran (1996) investigated the influence of water vapour permeance of the wall exterior surface and concluded that the amount of moisture accumulated in the wall cavity decreased as the water vapour permeance of the exterior surface increased and the rate of air exfiltration remained constant. This study suggested that higher air leakage rates would be tolerated when materials with higher vapour permeance are placed to the exterior. On the other hand, a study by Saber et al (2014) showed that the influence of water vapour permeance of the outboard insulation on the hygrothermal performance differed depending on the geographical location of a wall. For Vancouver and

St. John's climate, the moisture accumulation increased by increasing the water vapour permeance of the outboard insulation, whereas the water vapour permeance of the outboard insulation had insignificant effect on the moisture potential of walls constructed in Ottawa. In colder climates of Edmonton, increasing the water vapour permeance of outboard insulation helped in reducing the values of the mould index for walls without structural sheathing.

The study from Saber et al (2014) also showed that the structural sheathing had a positive effect on the hygrothermal performance of wood-frame walls for selected locations. Wall assemblies that included the structural sheathing performed better compared to the walls that were constructed without the structural sheathing. Air leakage rates of 0.1 and 0.075 L/(m²·s) at 75 Pa had a detrimental effect on the hygrothermal performance of wall assemblies and resulted in a risk of mould growth. Wall assemblies with an air leakage rate of 0.05 L/(m²·s) at 75 Pa (50% of the NBCC Part 9 maximum value) or lower were not susceptible to mould growth as the moisture accumulated during winter was able to dry out in the summer.

2.3.2 Modeling approaches

Heat, air, and moisture (HAM) analysis methods can range widely in terms of the physical phenomena that they include (Straube and Burnett 2001). On one end of the spectrum are simple steady-state models that include only heat conduction and vapor diffusion with constant material properties; on the other end are comprehensive computer models that include transient heat, vapor, liquid, and air transfer in as many as three dimensions, with

variable material properties and detailed descriptions of phenomena such as airflow and wind-driven rain.

Ojanen and Kumaran (1992) used a finite-difference technique to solve the transient heat, air, and moisture transfers in two-dimensional multilayer building structures to investigate the effect of exfiltration of indoor air on the moisture performance of the building envelope. They found that the moisture accumulation within the wall cavity due to air exfiltration highly depends on the indoor and outdoor climatic conditions, and the air exfiltration rate. If the indoor and outdoor climatic conditions allow moisture accumulation, any small air exfiltration rates may lead to high moisture contents in wall layers.

Karagiozis and Kumaran (1993) performed a steady state modeling as well as a transient two-dimensional hygrothermal modeling, using a finite-difference technique, to investigate the moisture performance of wood-frame walls. Their research examined the moisture accumulation in different wall components for six different vapour barriers. One conclusion was that the requirements for vapour barriers should be based on the transient weather data since the modeling with the steady state boundary conditions inadequately captured the moisture performance.

Ojanen and Kumaran (1996) further investigated the hygrothermal behaviour of wood-frame walls using a simple steady state hygrothermal modeling as well as a complex transient two-dimensional heat, air, and moisture transport model called TCCC2D (Transient-Coupled-Conduction and Convection in 2 Dimensions), developed at VTT Finland (VTT 1994). They analysed the amount of moisture accumulated in the wall cavity during the heating season and heat loss by modeling different air leakage paths and rates, varying indoor relative

humidity, vapour permeance and thermal resistance of exterior sheathing. They examined five air flow paths and found that the most critical case was when the air entered the wall cavity from the interior at the top of the wall and exited at the bottom. The next critical scenario was when the air entered the cavity from the bottom and exited at the top of the wall.

Kumaran and Haysom (2000) provided a guidance on the use of low-permeance materials towards the outside of wood-frame walls, for different climates in Canada. They explained the modeling procedure and the recommendations incorporated into the 1995 NBCC (NRC 1995) for low-permeance materials. Table 2.8 shows the 1995 NBCC requirement for the minimum required ratio of outboard to inboard thermal resistance, when low-permeance materials are placed within a wall assembly. The simulation described in their study investigated the required level of exterior insulation that would be necessary to prevent the moisture accumulation due to air exfiltration, and the minimum ratio of outboard to inboard thermal resistance was proposed for various locations in Canada. The study was based on the assumption that the indoor relative humidity during the heating season was 35%, and that there was a vapour barrier of $60 \text{ ng}/(\text{m}^2 \cdot \text{s} \cdot \text{Pa})$ (Type II) placed on the warm side. The air leakage rate was assumed to be $0.1 \text{ L}/(\text{m}^2 \cdot \text{s} \cdot \text{Pa})$ at 75 Pa as it was found to be the critical air leakage rate for exterior insulated walls (Ojanen and Kumaran, 1996).

Table 2.8: Minimum required ratio of outboard to inboard thermal resistance (1995 NBCC, Table 9.25.1.2)

Heating degree days of building location, Celsius degree-days	Minimum ratio, total thermal resistance outboard of material's inner surface to total thermal resistance inboard of material's inner surface
Up to 4999	0.20
5000 to 5999	0.30
6000 to 6999	0.35
7000 to 7999	0.40
8000 to 8999	0.50
9000 to 9999	0.55
10000 to 10999	0.60
11000 to 11999	0.65
12000 or higher	0.75

Chown and Mukhopadhyaya (2005) conducted a two-dimensional hygrothermal analysis, using computer modeling software hygIRC (2002), to determine the performance of building envelopes and to investigate whether the requirements from the 1995 NBCC Article 9.25.1.2 (Table 2.8) can be applied in climates such as coastal British Columbia (BC) where winter interior relative humidity above 35% is common. The analysis investigated the moisture accumulation in the stud space for different vapour barriers and concluded that the requirements from Table 9.25.1.2. of the NBCC can be applied to buildings located in milder BC climates, with a mild climate indicator (MCI) not exceeding 6300, and winter interior RH below 60%.

Brown et al (2007) developed a design protocol for the application of insulating sheathing to low-rise buildings with high interior relative humidity for various locations in Canada. The hygrothermal analysis was conducted using a time variant, two-dimensional, heat-air-

moisture (HAM) computer simulation program DELPHIN and the analysis considered 14 locations in Canada. The wall assembly was the same one that had been previously used by Ojanen and Kumaran (1992, 1996). The analysis investigated moisture accumulation in the stud cavity as well as the peak moisture content of the bottom wood plate due to different air leakage rates (0.024, 0.048 and 0.1 L/(m²·s) at 75 Pa). The results were presented in a similar way as the NBCC requirements for low air and vapour permeance sheathing, in terms of the minimum required outboard to inboard thermal resistance ratio and are summarized in Table 2.9. Their findings are suggested to be applied in cases where the air leakage rates would not exceed 0.048 L/(m²·s) at 75 Pa.

Table 2.9: Minimum required thermal resistance ratio when RH≤50% and RH≤60% (Brown et al 2007)

Location	HDD (Exterior temperature below 18°C)	Minimum Outboard/Inboard Thermal Resistance Ratio	
		RH≤50%	RH≤60%
Toronto, ON	3650	0.31	0.52
Yarmouth, NS	4100	0.34	0.55
Halifax, NS	4100	0.34	0.55
Montreal, QC	4250	0.36	0.57
Ottawa, ON	4600	0.38	0.57
Moncton, NB	4750	0.39	0.60
St. John's, NL	4800	0.40	0.61
Quebec City, QC	5200	0.43	0.64
Sudbury, ON	5400	0.44	0.65
Edmonton, AL	5400	0.44	0.65
Winnipeg, MB	5900	0.48	0.69
Saskatoon, SK	5950	0.49	0.70
Prince Albert, SK	6450	0.52	0.73
Fort McMurray, AB	6550	0.53	0.74

Saber et al (2014) used two-dimensional hygrothermal model hygIRC-C, developed by the National Research Council Canada (NRC), for modeling heat, air and moisture (HAM) transfer in investigating the hygrothermal performance of wood frame wall assemblies. The simulation results showed that the top and bottom portions of the wall assembly were the most critical locations for moisture accumulation based on the considered air leakage path, where air was assumed to leak into the wall through the opening at the bottom on the interior side and to exit to the exterior through a hole at the top of the wall. Also, it was observed that walls constructed using nominal 38 mm × 89 mm (2 × 4 in.) studs were less susceptible to mould growth compared to walls constructed with nominal 38 mm × 140 mm (2 × 6 in.) studs.

Glass (2013) in his research work used a one-dimensional transient hygrothermal modeling software WUFI[®] Pro 5.1 to investigate the moisture performance of residential wood-frame wall assemblies. All the assemblies considered in his study included oriented strand board (OSB) sheathing, and the moisture content and drying potential of the sheathing were investigated for a range of parameters, such as different exterior insulation materials, air exfiltration rates, wind-driven rain and wall orientations. He showed that the wall orientation and the type and vapour permeance of exterior insulation have a significant influence on the drying potential of the sheathing.

2.4 Summary

This chapter describes building code requirements and the research works that have previously been conducted related to the structural and hygrothermal performance of light wood-frame walls with insulated sheathing.

According to the Canadian Timber Design Standard CSA O86-14 (CSA 2014) shear wall strength is directly proportional to the strength of its nailed connections and the shear resistance per unit length of a wall can be calculated based on the individual nailed joint strength. Parameters that have the greatest influence on the strength of the nailed connection are nail diameter, lumber density and sheathing thickness. The CSA O86-14 standard prescribes design requirements for timber connections consisting of two or three wood-based members, whereas the connections including a layer of insulation between the sheathing and framing are not included in the standard. Although, the experimental studies on timber connections and shear walls which included a layer of intermediate insulation showed that the lateral capacity decreases significantly as the thickness of insulation increases (Plesnik 2014; Huber 2012), it has not been confirmed if the lateral capacity of a shear wall can be predicted based on the behavior of nail joint when insulation is inserted between the sheathing and framing.

The review of the studies that investigated the hygrothermal behavior of wood-frame walls included the findings which formed the basis for requirements and recommendations included in building codes in Canada, and described different hygrothermal modeling approaches. The 2015 NBCC (NRC 2015a) specifies the ratio of the thermal resistance values outboard and inboard of the innermost impermeable surface of the material within the wall

assembly. Applying those requirements would keep the inner surface of the low-permeable material warm enough during the heating season to avoid excessive moisture accumulation.

This project further investigated the influence of intermediate insulation on the structural performance of wood-frame shear walls and explored if the lateral capacity of the wall could be predicted based on its individual nailed connections. Additionally, the study investigated the moisture performance of the wall assembly where low-permeable insulation was inserted between the sheathing and framing and compared its performance to the case where this insulation was placed outboard to the structural sheathing. The hygrothermal analysis considered various air exfiltration rates, interior relative humidity and locations in Canada.

3 STRUCTURAL PERFORMANCE OF LIGHT WOOD-FRAME WALLS WITH INSULATED SHEATHING

3.1 Introduction

To investigate the influence of an insulation layer inserted between the sheathing and framing on the structural performance of light wood-frame walls, the experimental work was conducted on nailed connections as well as on shear walls. In this chapter the results from the experimental work will be presented and the predicted shear wall properties derived from nail joint results will be compared with shear wall test results.

The chapter begins with a description of all the materials used in this study including lumber studs, structural sheathing, fasteners, and insulation material. This is further followed by a description of the nail joint test program, test setup and procedure. The results from nail joint tests are analyzed and used for predicting the shear wall strength in accordance with the requirements from the CSA O86 (CSA 2014).

Experimental work on shear walls covered the testing of seven full-scale wall specimens (2.44 m by 2.44 m) under static racking load. Walls were constructed with intermediate insulation of different thickness and using different nailing. Finally, the chapter summarizes the experimental work discussing the influence of insulation thickness on shear wall performance and the influence of insulation layer on prediction of shear wall strength using nail joint properties.

3.2 Materials

3.2.1 Lumber

The most commonly used lumber for house construction in North America is Spruce-Pine-Fir (SPF) lumber due to its strength, light weight, low cost, and ease in cutting and nailing. SPF represents the largest reserve of commercial softwood in Canada and is used primarily for wall framing, roof framing, roof trusses and floor joists. High thermal resistance requirements for exterior walls mandated by building codes in Canada favorize 38 mm × 140 mm (nominal 2 × 6 in.) lumber pieces to be the most commonly used in wall construction as they can accommodate more insulation into the wall cavity.

Lumber pieces used for fabricating nailed joints in this study were cut from 38×140 mm (nominal 2×6 in.) SPF dimension lumber and were purchased from a local building supply store in Edmonton, Alberta.

Testing of shear walls was conducted at the University of New Brunswick (UNB) and the wall specimens were constructed using lumber pieces cut from 38×89 mm (nominal 2×4 in.) SPF dimension lumber that were purchased locally in New Brunswick.

After each test, a small piece of wood was cut from each tested specimen to measure lumber density, whereas the moisture content was measured using oven-drying method, as shown in Appendix A. At the time of testing, the lumber used for making nail joints had a mean ± SD density of $0.41 \pm 0.03 \text{ g/cm}^3$, whereas the density of lumber pieces used for shear walls was

$0.46 \pm 0.03 \text{ g/cm}^3$, as shown in Appendix A. This variability in the lumber density contributed to the variability of the test results.

3.2.2 Sheathing

Nail joint specimens and shear walls considered in this study had Oriented Strand Board (OSB) as a structural sheathing. The OSB boards were purchased from a local supplier and were delivered in standard 1220×2440 mm panel size and were 15.9 mm thick. For nail joint fabrication OSB panels were cut into 100×660 mm strips whereas the whole boards were used for wall construction.

3.2.3 Insulation

Extruded polystyrene (XPS) rigid foam insulation was selected to be used as an intermediate insulation material. Four different insulation thicknesses were used in the study: 12.7 mm, 25.4 mm, 38.1 mm, and 50.8 mm. For the fabrication of nail joints, insulation boards of 610×2440 mm were cut to the appropriate size, whereas the shear wall construction included full size 1220×2440 mm panels.

3.2.4 Fasteners

Canadian Timber Design Standard CSA O86-14 (CSA 2014) gives provisions for lateral resistance of nailed connections, as described in 2.2.1, which can only be applied to connections constructed with common round steel wire nails.

Nail joint and shear wall specimens in this study were constructed using three different nail types in order to investigate the influence of nail length and nail diameter on the connection strength: 10d (3.66 mm × 76 mm) common wire nails, 16d (4.06 mm × 89 mm) common wire nails, and power-driven (PD) nails (3.33 mm × 102 mm). 10d and 16d common wire nails meet the requirements of CSA O86-14 and can be used for calculating the shear resistance of the wall. Also, 16d nails are 89 mm long which theoretically allows for a thicker insulation (50.8 mm) to be placed between the sheathing and framing, while meeting the minimum requirements for nail penetration into the lumber.

To investigate the nail joint and shear wall behaviour when constructed with longer nails that are different from the common wire nails, PD nails were used. PD nails are widely used in the construction practice in North America and the nails considered in this study were 102 mm long, with a 3.33 mm diameter. Additionally, PD nails included a layer of coating to enhance the withdrawal resistance. Figure 3.1 shows different nail types used in this study.



Figure 3.1: Nails used in the study: 10d, 16d, PD (left to right)

3.2.4.1 Nail Bending Test Results

Nail bending strength is required as input property to calculating design strength of nail connection. The bending yield moment of the nails, used in this study, was determined in accordance with the Standard Test Method for Determining Bending Yield Moment of Nails (ASTM 2008). The center-point bending test involved simply supporting each nail and applying a point load in the middle at a constant deformation rate of 3.0 mm/min, as shown in Figure 3.2.

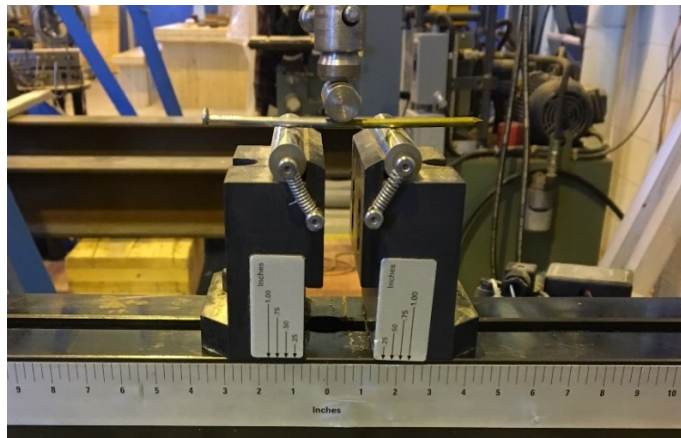


Figure 3.2: Center-point nail bending test setup

Nail bending tests were conducted for 10d, 16d and PD nails and three nail specimens were randomly selected from each of the nail types. The results of center-point nail bending tests are presented in Table 3.1. Mean response curves are plotted in Figure 3.3 and the response curves of all the nails tested can be found in Appendix E.

Table 3.1: Center-point nail bending test result

Nail Type	Mean Nail Diameter [mm]	Bending Yield Strength [MPa]	CSA O86 Strength [MPa]	ASTM F1667 Strength [MPa]
10d	3.75	548	613	620.5
16d	4.12	642	594	620.5
PD	3.24	742	-	689.5

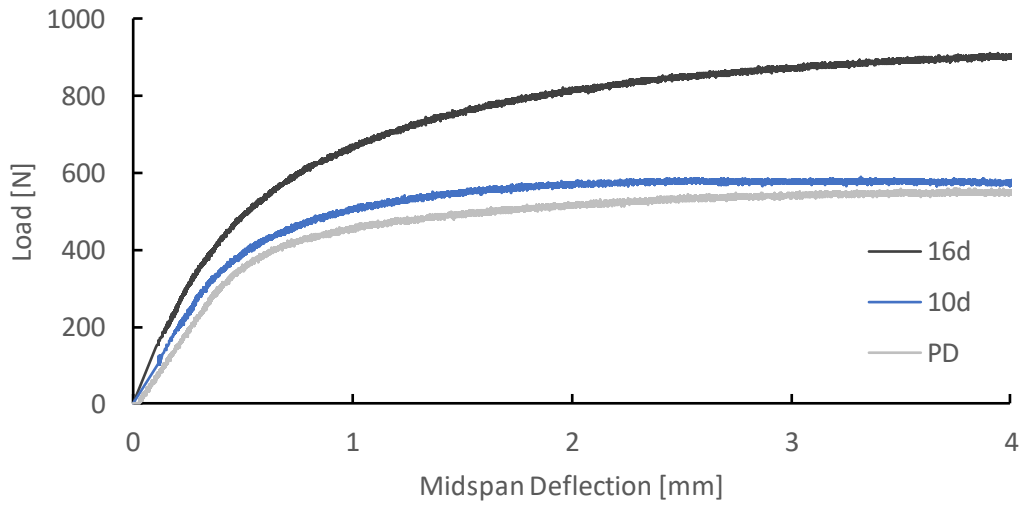


Figure 3.3: Center-point nail bending test results

3.3 Properties of Nailed Joints

3.3.1 Nail Joint Test Program

The nail joint test program covered, in total, 30 nail joint specimens fabricated with a layer of intermediate insulation which thickness varied between 0 and 50.8 mm, with a 12.7 mm increment. Nail joint specimens that did not include the insulation layer between the sheathing and framing served as a reference case for determining the effect of insulation on structural performance. Sheathing thickness was 15.9 mm in all the considered cases. To investigate the impact of nail diameter and nail length on the connection performance, three different nail types were considered in this study. Table 3.2 lists the details on number of test specimens and the different combinations of nail type and insulation thickness that were considered.

Table 3.2: Nail Joint Test Program

Insulation thickness [mm]	Number of specimens		
	10d nails 3.66 mm × 76 mm	16d nails 4.06 mm × 89 mm	PD nails 3.33 mm × 102 mm
0	3	3	-
12.7	3	3	-
25.4	3	3	-
38.1	-	3	3
50.8	-	3	3

3.3.2 *Nail Joints Test Setup*

The test setup used for testing of nail joints was similar to the one previously used by Wang (2009) and Plesnik (2014) and consisted of two segments - the test section at the top, and a dummy section at the bottom. During the fabrication of the specimens, lumber pieces that did not include any visible defects such as knots or splits were selected for making the test section, whereas the lumber pieces that contained such imperfections were used for the dummy end. The purpose of the dummy section was only to maintain the geometry of the specimen and was fabricated using six 12-gauge screws that provided the dummy section with high stiffness and such preventing any movement of that end. The test section was constructed with four nails and consisted of 38 mm × 140 mm (nominal 2 × 6 in.) stud, and insulation boards and the OSB on both sides. The reason for using 38 mm × 140 mm studs as the main member was to accommodate enough space for nails which were driven on both sides and prevent any interference between the nails. OSB panels were cut parallel to the face grain to 100 mm × 665 mm strips and outer strands of the OSB were parallel to the direction of loading. The specimen was symmetric with respect to the vertical axis. All specimens were stored in the laboratory ambient conditions for at least 2 weeks after fabrication to allow for wood relaxation around the nails.

Both wood sections were clamped using steel plates and threaded rods which helped in levelling the specimen and keeping the line of loading to be directly through the center of the specimen. Grip blocks were welded to the outer side of steel plates and the bottom plate was clamped to the testing machine, whereas the top end was connected to the machine using a pin connection. Figure 3.4 illustrates the nail joint test setup used in this study.

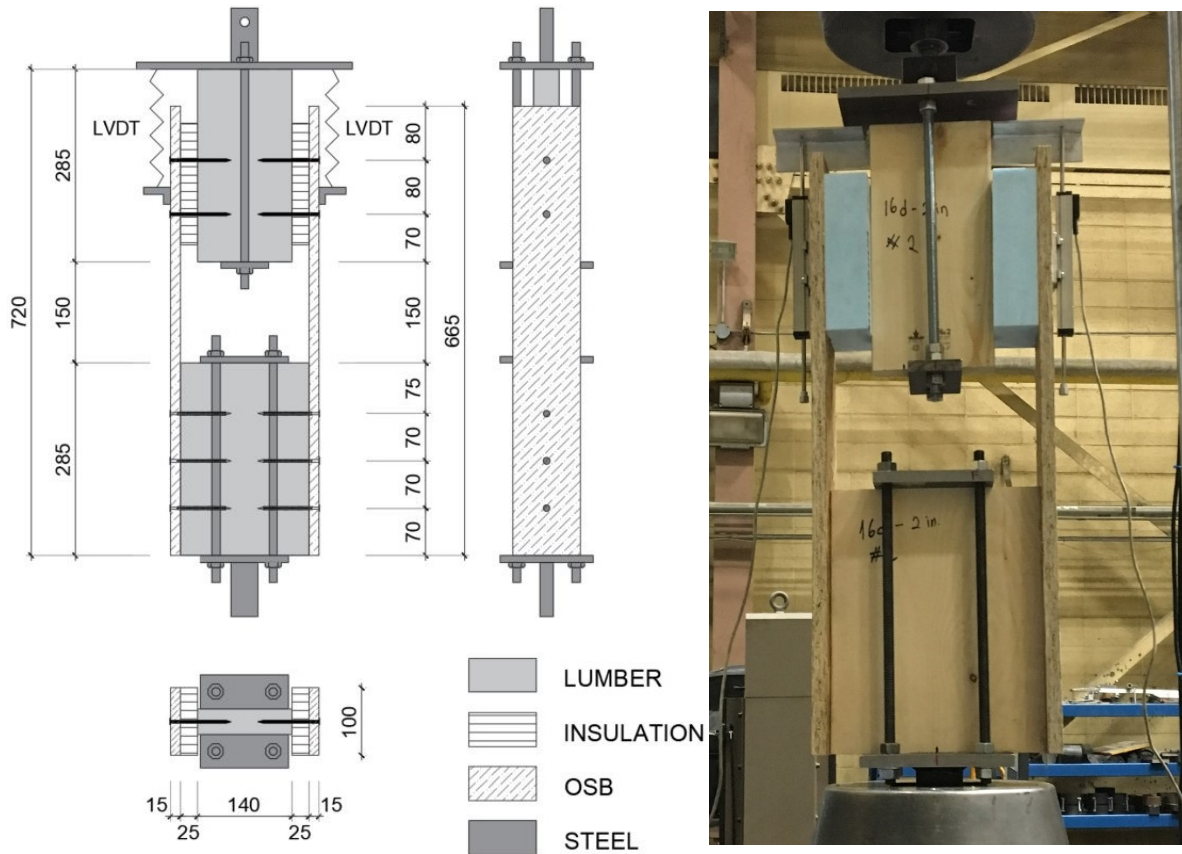


Figure 3.4: Nail Joint Test Setup

3.3.3 Instrumentation and Test Procedure

Nail joint specimens were subjected to monotonic loading with an applied pre-programmed displacement rate of 3.0 mm/minute. Two Linear Variable Differential Transformers (LVDTs) were attached to both sides of the specimen to record the relative displacement between lumber and the OSB. The brackets holding the LVDTs were attached to the OSB between the nail heads on each side of the specimen and pointing into a steel plate attached to the test stud.

The NBCC (NRC 2015a) prescribes a limit on wall drift of a maximum 2.5% of the wall height, which for a standard 2.44 m × 2.44 m wall translates into a maximum of 61 mm. Plesnik (2014) showed that an individual nailed connection that is part of a shear wall of any design will experience at most 10 mm of deflection at this level of wall drift. Nail joint tests in this study were stopped when the testing machine reached 25 mm displacement.

3.3.4 Nail Joint Test Results

Table 3.3 shows the mean values of the maximum recorded load for all nail joint specimens tested in this study. Additionally, the table provides information on the drop of lateral capacity when the insulation thickness increases, as well as the coefficient of variation.

Table 3.3: Nail Joint Test Results

Insulation Thickness [mm]	10d Nails			16d Nails			PD Nails ⁽¹⁾	
	Max Load [kN]	COV	Decrease in capacity [%]	Max Load [kN]	COV	Decrease in capacity [%]	Max Load [kN]	COV
0	1.40	0.02	100	1.51	0.06	100	-	-
12.7	1.10	0.05	78	1.16	0.03	77	-	-
25.4	0.69	0.03	50	0.82	0.04	54	-	-
38.1	-	-	-	0.58	0.03	38	0.95	0.11
50.8	-	-	-	0.38	0.08	25	0.71	0.01

⁽¹⁾ Specimens fabricated with PD nails did not experience a failure before the test was stopped. Load recorded at 25 mm displacement.

It can be noticed that nail joints fabricated with 10d nails experienced similar drop in strength, compared to specimens with 16d nails, as the insulation thickness increased. The maximum mean load of the connection constructed with 10d nails and without insulation, was 1.40 kN

per nail, whereas it was 1.51 kN for specimens constructed with 16d nails. Specimens that included 12.7 mm thick insulation layer retained 78% and 77% of the base case strength, for 10d and 16d nails respectively. Additionally, increasing the intermediate insulation to 25.4 mm caused the strength to drop to 50% and 54% of the base case load, for 10d and 16d nail respectively. Specimens with 10d nails and insulation thicknesses of 38.1 mm and 50.8 mm were not considered in the study.

Nail joint specimens with 38.1 mm and 50.8 mm of intermediate insulation and constructed with PD nails performed markedly better when compared to same specimens fabricated with 16d nails. Even though PD nails had the smallest diameter of the three considered nail types, nail joints constructed with these nails did not experience the failure before the test was stopped at 25 mm displacement. Figure 3.5 graphically shows the mean load-displacement curves per nail for specimens constructed with 10d, 16d, and PD nails, respectively.

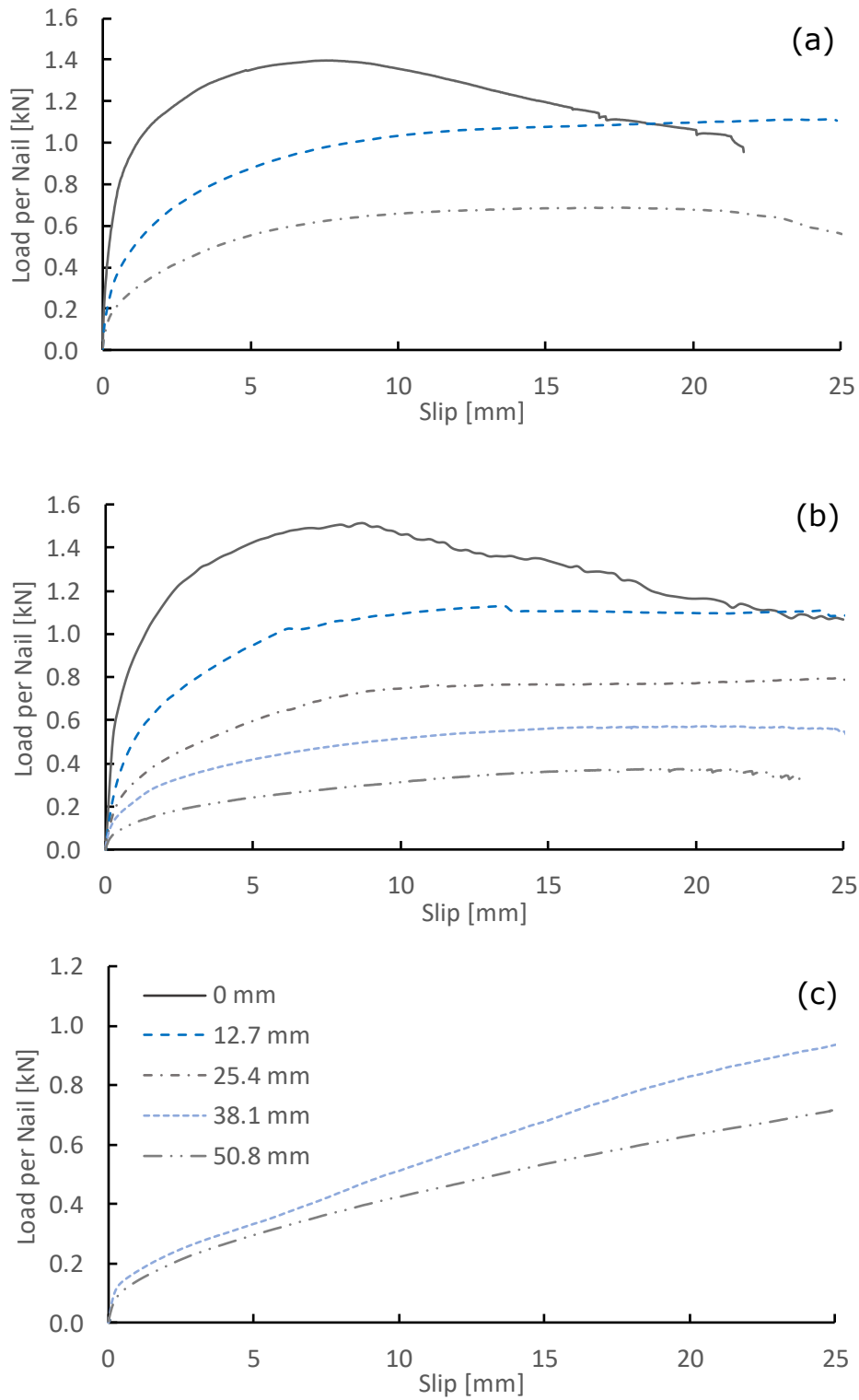


Figure 3.5: Mean Load-Displacement Response of Nail Joints Constructed with: (a) 10d Nails; (b) 16d Nails; (c) PD Nails

3.3.5 Failure Modes of Nail Joints

It was observed that the predominant failure mode of nail joints under monotonic loading was the bending of nails. Figure 3.6. shows a typical failure of the specimens constructed with common wire nails (10d and 16d). It can be seen that as the insulation thickness increased the nail bending angle decreased. Additionally, it was observed that nail joint specimens that included 50.8 mm thick insulation layer and 16d nails failed when nails started pulling out of lumber even though the nail penetration length in point side member (22.2 mm) met the CSA O86-14 requirement of $5d_f$ (20.3 mm). Therefore, the minimum nail penetration length of $5d_f$ (five times the nail diameter) in point side member, required by the CSA O86-14 for wood connections might not be enough when the connection includes a layer of intermediate insulation.

Nailed connections constructed with PD nails did not experience the failure before the test was stopped at 25 mm displacement. In these connections, it was observed that as the displacement was increasing the OSB sheathing was squashing the insulation against the lumber and such increasing the connection capacity. This was the opposite scenario compared to the failure of the specimens with 50.8 mm insulation constructed with 16d nails, where the OSB was moving away from the lumber and nails started pulling out under higher displacements. More photos of tested nail joints can be found in Appendix C.

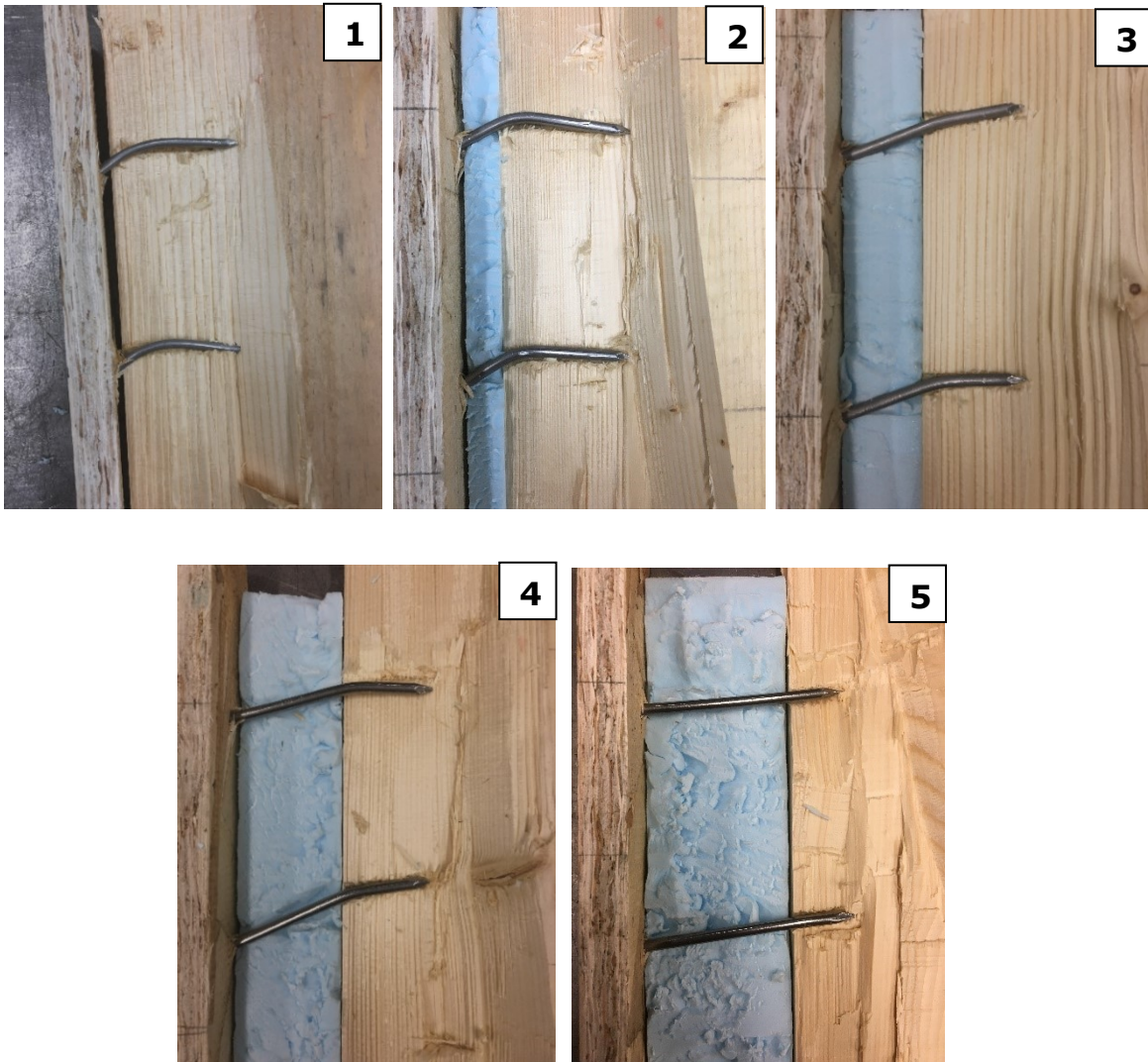


Figure 3.6: Typical failure mode of nail joints constructed with common wire nails (10d and 16d): 1 – 0 mm insulation; 2 – 12.7 mm insulation; 3 – 25.4 mm insulation; 4 – 38.1 mm insulation; 5 – 50.8 mm insulation

3.3.6 Shear Wall Strength Predicted Using Nail Joint Properties

According to CSA O86-14 (CSA 2014), the strength of wood-frame shear walls can be calculated based on the resistance of individual sheathing nail joints, as shown in Equation (3.1).

$$V_d = \frac{N_u}{s} \times L_S \quad (3.1)$$

where:

N_u - lateral resistance of individual nailed connection, [N]

s - fastener spacing along panel edges, [mm]

L_S - shear wall length, [m]

Table 3.4 lists the shear wall strength derived by using this equation and the lateral resistance values of tested nail joints.

Table 3.4: Shear Wall Strength Predicted Based on Nail Joint Strength

Insulation Thickness [mm]	Nail Joints (tested) [kN]			Shear Wall (predicted) [kN]		
	10d Nails	16d Nails	PD Nails	10d Nails	16d Nails	PD Nails
0	1.40	1.51	-	22.8	24.6	-
12.7	1.10	1.16	-	17.9	18.9	-
25.4	0.69	0.82	-	11.2	13.3	-
38.1	-	0.58	0.95	-	9.4	*
50.8	-	0.38	0.71	-	6.2	*

* Nail joints constructed with PD nails did not reach a peak load

3.4 Shear Wall Performance

3.4.1 Shear Wall Test Program

The shear wall test program included seven shear walls which were fabricated and tested in accordance with the ASTM E72-15 Standard (ASTM 2015). Walls were constructed using the same materials as nail joint specimens and the objective was to investigate if the strength of the wall with intermediate insulation can be predicted based on the properties of its individual nailed connection. Additionally, the study investigated the influence of nail spacing along the panel edge considering two wall configurations (S5 and S6) with same construction details except for nail spacing. Table 3.5 summarizes the shear wall test program.

Table 3.5: Shear wall Test Program

Shear Wall	OSB thickness [mm]	Insulation thickness [mm]	Nails diameter/length [mm]	Panel edge nail spacing [mm]	Field nail spacing [mm]
S1	15.9	-	10d 3.66/76	150	300
S2	15.9	12.5	10d 3.66/76	150	300
S3	15.9	25	10d 4.06/89	150	300
S4	15.9	25	16d 4.06/89	150	300
S5	15.9	50	16d 4.06/89	150	300
S6	15.9	50	16d 4.06/89	75	300
S7	15.9	50	PD 3.33/102	150	300

3.4.2 *Shear Walls Test Setup*

Full-scale shear walls tested in this study were 2.44 m by 2.44 m (8 by 8 ft) in size and the wall frames were assembled in accordance with ASTM E72-15 Standard (ASTM 2015) using 38 by 89 mm (nominal 2 × 4 in.) SPF stud members. All walls consisted of double end studs that were nailed together, and vertical studs in the middle spaced at 610 mm (24 in.) on centres. To meet the CSA O86-14 (CSA 2014) requirement for nail edge spacing at adjoining panel edges, walls constructed using 16d nails (4.06 mm diameter) included a double mid-stud (two 2 × 4 members nailed together). During the fabrication of wall specimens, nails were driven manually using a hammer. Top and bottom plates of a shear wall were connected to steel frame beams with 15.9 mm (5/8 in.) bolts which were designed to prevent wall slip along the top and bottom supports during the test. Bolt holes in the supporting beams were minimally oversized, whereas the holes in wood top and bottom plates were the same width as bolts. Additional wood plate was inserted between the steel frame and bottom and top plates of the wall allowing the structural sheathing to rotate freely without interference with the steel frame beam during the racking of the wall. To overcome the tendency of one end of the wall panel to rise as the racking load was applied hold-downs were provided at the wall bottom ends anchoring the wall to the steel frame. Simpson HTT22 hold-downs were installed per manufacturer's specifications and raised off the bottom plate by 25.4 mm.

The steel beam at the top plate distributed the racking load from a programmable hydraulic actuator. The actuator, with a displacement range of ±160 mm, was secured between the support and the distribution steel beam by means of the hinged connections. The test setup included a lateral support with minimal friction in order to ensure in plane wall deflection.

Figure 3.6 illustrates the shear wall assembly including the instrumentation and shows a picture of the shear wall test setup.

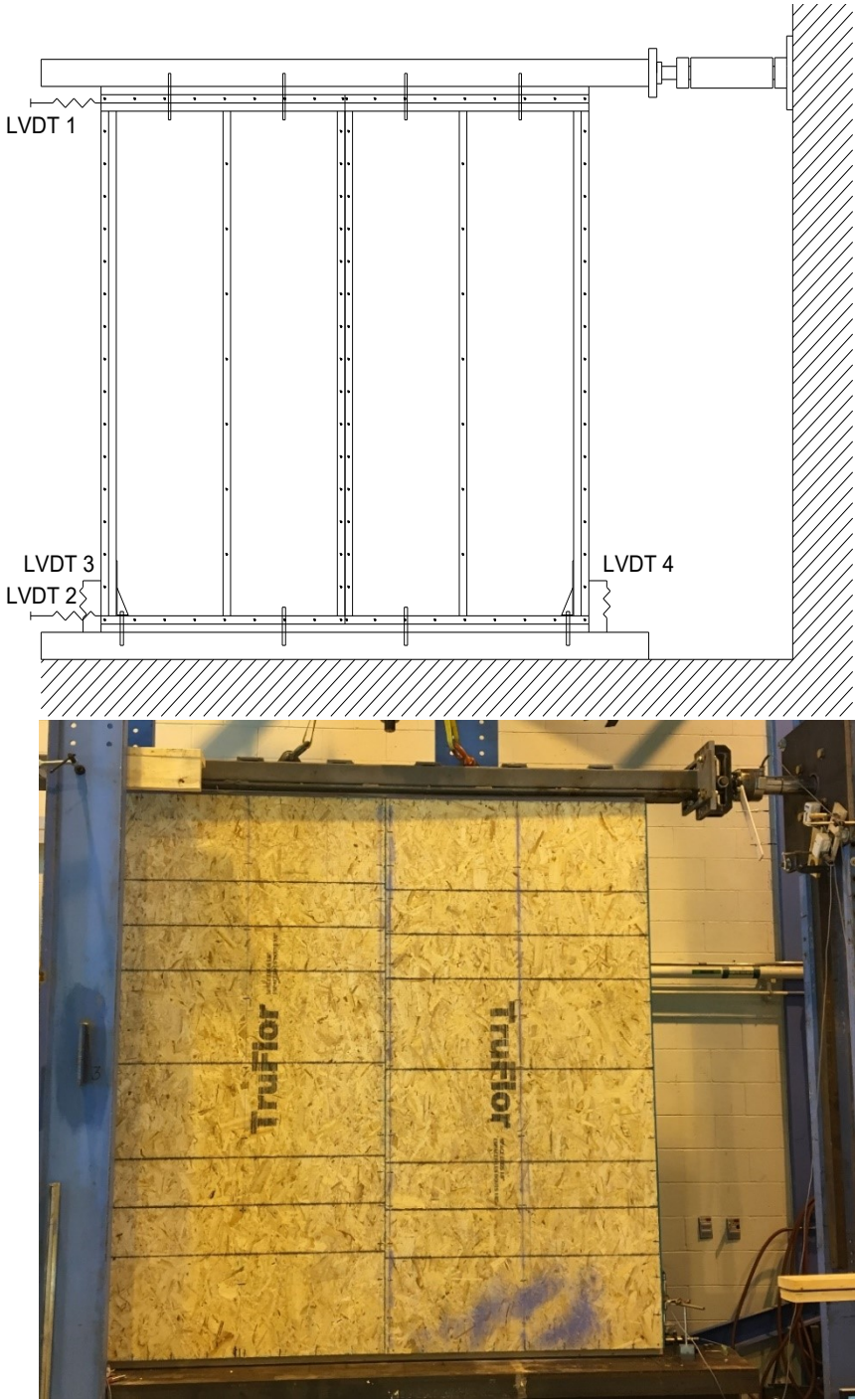


Figure 3.7: Shear Wall Test Setup

3.4.3 Instrumentation and Test Procedure

Testing of shear walls was conducted by displacing the top of the wall specimen at a constant rate of 3.0 mm/minute in three stages, in accordance with ASTM E72-15 Standard (ASTM 2015). Displacement was applied with a hydraulic actuator using a steel distribution beam bolted to the wall top plates, until the machine stroke was reached at 160 mm. To measure the displacement of the wall specimen, four linear displacement measuring devices were provided: two horizontal LVDTs placed at the centerline of the top plate and the bottom plate, and the vertical LVDTs at the centre of the tension stud and the compression stud, in accordance with ASTM E72-15.

3.4.4 Shear Wall Test Results

Figure 3.8 presents load-deflection curves of shear wall test specimens constructed with 10d nails (S1, S2 and S3). Comparing the responses of these three shear walls, where the insulation thickness increased from 0 mm to 12.7 mm and 25.4 mm, the maximum recorded load dropped from 100% to 79%, and 58%, respectively. This trend of decrease in lateral capacity of shear walls compares well with the decrease of the lateral resistance of nail joints constructed with same materials: 100%, 78%, and 50% respectively. Putting a layer of insulation between the sheathing and framing markedly reduces the racking resistance of the wall and increasing the thickness of that insulation leads to a significant drop of the wall lateral capacity.

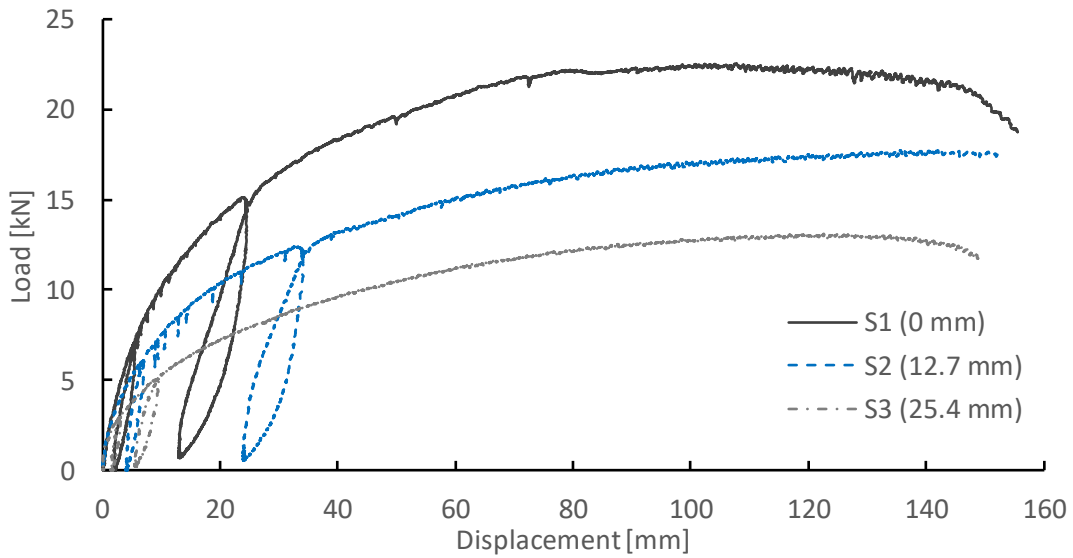


Figure 3.8: Load-Displacement Responses of Shear Walls Constructed with 10d Nails

Comparing the responses of wall specimens S3 and S4, Figure 3.9, where the diameter of nail was increased from 3.66 mm to 4.06 mm, and the insulation thickness was 25.4 mm, the lateral resistance of the wall increased by 151%.

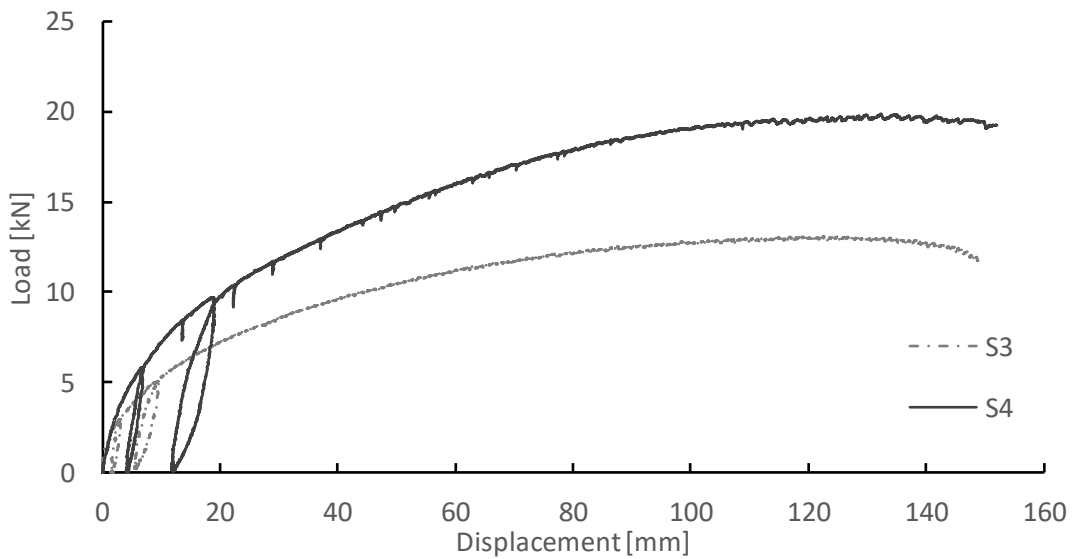


Figure 3.9: Load-Displacement Responses of Shear Walls S3 (10d) and S4 (16d)

Figure 3.10 shows load-displacement curves of wall specimens constructed with 16d nails (S4, S5, and S6). It can be seen that adding 50.8 mm of insulation between the sheathing and framing (S5) caused a drop in lateral capacity to 49% relative to the wall constructed with 25.4 mm of insulation (S4). This agrees well to the drop in the lateral capacity of nail joint having the same configuration and 16d nails, where the capacity decreased to 46%. Reducing the nail edge spacing by half, from 150 mm to 75 mm (S6), caused the increase of the wall strength by 210% which confirmed that the shear wall strength can be recovered by using a closer nail spacing even for wall configurations including the layer insulation between the sheathing and framing.

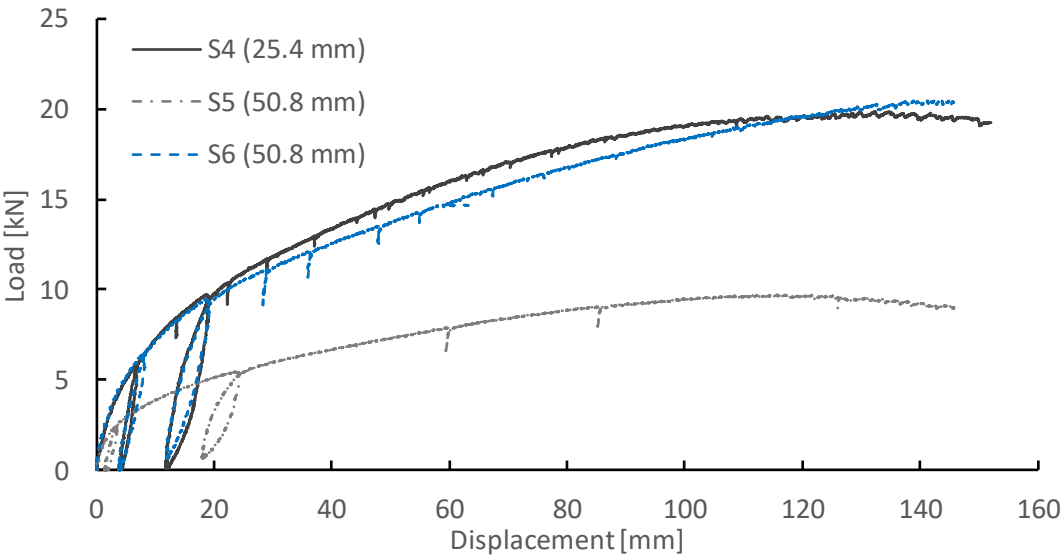


Figure 3.10: Load-Displacement Responses of Shear Walls Constructed with 16d Nails

Comparing the wall specimen constructed with PD nails and 50.8 mm insulation (S7) to the same configuration constructed with 16d nails (S5), Figure 3.11, it can be concluded that these two walls exhibited similar response compared to their individual nailed connections, as shown in 3.3.4. Shear wall constructed with PD nails did not experience the failure before

the maximum displacement of 160 mm was reached and had a higher lateral capacity, even though PD nails had a smaller nail diameter.

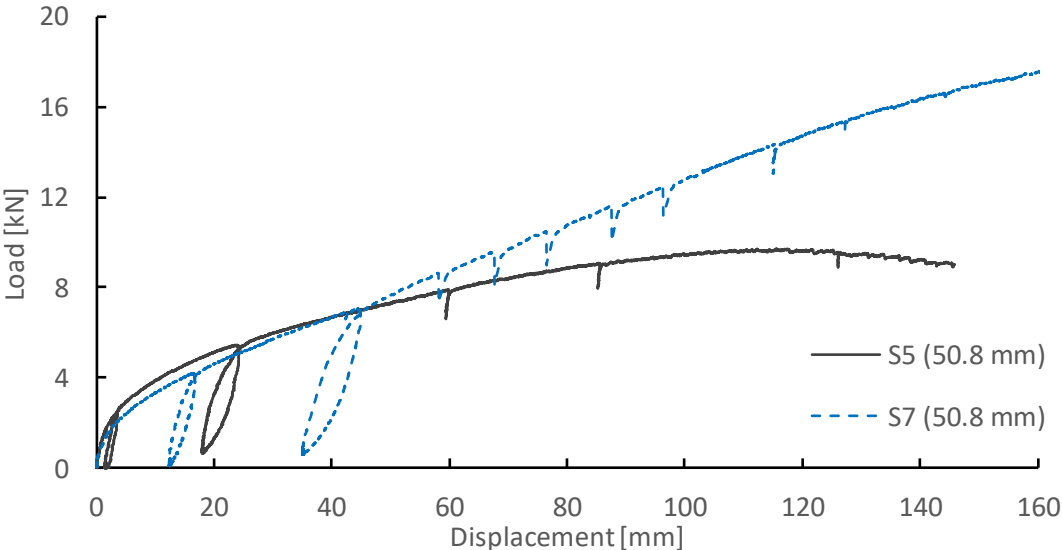


Figure 3.11: Load-Displacement Responses of Shear Walls S5 (16d) and S7 (PD)

Table 3.6 summarizes the results from shear wall tests. Additionally, the initial stiffness of each shear wall specimen was derived based on the equivalent energy elastic-plastic (EEEP) method (ASTM 2011). The initial stiffness is calculated as a slope from the origin to the point on the ascending curve where the resistance is equal to 0.4 times of the peak load, $0.4F_{max}$. It can be seen that as the insulation thickness increases, the wall strength and stiffness both exhibit a steep reduction.

Table 3.6: Shear Wall Test Results

Shear Wall	Insulation thickness [mm]	Nail Type	Panel edge nail spacing [mm]	Peak Load [kN]	Change in Capacity [%]	Initial Stiffness [kN/mm]
S1	-	10d	150	22.55	Base Case 1	1.12
S2	12.5	10d	150	17.73	79 ⁽²⁾	0.75
S3	25	10d	150	13.13	58 ⁽²⁾	0.53
S4	25	16d	150	19.87	Base Case 2	0.67
S5	50	16d	150	9.72	49 ⁽³⁾	0.39
S6	50	16d	75	20.45	210 ⁽³⁾	0.62
S7	50	PD	150	17.06 ⁽¹⁾	-	0.15

⁽¹⁾ Shear wall constructed with PD nails did not fail, peak load recorded at 160 mm displacement

⁽²⁾ Relative to shear wall S1 (Base Case 1)

⁽³⁾ Relative to shear wall S4 (Base Case 2)

3.4.5 Failure Modes of Shear Walls

The reference case specimen, which was the wall that did not include a layer of intermediate insulation (S1), failed predominantly due to nail bending. However, splitting of the bottom wood plate was also observed as well as tearing of the sheathing and nail head pull-through close to the panel edges, as shown in Appendix D.

Shear wall specimens S2, S3, and S4 failed mainly due to the failure of edge nail joints caused by bending of nails under large rotation of the sheathing panels. No other failure modes were observed in these wall specimens.

Additional failure mode was observed in walls that included 50.8 mm of insulation and constructed with 16d nails (S5 and S6), where some nails pulled out of the framing members under large lateral displacement.

The only wall specimen that did not experience a failure before the test was stopped at 160 mm deflection was the one constructed with PD nails. During the racking of the wall it was observed that as the displacement increased and nails were bent more, sheathing panels were squashing the insulation against the framing and thus increasing the lateral capacity of the wall, as shown in Appendix D for S7 wall.

3.5 Influence of Insulation Layer on Prediction of Shear Wall Strength using Nail Joint Properties

According to the Canadian timber design standard CSA O86-14 (CSA 2014), the lateral resistance of wood shear walls can be calculated based on the resistance of sheathing-to-framing nail joints. This section compares the lateral resistance values of shear walls predicted based on the nail joint properties with the values obtained from full-scale shear wall tests. This comparison is shown in Table 3.7.

Comparing the predicted and tested values of shear wall lateral capacity, it can be seen that the shear wall lateral resistance can be accurately predicted based on nail joint properties, for specimens constructed with 10d nails. Additionally, wall specimens constructed with 10d nails experienced a drop in the capacity from 100% to 79% and 58%, which closely compares to the predicted lateral capacity drop from 100% to 78% and 50%, as the insulation increased from 0 mm to 12.7 mm and 25.4 mm, respectively.

Table 3.7: Predicted and Tested Shear Wall Lateral Resistance

Insulation Thickness [mm]	Shear Wall Predicted Capacity [kN]			Shear Wall Tested Capacity [kN]		
	10d Nails	16d Nails	PD Nails	10d Nails	16d Nails	PD Nails
0	22.8	24.6	-	22.6	-	-
12.7	17.9	18.9	-	17.7	-	-
25.4	11.2	13.4	-	13.1	19.9	-
38.1	-	9.5	*	-	-	-
50.8	-	6.2	*	-	9.7	*

* Nail joints and shear walls constructed with PD nails did not experience a failure before the test was stopped

Nail joint and shear wall specimens constructed using 16d nails experienced similar drop in strength, however, the test values were higher compared to the values calculated based on nail joint properties. The reason for this anomaly could be attributed to the differences in fabrication process between nail joints and shear walls, as well as to the differences in lumber density. Nail joints were fabricated and tested at the University of Alberta and the nail joints constructed with 16d nails had a mean \pm SD density of $0.39 \pm 0.02 \text{ g/cm}^3$. Shear walls, on the other hand, were fabricated and tested at the University of New Brunswick and the density of lumber pieces was $0.46 \pm 0.03 \text{ g/cm}^3$.

Nail joints and shear walls constructed using PD nails exhibited similar load-displacement behavior and did not experience a failure before the tests were stopped. In both cases, it was observed that as the displacement was increasing OSB panel was squashing the insulation against the lumber and the tests were stopped when the loading actuator reached a maximum displacement of 160 mm.

3.6 Summary

The experimental portion of this study covered the testing of nail joints and full-scale shear walls under monotonic load in order to investigate the influence of insulation layer inserted between the sheathing and framing on the structural performance of wood-frame walls. The study included various nail joint and shear wall configurations where the insulation thickness varied between 0 and 50.8 mm. Additionally, three different nail types were used in fabricating the specimens, varying the nail diameter, length and the nail edge spacing. All specimens were constructed using SPF dimension lumber and 15.9 mm thick OSB structural sheathing. The purpose of this work was to evaluate if the same mechanics-based design method addressed in the 2014 edition of CSA O86-14 (CSA 2014) can be applied to the shear walls constructed with insulated sheathing and to investigate how accurately shear wall lateral capacity can be predicted based on the nail joint properties.

It was noticed that the failure mode of both nail joints and shear walls was largely due to the bending of nails. Specimens constructed with 16d nails and included 50.8 mm thick insulation between the sheathing and framing failed when nails started to pull out of lumber, but slight nail bending was also noticed. Based on this observation it is recommended that a minimum nail penetration into lumber is higher than five times the nail diameter as required by the CSA O86-14 for wood-member connections. Nail joint and shear wall specimens constructed with PD nails showed similar behavior and did not experience a failure before the tests were stopped when the stroke of the displacement sensor was reached.

Based on the results from nail joint and shear wall tests it can be concluded that the specimens fabricated with 10d and 16d nails experienced a similar decrease in lateral capacity as the

insulation thickness increased. On average, the capacity decreased to 78%, 54%, 38%, and 25%, when the insulation thickness increased from zero to 12.7 mm, 25.4 mm, 38.1 mm, and 50.8mm, respectively. Both nail joints and shear walls constructed with larger diameter nails had higher lateral resistance under monotonic load.

Overall, comparing the predicted and tested values of shear wall lateral capacity, it can be concluded that the shear wall lateral resistance can be accurately predicted based on nail joint properties.

4 HYGROTHERMAL PERFORMANCE OF LIGHT WOOD-FRAME WALLS WITH INSULATED SHEATHING

4.1 Introduction

A popular way of increasing the thermal resistance of light wood-frame wall assemblies is putting a continuous foam insulation exterior to the wall cavity. This insulation also has the benefit of reducing a thermal bridging and can be placed either outboard to the structural sheathing or inserted between the sheathing and framing. A sensitivity analysis was performed using one- and two-dimensional hygrothermal modeling to investigate the hygrothermal performance of wood-frame wall assemblies with low-permeance exterior insulation. The two-dimensional analysis investigated the thermal performance of different wall assemblies comparing their heat flux values, and investigated the critical locations within the wall for moisture accumulation. The one-dimensional analysis further investigated the moisture accumulation in different wall layers considering a range of parameters, such as outdoor climate, indoor relative humidity, air exfiltration rate and the position and thickness of exterior insulation. For each case, the analysis suggested the amount of exterior insulation required to prevent excessive moisture accumulation and mould growth within the wall.

This chapter begins with a description of the wall assemblies and simulation parameters considered in the analysis. The simulation parameters include a hygrothermal material properties, exterior and interior climate conditions, and air exfiltration modeling. This is followed by the results of the analysis and the discussion on the influence of low-permeance insulation. The chapter summarizes the key findings and discusses the effect of low-

permeance insulation, when placed outboard and inboard to the structural sheathing, on the wall hygrothermal performance.

4.2 Wall Assembly Configurations

Hygrothermal analysis investigated and compared the moisture performance of two types of light wood-frame wall construction. First, where the structural sheathing was nailed directly to the framing and the low-permeance insulation was placed exterior to the sheathing: “Insulation-Sheathing-Framing” (ISF) configuration. In the second configuration, the low-permeance insulation was inserted between the sheathing and framing: “Sheathing-Insulation-Framing” (SIF). Figure 4.1 illustrates these two wall assemblies showing wall component layers considered in this study. Both wall assemblies, ISF and SIF, were clad with 19 mm stucco siding and included a spunbonded polyolefin weather-resistive barrier (WRB) behind it. The structural sheathing was a 12.5 mm OSB and the stud cavity was filled with fiber-glass batt insulation. On the interior side of the cavity a vapor barrier, that met the NBCC 2015 9.25.4.2 (NRC 2015a) minimum requirement for vapour permeance of $60 \text{ ng}/(\text{m}^2 \cdot \text{s} \cdot \text{Pa})$, was placed and the assemblies included a 12.5 mm thick interior gypsum board. A 2-D hygrothermal sensitivity analysis compared the performance of the two assemblies constructed with 38.1 mm extruded polystyrene (XPS) insulation, whereas a 1-D analysis investigated the performance of ISF and SIF wall assemblies where the thickness of XPS insulation varied between 0 and 50 mm.

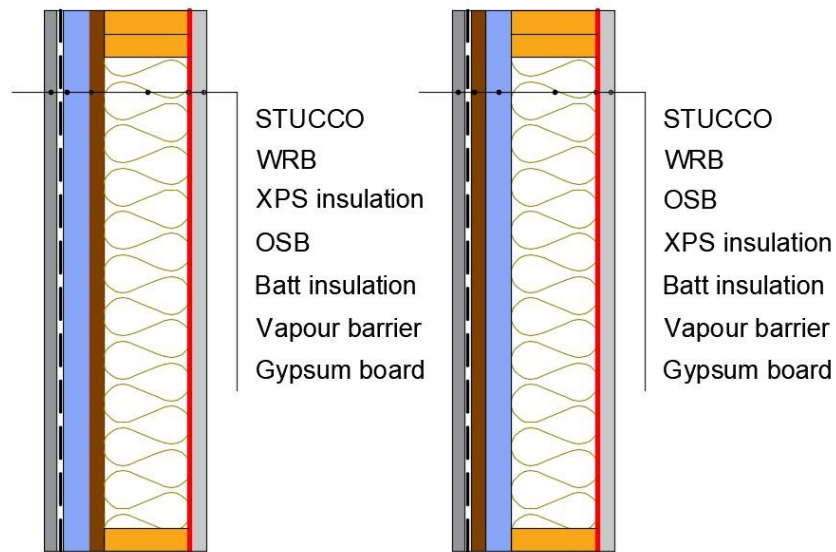


Figure 4.1: Wall Assemblies: ISF (left) and SIF (right)

4.3 Simulation Parameters

4.3.1 *Material Properties*

The hygrothermal properties of all materials used in simulations were derived from NRC hygrothermal property databases (Kumaran, et al 2002b and Kumaran 2002c) and from WUFI database (IBP 2018). The basic material properties assumed for the wall assemblies evaluated are summarized in Table 4.1, whereas the moisture storage functions and the moisture dependency on transport mechanisms for each material are presented in Appendix F.

Table 4.1: Basic Material Properties (Kumaran, et al 2002b and Kumaran 2002c)

Property	Units	STUCCO	XPS	OSB	Fiber Glass	Lumber (Spruce)	Gypsum Board
density	[kg/m ³]	1769	28.6	650	30	400	625
porosity	[m ³ /m ³]	0.27	0.99	0.95	0.99	0.9	0.706
heat capacity	[J/kg·K]	840	1470	1880	840	1880	870
saturation MC	[m ³ /m ³]	0.265	0.008	0.47	0.046	0.845	0.43
thermal conductivity	[W/m·K]	0.343	0.028	0.092	0.035	0.086	0.16
WV Permeability	[ng/m·s·Pa]	*	1.22	*	151	*	*

* Moisture dependant property – presented in Appendix F

4.3.2 *Locations and Weather*

The 2-D analysis investigated and compared the hygrothermal performance of walls constructed in Edmonton, whereas the 1-D simulations were performed for climate conditions of eight locations across Canada, covering climate zones 4 through 8, as shown in Table 4.2. Exterior boundary conditions included outdoor temperature and relative humidity, whereas solar radiation and the effect of rain were omitted. Wind speed and wind direction, on the other hand, were accounted for in determining the rate of air exfiltration. The analysis considered twenty years of hourly weather data, obtained from Environment Canada, for each location. The heating degree-days (HDD) for exterior temperature below 18°C were calculated for the heating season (October 1 to April 1) and the coldest winter was identified. The hygrothermal analysis considered two years: a year that preceded the coldest winter and the following year. After these two years the weather cycle repeated. Figure 4.2 shows the

exterior climate conditions for Edmonton for the years 1995 and 1996, as the winter between these two years was identified as the coldest.

Table 4.2: Locations and Climate Zones considered in 1-D analysis

Location	HDD	Climate Zone
Vancouver	2900	4
Toronto	3650	5
Ottawa	4600	6
St. John's	4800	6
Edmonton	5400	7A
Winnipeg	5900	7A
Fort McMurray	6550	7B
Yellowknife	8500	8

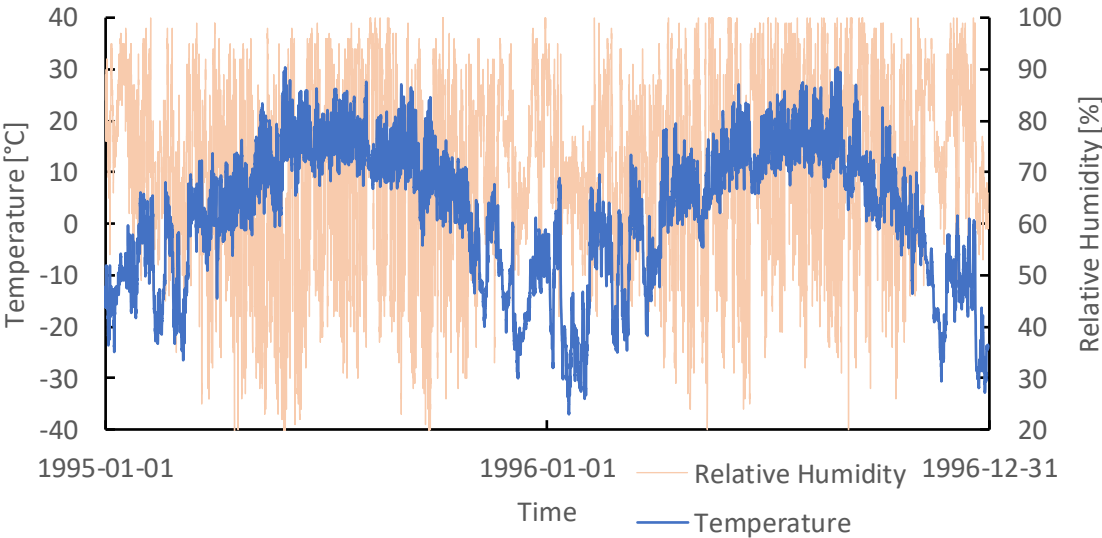


Figure 4.2: Hourly outdoor temperature and relative humidity for Edmonton climate

4.3.3 Indoor Conditions

The indoor temperature was derived based on ASHRAE 160-2016 Standard (ASHRAE 2016) and set at 21.1°C when the 24-hour average outdoor temperature was below 18.3°C, and 2.8°C above the 24-hour average outdoor temperature when the outdoor temperature was above 18.3°C. The indoor temperature had a maximum of 23.9°C.

Health Canada recommends that the indoor relative humidity level be kept between 30 and 55 percent during winter. Lower relative humidity could cause skin allergies and respiratory infections, whereas higher humidity levels increase the spread of viruses, mould and bacteria (Health Canada 2016). On the other hand, ASHRAE suggests a 30 to 60 percent indoor humidity as an acceptable range (ANSI/ASHRAE 1989).

In this study, the indoor relative humidity was calculated based on hourly exterior temperature and RH using a moisture balance Equation (4.1), proposed by Roppel et al (2007).

$$P_i = \frac{I}{I+\alpha} P_o + \frac{Q_{\text{source}} P_{\text{total}}}{0.622 \rho v (I+\alpha)} + \frac{\beta P_{\text{sat}}}{I+\alpha} \quad (4.1)$$

where:

P_i - indoor air vapour pressure, [Pa]

P_o - outdoor air vapour pressure, [Pa]

P_{sat} - saturation vapour pressure of indoor air, [Pa]

P_{total} - total atmosphere pressure, [Pa]

Q_{source} - moisture generation rate, [kg/h]

I - air exchange per hour (ACH)

ρ - density of air, 1.22 kg/m³

v – volume of space, [m^3]

α & β – moisture admittance factors (0.6 & 0.4), [h^{-1}]

The analysis considered a small apartment of 80 m^2 (195 m^3) with an average moisture load of 7 L/day , a value suggested by ASHRAE 160-2016 for a 1-bedroom apartment. The rate of ventilation (ACH) varied such that the Equation (4.1) yielded the winter average relative humidity values of 35, 45 and 55 percent, respectively, for each location. Figure 4.3 illustrates indoor conditions for Edmonton climate when the average indoor relative humidity during winter was 35%.

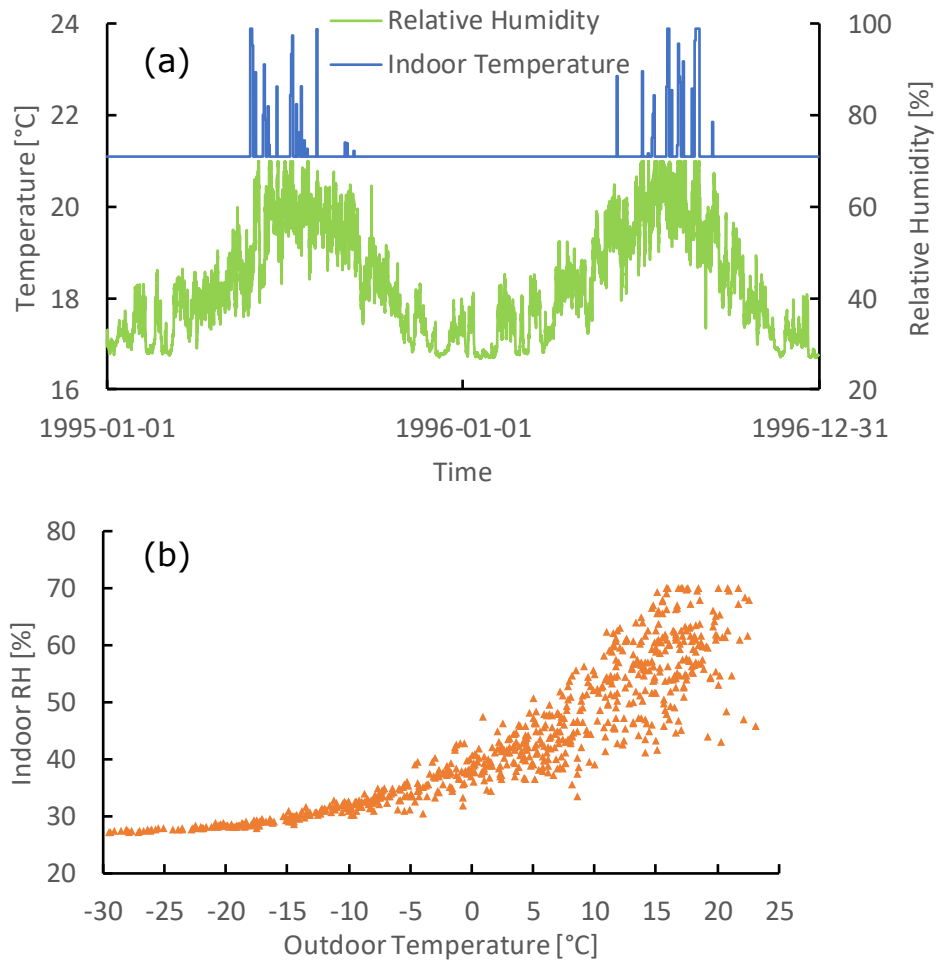


Figure 4.3: Indoor conditions for Edmonton climate: (a) Hourly temperature and relative humidity; (b) Indoor RH dependence on the outdoor temperature

4.3.4 Air Exfiltration

The hygrothermal analysis considered the effect of air exfiltration into the wall assemblies through cracks and holes, as this moisture transport mechanism had been found to be the dominating one and can carry significantly larger volumes of water vapour compared to vapour diffusion (ASHRAE 2009). The air pressure difference across the wall is the driving force for air flow and depends on buoyancy (stack effect), wind direction and velocity, and the pressure differences due to mechanical ventilation systems. This study, however, neglected the influence of the mechanical ventilation on the air pressure difference ($\Delta P_{\text{vent}} = 0$). The amount of air leaking into the wall assembly was calculated as:

$$Q = \alpha \times \Delta P_{\text{tot}}^n \quad (4.2)$$

where:

Q – air flow rate, [$\text{m}^3/(\text{m}^2 \cdot \text{s})$]

α – coefficient determined to satisfy the condition at which the air leakage rate was $0.10 \text{ L}/(\text{m}^2 \cdot \text{s})$ at $\Delta P_{\text{tot}}=75 \text{ Pa}$, while the exponent $n=0.7$ (Saber et al, 2014)

$$\Delta P_{\text{tot}} = \Delta P_{\text{wind}} + \Delta P_{\text{stack}} + \Delta P_{\text{vent}} \quad (4.3)$$

Stack effect

The study considered an apartment located at the third story of a three-storey building and the stack effect was calculated for the top of that storey, since this location is subjected to the highest exfiltration rate. Figure 4.4 shows the air pressure differential due to stack effect for Edmonton climate. The stack effect was calculated using the following equation:

$$\Delta P_{\text{stack}} = \rho \times \left(\frac{T_o - T_i}{T_i} \right) \times g \times \frac{H}{2} \quad (4.4)$$

where:

ρ – density of air, 1.22 kg/m³

T_o – outdoor temperature, [°C]

T_i – indoor temperature, [°C]

g – gravitational acceleration, [m/s²]

$H = 7.5$ m – building height

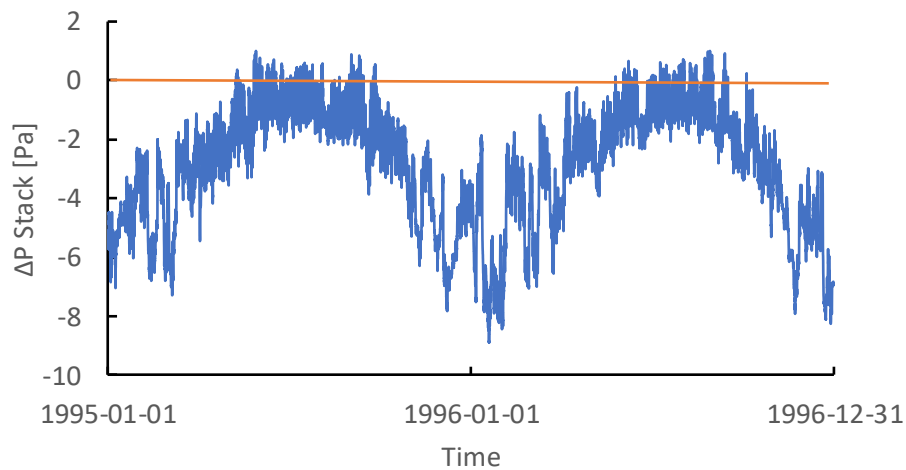


Figure 4.4: Stack pressure at the top of three-storey building located in Edmonton

Wind effect

The air pressure differential caused by wind was calculated according to Equation (4.5). For each location, an hourly wind data (wind speed and direction) was analyzed and the air pressure was calculated for each wall orientation using surface pressure coefficient of wind proposed Saber (Saber et al, 2014). The orientation of the wall with the highest yearly average negative wind pressure (pressure causing air exfiltration) was selected for the analysis. Figure 4.5 shows the wind pressure analysis for Edmonton climate and it can be seen that the wall

facing south southwest had the highest yearly average negative air pressure and therefore the air exfiltration rate. The corresponding hourly wind pressure of that wall is shown in Figure 4.6.

$$\Delta P_{\text{wind}} = \frac{1}{2} \times C_{\text{wp}} \times \rho \times v^2 \tag{4.5}$$

where:

C_{wp} – surface pressure coefficient of wind calculated using Saber’s correlation (Saber et al, 2014)

ρ – density of air, 1.22 kg/m³

v – wind velocity, [m/s]

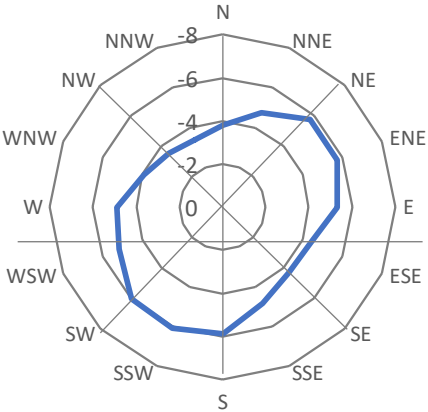


Figure 4.5: Wind pressure: Average yearly negative wind pressure [Pa] for Edmonton climate

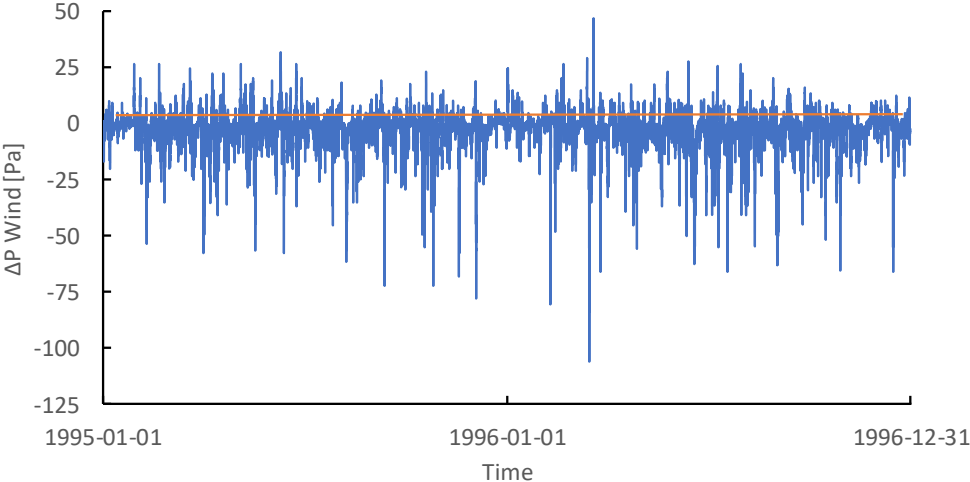


Figure 4.6: Hourly wind pressure of wall facing south southwest (Edmonton climate)

4.4 Moisture Accumulation and Thermal Performance of Wood-Frame Walls with Exterior Insulation

4.4.1 Modeling Approach

To investigate and compare the hygrothermal performance of the two wall assemblies where a low-permeance insulation is placed either outboard or inboard to the structural sheathing, a two-dimensional computer program DELPHIN (version 6.0.2) was selected. DELPHIN is a time variant, two-dimensional, heat-air-moisture (HAM) computer simulation program, developed and maintained at the Technical University of Dresden (TUD). The program can simulate the combined effects of heat, air and moisture flows. Heat flow mechanism is considered through conduction, convection, radiation and phase change, whereas the moisture flow is simulated through convection, vapour diffusion, capillary suction and adsorption, and includes moisture movement through common construction materials including air.

Air flow through the wall assembly was modeled as laminar flow. The modeling assumed that the air flow path extended from an opening in the interior above the bottom plate, through the stud cavity, and exited through an opening in the exterior at the top of the wall, as shown in Figure 4.7. This air leakage path was one of the worst-case scenarios for moisture accumulation in the study by Ojanen and Kumaran (1996) and was also used in the study by Chown and Mukhopadhyaya (2005). The air pressure difference across the wall was calculated for each hour of the weather data, using Equation (4.3), and provided as a boundary condition in the modeling software.

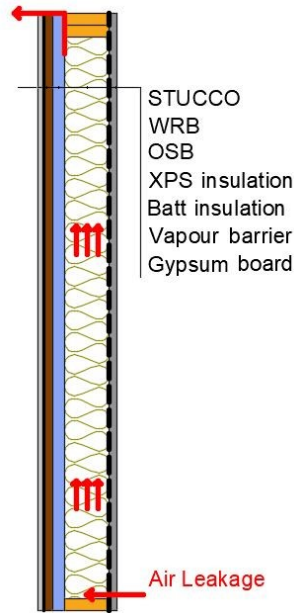


Figure 4.7: Air Leakage Path considered in 2-D hygrothermal analysis

The effect of the position of exterior low-permeance XPS insulation was investigated for Edmonton climate and the thickness of the insulation was 38.1 mm. This insulation thickness was selected to meet the 2015 NBCC 9.25.5.2. (NRC 2015a) requirement for the minimum ratio of outboard to inboard thermal resistance of 0.30 for Edmonton climate, as shown in Table 2.8. The determination of this ration is shown in 4.4.3. The winter average interior relative humidity was 35% as shown in

Figure 4.3 and the rate of air exfiltration was $0.10 \text{ L}/(\text{m}^2 \cdot \text{s})$ at 75 Pa. This air exfiltration rate was selected to meet the NBCC Part 9 maximum allowable air leakage rate when the indoor humidity level does not exceed 35%.

The analysis considered a $38 \text{ mm} \times 140 \text{ mm}$ ($2 \times 6 \text{ in.}$) stud wall and compared the moisture accumulation and the thermal performance of three selected wall assemblies:

1. Wall without exterior insulation – base case wall (BC)

2. Wall with XPS insulation placed outboard to the sheathing (ISF)
3. Wall with XPS insulation placed between the sheathing and framing (SIF)

The simulation was started on July 1 and run for two years using 1-h time step. The initial temperature in each component was set to 20°C, whereas the initial RH was 80%.

4.4.2 Influence of exterior insulation on the moisture accumulation

Figure 4.8 illustrates the distribution of the relative humidity during winter in BC, SIF and ISF assemblies, respectively. It can be seen that the wall assembly where the low-permeance insulation is inserted between the sheathing and framing (SIF) has markedly higher humidity levels at the XPS-Batt interface, whereas in the ISF wall assembly the relative humidity of the OSB sheathing is higher. Additionally, it can be concluded that the location with highest relative humidity is the bottom corner of sheathing-to-framing interface. Therefore, the analysis investigated and compared the moisture contents of the bottom wood plate, bottom portion (15 cm high) of the OSB sheathing, as well as the moisture accumulation in batt insulation.

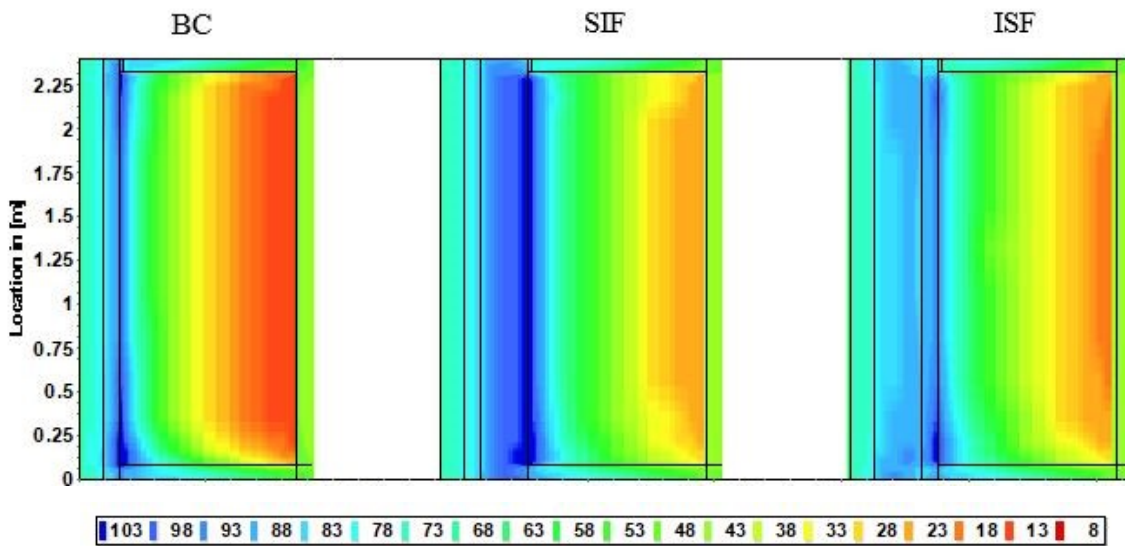


Figure 4.8: Relative humidity distribution during winter (Edmonton)

Adding a layer of exterior insulation significantly reduces the moisture accumulation in the bottom plate, as it can be seen in Figure 4.9. The moisture content (MC) of the bottom plate does not show any dependency on the position of the exterior insulation when excessive moisture accumulation is prevented (0.3 ratio of outboard-to inboard thermal resistance for Edmonton climate) and the MC exhibit a similar change in both ISF and SIF assemblies.

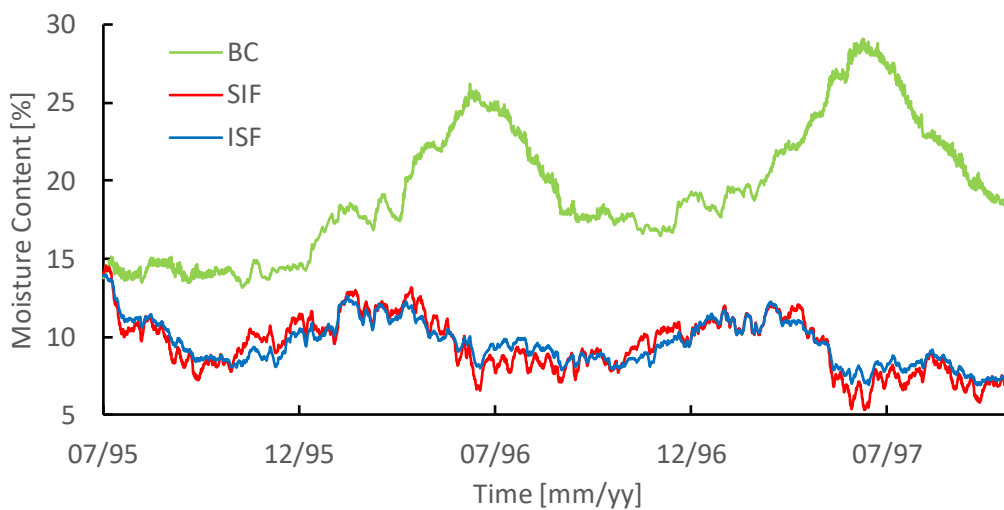


Figure 4.9: Bottom Wood Plate Moisture Content at Sheathing-Batt Interface

Comparing the moisture content of the OSB sheathing, presented in Figure 4.10, it can be seen that the OSB in the ISF assembly accumulates considerably higher amounts of moisture when compared to the SIF assembly. Moisture content of the bottom portion of the OSB in the ISF assembly reaches 30% during winter. However, this moisture dries out during Summer. In addition, the average moisture content of the whole OSB sheathing in the ISF assembly varies between 13 and 18 percent. On the other hand, the OSB moisture content in the SIF assembly remains below 10% throughout the year as there is no insulation to prevent drying.

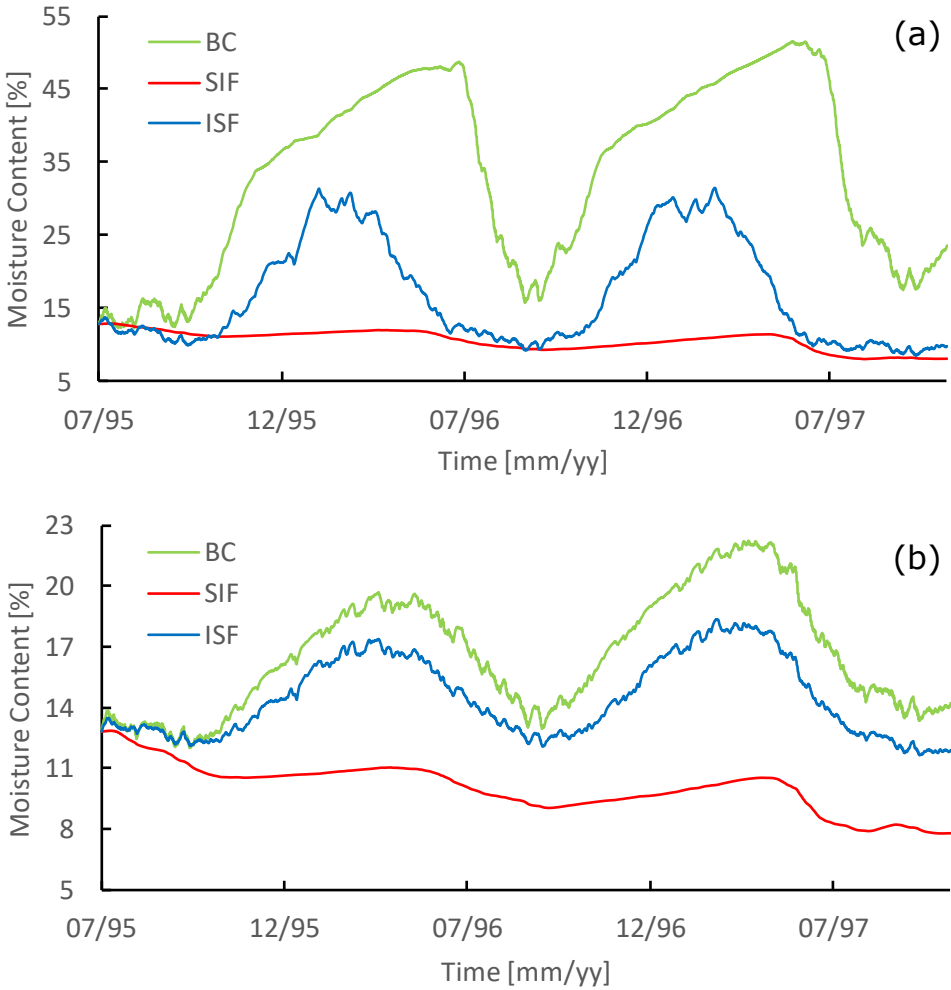


Figure 4.10: OSB Moisture Content: (a) Bottom 15 cm, (b) Average MC for the whole OSB layer

Comparing the amount of moisture accumulated in the stud cavity, as presented in Figure 4.11, it can be seen that in the SIF assembly most of the moisture is accumulated in batt insulation. Moisture accumulated within the cavity during winter dries completely during Summer in all three assemblies.

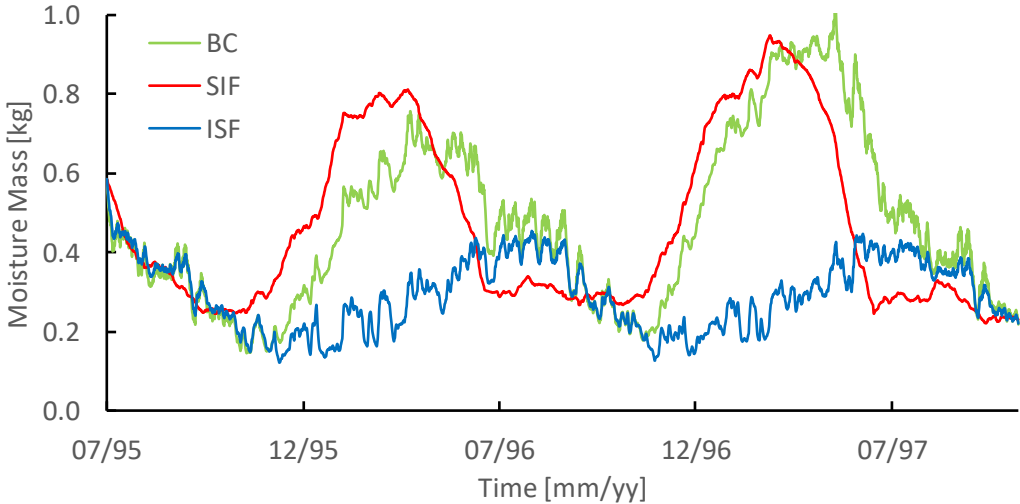


Figure 4.11: Moisture Content of the Batt Insulation

Summarizing the results from Figures 4.9 to 4.11, it can be concluded that most of the moisture accumulated within the wall, due to air convection and vapour diffusion, is absorbed by the OSB sheathing in the ISF assembly, whereas in the SIF assembly that moisture is absorbed by the batt insulation. When enough insulation is placed exterior to the cavity, the moisture accumulated during winter dries completely during summer in both ISF and SIF assemblies.

4.4.3 Influence of exterior insulation on the thermal performance

The National Energy Code for Buildings (NRC 2015b) prescribes requirements on the minimum effective thermal resistance (R-Value) of above grade wall assemblies, accounting for the thermal bridging effect between the framing elements and the cavity insulation. According to this standard, the minimum required effective R-Value for the exterior wall constructed in Edmonton is 27. Wall assemblies considered in this analysis, ISF and SIF, constructed with 38.1 mm of XPS meet this requirement and both assemblies have the effective R-Value of 27.5. Table 4.3 shows effective R-Value and outboard-to-inboard¹ insulation ratio for ISF and SIF assembly constructed with 38.1 mm.

Table 4.3: Effective R-Value and Outboard to Inboard Insulation Ratio

		Wall Assembly Component	R-Value
		1. Exterior air film	0.17
		2. STUCCO (19 mm)	0.31
		3. WRB	0
		4. XPS (38.1 mm)	7.5
		5. OSB (12.5 mm)	0.77
		6. Fiber Glass (2×6 framing filled with R22.7 at 24” o.c.)	17.6
		7. Vapour Barrier	0
		8. Gypsum Board (12.5 mm)	0.44
		9. Interior air film	0.68
	Effective R-Value	27.5	
	Nominal R-Value	32.6	
Outboard to Inboard Ratio	SIF assembly	0.37	
	ISF assembly	0.32	

¹ According to the 2015 NBCC, when a low air- and vapour-permeance (equal to or less than 60 ng/m²·s·Pa water vapour permeance) material is located within the assembly, innermost surface of that material divides outboard and inboard insulation.

To investigate if the position of the exterior insulation has an impact on the thermal performance, the analysis examined the heat flux through the interior surface. Figure 4.12 graphically presents mean heat conduction values through the interior surface of the selected wall assemblies. In addition, Table 4.4 shows the winter average (October 1 to April 1) heat flux values of the BC, ISF and SIF walls, respectively. It can be seen that the heat conduction value of the SIF wall is approximately 1% higher compared to the ISF wall. The reason for this difference is due to higher moisture content of the batt insulation in the SIF assembly, as shown in Figure 4.11, and the thermal conductivity of fiber glass insulation increases as the moisture content increases, as shown in Appendix F.

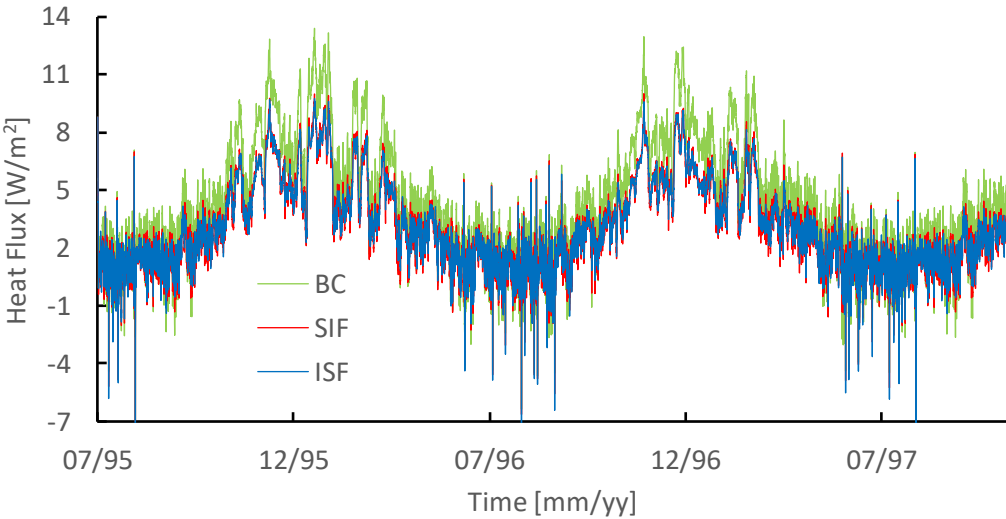


Figure 4.12: Heat Flux through the Interior Surface

Table 4.4: Winter Average Heat Flux through the Interior Surface

Wall Assembly	Heat Flux [W/m^2] (winter average)	Standard deviation
BC	7.11	2.54
ISF	5.18	1.85
SIF	5.23	1.92

4.5 The Effect of Air Leakage Rate and Indoor Relative Humidity on the Hygrothermal Performance

The hygrothermal behavior of any building component is determined by the complex interaction of heat, air, and moisture processes. Factors that have the highest influence on the wall hygrothermal performance are the air leakage rate, indoor relative humidity, exterior weather conditions and the material properties (Ojanen and Kumaran, 1996). To investigate the influence of air exfiltration rate and indoor relative humidity on moisture accumulation of ISF and SIF wall assemblies, a one-dimensional analysis was performed for eight locations in Canada, listed in Table 4.2. For each location, the analysis considered three air leakage rates (0.02; 0.05 and 0.10 L/m²·s at 75 Pa air pressure difference) and three indoor winter average relative humidity levels (35, 45 and 55%). The results from the parametric study were analysed for excessive moisture accumulation and the amount of exterior insulation that would prevent the mould growth is suggested. Computer modeling software used for this analysis was Wärme und Feuchte instationär (WUFI® Pro 6.2, Transient Heat and Moisture) developed by the Fraunhofer Institute for Building Physics (IBP 2018).

4.5.1 Modeling Approach and Input Parameters

Wall assemblies, ISF and SIF, were simulated as having been constructed with wood framing, either 38 by 89 mm (nominal 2×4 in.) or 38 by 140 mm (nominal 2×6 in.). Wood framing, however, was not modeled as the simulation was one-dimensional and included a section through the insulated cavity rather than the framing. Identification codes for the different wall constructions are presented in Table 4.5.

Table 4.5: Wall Assembly Codes

Exterior Insulation	Wall Code	
	ISF assembly	SIF assembly
0 mm	ISF-0	SIF-0 ⁽¹⁾
12.7 mm	ISF-12.7	SIF-12.7
25.4 mm	ISF-25.4	SIF-25.4
38.1 mm	ISF-38.1	SIF-38.1
50.8 mm	ISF-50.8	SIF-50.8

⁽¹⁾ OSB sheathing in this assembly was modeled without the moisture storage function so that the moisture would accumulate within the batt insulation making this the base case wall for the SIF assembly

Three different air leakage rates were simulated for each location. The lower limit was chosen to comply with the NBCC Part 5 allowable maximum air leakage rate of 0.02 L/(m²·s), whereas the upper air leakage limit was set at 0.1 L/(m²·s), the NBCC Part 9 allowable maximum. Additionally, the air leakage rate of 0.05 L/(m²·s) was chosen as an intermediate value. All air leakage rates were assumed to have been measured at an air pressure difference of 75 Pa.

WUFI[®] Pro 6.2 models the deposition of water vapour carried by exfiltrating air by introducing a moisture source at the location where it is most likely for this moisture to accumulate (i.e. OSB sheathing in ISF configuration and at the XPS-Fiberglass interface in SIF configuration), neglecting the thermal effects of exfiltrating air and water vapour phase change. The air leakage rate was calculated using hourly weather data for each geographic location and a transient moisture source was introduced in WUFI by the following equation:

$$m = Q \times (c_i - c_{sat,T}) \quad (4.6)$$

where:

m – moisture source, [$\text{kg}/(\text{m}^2 \cdot \text{s})$]

c_i – indoor water vapour concentration, [kg/m^3]

$c_{\text{sat},T}$ – water vapour concentration at saturation at the deposition site, [kg/m^3]

Figure 4.13 illustrates an example of the transient moisture source, calculated by using Equation (4.6), that was provided in WUFI for the SIF-38.1 wall for Edmonton climate, 35% indoor relative humidity and $0.1 \text{ L}/(\text{m}^2 \cdot \text{s})$ air leakage rate.

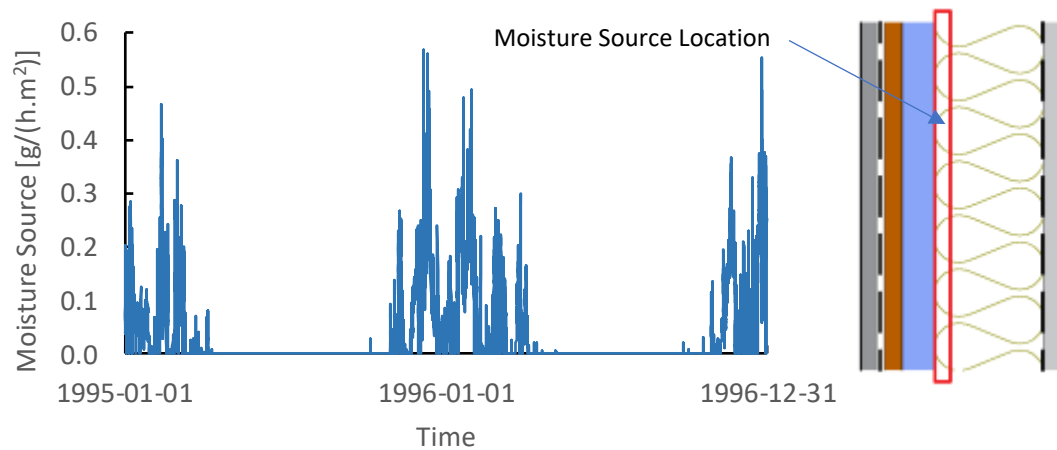


Figure 4.13: Transient Moisture Source (SIF-38.1; 35% indoor RH; Air Leakage rate $0.1 \text{ L}/(\text{s} \cdot \text{m}^2)$ at 75 Pa)

4.5.2 Performance Criteria

The analysis investigated the total moisture content per unit area of a wall, as well as the moisture content changes of the OSB sheathing in the ISF and of the batt insulation in the SIF assembly.

The analysis also investigated a mould growth potential of the OSB sheathing in the ISF assembly and at the XPS-Batt interface in the SIF assembly, since these locations were found to be at highest risk for mould growth, as shown in 4.4.2. The mould model developed by Ojanen et al (2010) was used in determining the mould index (MI) of different materials and

assessing the mould growth potential. The descriptions of the mould index levels are provided in Table 4.6. This model classifies materials into four sensitivity classes, namely, very sensitive, sensitive, medium resistant and resistant, as shown in Table 4.7. Each material was assigned a sensitivity category, or more specifically, the sensitivity class of OSB layer was “sensitive” whereas the sensitivity class of fiber glass and XPS insulation was set as “medium resistant”.

Table 4.6: Mould Index (MI) Description (Ojanen et al, 2010)

Mould Index (MI)	Description of Growth Rate
1	No growth
2	Small amounts of mould on surface (microscope), initial stages of local growth
3	Visual findings of mould on surface, < 10% coverage, or < 50% coverage of mould (microscope)
4	Visual findings of mould on surface, 10%–50% coverage, or > 50% coverage of mould (microscope)
5	Plenty of growth on surface, > 50% coverage (visual)
6	Heavy and tight growth, coverage about 100%

Table 4.7: Material sensitivity classes (Ojanen et al, 2010)

Sensitivity Class	Materials	RH _{min} [%] ⁽¹⁾
Very Sensitive	Pine sapwood	80
Sensitive	Glued wooden boards, PUR with paper surface, spruce	80
Medium Resistant	Concrete, aerated and cellular concrete, glass wool, polyester wool	85
Resistant	PUR with polished surface	85

⁽¹⁾ Minimum relative humidity needed for mould growth

The analysis investigated the required thickness of exterior insulation that would be necessary to prevent the mould growth in wall assemblies. The results of the analysis are presented using a similar approach to the NBCC 9.25.5.2. (NRC 2015a) requirement for the position of low air- and vapour- permeance sheathing, in terms of the minimum required thermal resistance ratio of materials placed outboard of the innermost impermeable surface and materials placed inboard of that surface.

All simulations started on January 1 and were run for a period of four years using 1-h time step. The initial temperature in each component was set to 0°C and each material composing the wall was assigned a typical built-in moisture content from the WUFI database, except for OSB sheathing which initial moisture content was set at 17%.

4.5.3 Results and Discussion

Figures 4.14 to 4.18 graphically present the simulation results for Edmonton climate. The indoor average winter relative humidity was set at 35% and the air leakage rate was 0.1 L/(s·m²) at 75 Pa. These simulation parameters were chosen to match the parameters used in the 2-D analysis.

Figure 4.14 shows the average moisture content values of the whole OSB layer in the ISF assembly. The values obtained from 1-D and 2-D analysis for the ISF-38.1 wall match closely and the OSB average moisture content varies between 13 and 18 percent. It can be seen that the thickness of the exterior insulation has a significant effect on OSB moisture content and its drying potential. Putting insufficient amount of low-permeance insulation exterior to the sheathing could trap the moisture and the OSB moisture content increases over time (i.e. ISF-

12.7). Figure 4.15 presents the changes of the mould index in the ISF assembly. It can be seen that 38.1 mm thick XPS insulation would be required to keep the MI below 3 (visual findings of mould on surface), whereas a thinner XPS layer would cause the MI to increase over time and lead to mould problems.

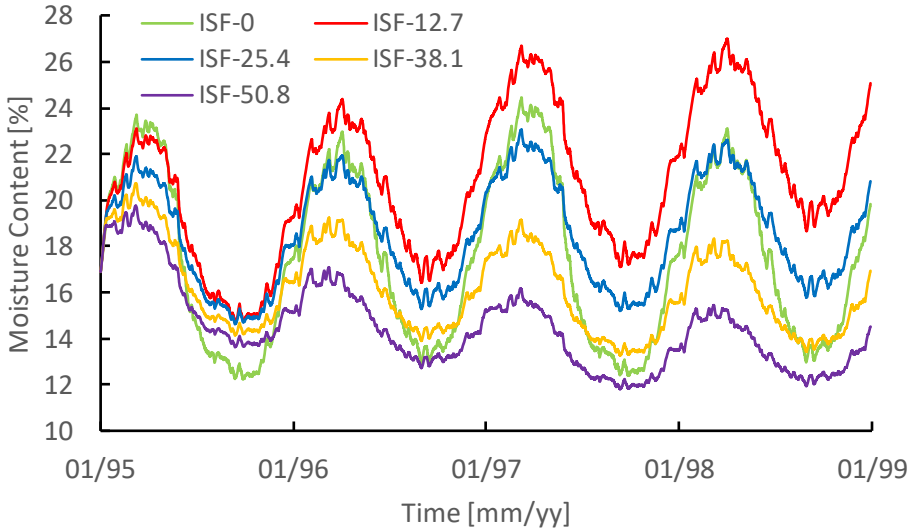


Figure 4.14: OSB Moisture Content (ISF assembly)

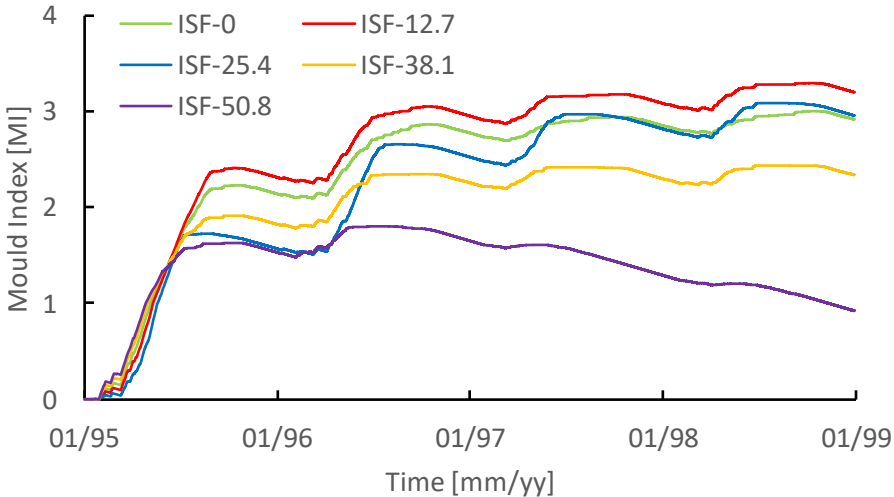


Figure 4.15: OSB Mould Index (ISF assembly)

In the SIF wall assembly, the amount of moisture accumulated within the cavity during winter dries out during summer for any thickness of XPS insulation, as shown in Figure 4.16. However, from Figure 4.17 it can be seen that if the thickness of XPS insulation is lower than 38.1 mm, the mould index keeps increasing from year to year and the moisture accumulated within the cavity could stimulate mould growth at XPS-Batt interface. Therefore, both assemblies for a given climate require a minimum of 38.1 mm of exterior insulation.

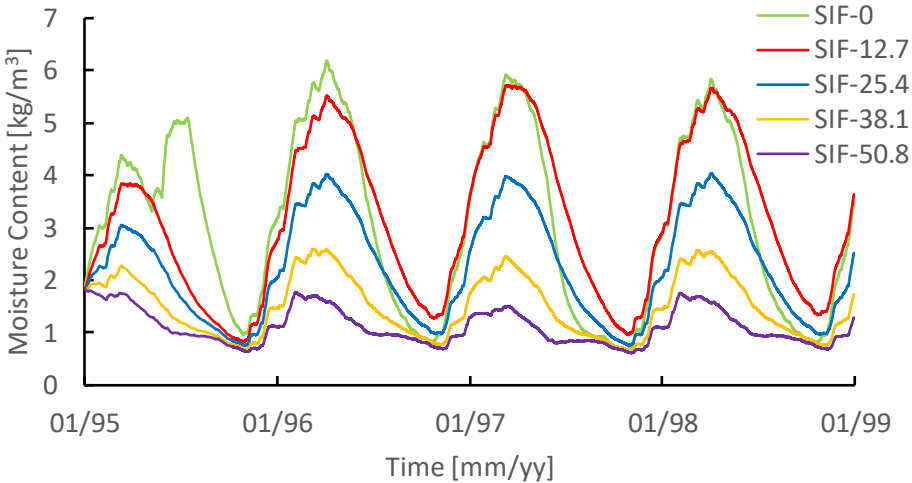


Figure 4.16: Cavity Insulation Moisture Content (SIF assembly)

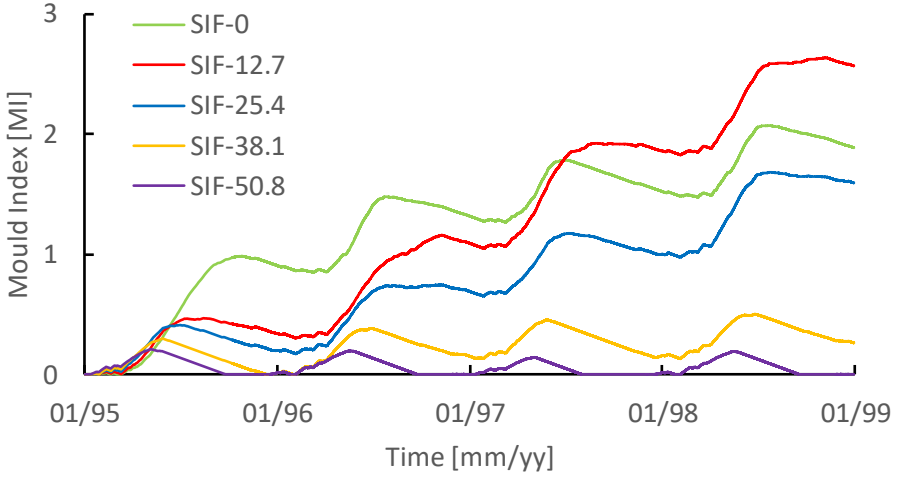


Figure 4.17: Mould Index at XPS-Batt Interface (SIF assembly)

Figure 4.18 compares the total amount of moisture deposited in all wall layers per square meter of a wall. It can be seen that, when the performance requirement (no mould growth) is met, and there is enough exterior insulation to prevent excessive moisture accumulation, both ISF and SIF assemblies exhibit the same wetting and drying potentials. The difference between two curves on the graph is because the OSB sheathing in the SIF assembly dries faster to the exterior and has moisture contents much lower than the initial 17%.

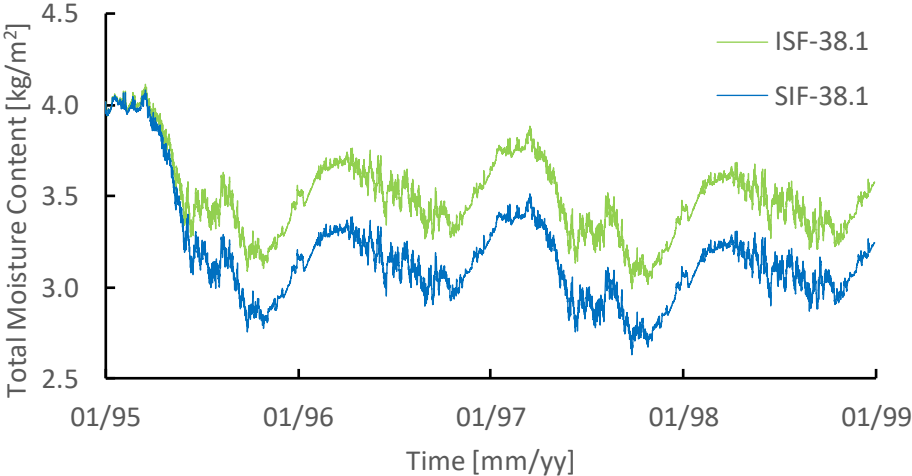


Figure 4.18: Total Moisture Content per square meter of a wall

The analysis investigated the hygrothermal performance of SIF and ISF wall assemblies constructed with standard 38 mm × 89 mm (2 × 4 in.) and 38 mm × 140 mm (2 × 6 in.) framing members and exterior XPS insulation which thickness varied from 0 mm to 50.8 mm. For each considered wall assembly, the outboard-to-inboard thermal resistance ratio was calculated in accordance with the 2015 NBCC (NRC 2015a), following the principal shown in Table 4.3, and the values of this ratio for each considered wall are shown in Table 4.8. It can be seen that inserting insulation between the sheathing and framing (SIF), instead of placing that same insulation outboard to the sheathing (ISF), could increase this ratio by

approximately 0.07 and 0.04 for 38 mm × 89 mm and 38 mm × 140 mm stud cavity walls, respectively.

Table 4.8: Ratio of Outboard to Inboard Thermal Resistance

Insulation thickness	2 × 4 Framing		2 × 6 Framing	
	ISF	SIF	ISF	SIF
12.7 mm	0.18	0.24	0.12	0.16
25.4 mm	0.34	0.40	0.22	0.26
38.1 mm	0.49	0.56	0.32	0.37
50.8 mm	0.64	0.72	0.43	0.47

The hygrothermal analysis investigated the minimum required thickness of exterior insulation necessary to prevent the mould growth and excessive moisture accumulation within the wall. The results are presented in terms of minimum outboard-to-inboard thermal resistance ratio and are summarized Table 4.9 for each considered location, indoor RH and air leakage rate. Additionally, for each scenario (building location, indoor RH and air leakage rate), the specified ratio can be applied to both ISF and SIF wall assemblies as it was found that these two assemblies exhibit the same wetting and drying potentials and require the same outboard-to-inboard thermal resistance ratio to prevent excessive moisture accumulation. The values of the outboard-to-inboard ratio from Table 4.8 are meant to serve as a guide in selecting an appropriate wall assembly for different conditions shown in Table 4.9. Empty cells (-) in this table (Table 4.9) indicate that even the highest considered ratio of 0.72 was not sufficient to prevent the possibility of mould growth. It can be seen that the indoor RH and air leakage rate have a significant effect to the selection of required ratio and that as the indoor RH and air leakage rate increase the outboard-to-inboard ratio increases as well.

Interior relative humidity of 55% has proven to be the critical for the hygrothermal performance and wall assemblies considered in this study require high levels of exterior insulation to prevent the mould growth.

Table 4.9: Minimum Required Outboard to Inboard Ratio of Thermal Resistance

Location	Interior RH 35%			Interior RH 45%			Interior RH 55%		
	Air Leakage [L/m ² ·s at 75 Pa]			Air Leakage [L/m ² ·s at 75 Pa]			Air Leakage [L/m ² ·s at 75 Pa]		
	0.02	0.05	0.10	0.02	0.05	0.10	0.02	0.05	0.10
Vancouver	0	0	0	0	0	0	0	0.22	0.32
Toronto	0	0	0	0	0.22	0.40	0.49	0.64	-
Ottawa	0	0	0.22	0.37	0.43	0.49	0.64	-	-
St. John's	0	0	0.22	0.37	0.43	0.49	0.64	-	-
Edmonton	0	0.22	0.32	0.43	0.49	0.64	-	-	-
Winnipeg	0.12	0.32	0.43	0.49	0.64	-	-	-	-
Fort McMurray	0.18	0.32	0.43	0.49	0.64	-	-	-	-
Yellowknife	0.40	0.49	0.64	-	-	-	-	-	-

Figure 4.19 illustrates the effect of the air leakage on the OSB moisture content of the ISF wall, whereas, Figure 4.20 shows the OSB moisture content dependency on the indoor relative humidity. The results show that both the air leakage rate and the indoor relative humidity have a significant influence on the moisture performance of the wall and should be considered as key factors in building envelope design.

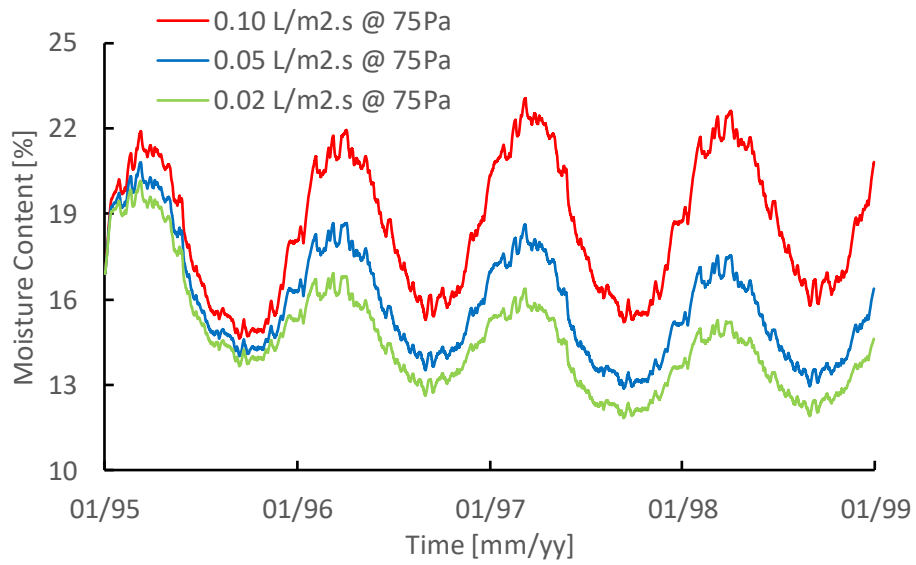


Figure 4.19: OSB Moisture Content of ISF-38.1 wall (Edmonton; indoor RH 45%)

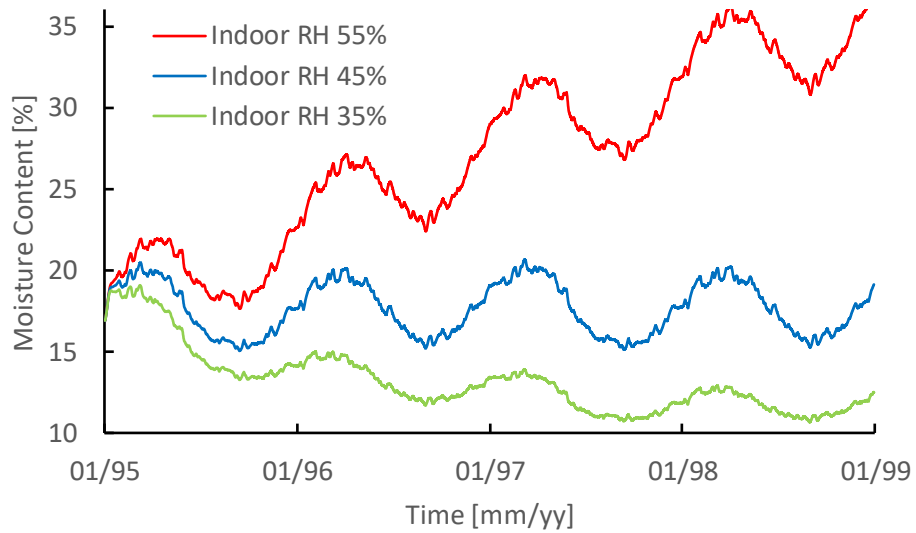


Figure 4.20: OSB Moisture Content of ISF-50.8 wall (Edmonton; air leakage 0.02 L/(m²·s) at 75Pa)

4.6 Summary

A sensitivity analysis was performed to investigate the hygrothermal performance of wood-frame walls with low-permeance exterior insulation. As the low-permeance insulation, the analysis considered extruded polystyrene (XPS) insulation placed either outboard (ISF assembly) or inboard (SIF assembly) to the structural sheathing. The hygrothermal analysis included one- and two-dimensional hygrothermal modeling and was conducted for eight locations in Canada, three different air leakage rates and three indoor relative humidity levels.

The analysis showed that a location at the highest risk for moisture accumulation within the wall is the bottom corner of sheathing-to-framing interface. Also, when excessive moisture accumulation within the wall was prevented, the moisture content of the bottom wood plate was the same in both ISF and SIF wall assemblies and these assemblies exhibited the same wetting and drying potentials.

Both 1-D and 2-D analysis showed that most of the moisture accumulated within the wall, due to air convection and vapour diffusion, was absorbed by the OSB sheathing in the ISF assembly, whereas in the SIF assembly that moisture was absorbed by the batt insulation. Additionally, the analysis showed that the heat flux values of the SIF walls were slightly higher compared to that of the ISF walls due to higher moisture contents of the batt insulation in the SIF assembly.

The analysis suggested the minimum required thickness of exterior insulation necessary to prevent the mould growth and excessive moisture accumulation within the wall assemblies. The results were presented in terms of the minimum outboard-to-inboard thermal resistance ratio for each considered location, indoor RH and air leakage rate. Since both ISF and SIF

wall assemblies showed the same wetting and drying potentials when constructed with the same ratio of outboard to inboard thermal resistance, the specified ratio can be applied to both wall assemblies. However, putting exterior insulation between the sheathing and framing (SIF), instead of placing that same insulation outboard to the sheathing (ISF), increased the outboard-to-inboard ratio by approximately 0.07 and 0.04 for 38 mm × 89 mm (2 × 4 in.) and 38 mm × 140 mm (2 × 6 in.) stud cavity walls, respectively. Consequently, the SIF wall assemblies could, in some cases, meet the minimum requirement for the outboard-to-inboard thermal resistance ratio using a thinner exterior insulation when compared to the ISF wall assemblies.

5 CONCLUSIONS AND RECOMMENDATIONS

5.1 Summary

This study investigated and compared the structural and hygrothermal performance of light wood-frame walls with insulated sheathing. The structural performance was investigated through experimental testing of nail joints and full-scale shear walls considering different nail sizes and thicknesses of exterior insulation. The analysis evaluated the effect of exterior insulation placed between the sheathing and framing on the lateral resistance of a wall, and the purpose of this work was to evaluate if the same mechanics-based design procedure addressed in the 2014 edition of CSA O86 (CSA 2014) can be applied to the shear walls built with insulated sheathing. The hygrothermal analysis included one- and two-dimensional computer modeling investigating the effect of low-permeance insulation, placed either outboard or inboard to the structural sheathing, on the moisture accumulation. The modeling was performed for eight locations in Canada different simulation parameters such as indoor relative humidity, air exfiltration rate and the thickness of exterior insulation.

This chapter discusses the conclusions derived from this study and recommends the areas for further research.

5.2 Conclusions

The conclusions from this study are as follows:

Nail joints and shear walls with intermediate insulation

1. Based on the results from nail joint and shear wall tests it was found that there was a significant drop in lateral capacity and stiffness as the intermediate insulation thickness increased. Additionally, both nail joints and shear walls constructed with larger diameter nails had larger lateral resistance.
2. Specimens fabricated with common wire 10d (3.66 mm by 76 mm) and 16d (4.06 mm by 89mm) nails experienced similar drop in lateral capacity as the insulation thickness increased. That drop was roughly from 100% to 78%, 54%, 38%, and 25%, when the insulation thickness increased from 0mm to 12.7 mm, 25.4 mm, 38.1 mm, and 50.8mm, respectively.
3. Doubling the number of nails or reducing the nail spacing to half led to a two-fold increase in shear strength of the shear wall.
4. It was noticed that the failure mode of both nail joints and shear walls was largely due to the bending of nails. However, nail pullout failure mechanism was observed when specimens were constructed with 16d nails and included 50.8 mm thick intermediate insulation. Based on this observation it is recommended that a minimum nail penetration into lumber be higher than five times the nail diameter as required by the CSA O86 (CSA 2014) for wood-member connections.

5. Nail joint and shear wall specimens constructed with power-driven nails did not experience a failure before the tests were stopped when the stroke of the displacement sensor was reached.
6. Comparing the shear wall lateral capacity values obtained from the full-scale tests and the lateral capacity values derived based on the nail joint tests, it was concluded that the lateral resistance of a shear wall with intermediate insulation can be accurately predicted based on the nail joint properties.

Hygrothermal performance of wood-frame walls with exterior insulation

1. The analysis results showed that the location at the highest risk of moisture accumulation and mould growth within a wall was the bottom portion of sheathing-to-framing interface.
2. The moisture accumulated within the wall due to air convection and vapour diffusion was absorbed by the OSB sheathing in the assembly where exterior insulation was placed outboard to the sheathing (ISF). On the other hand, in the assembly where the insulation was inserted between the sheathing and framing (SIF), the moisture was absorbed by the batt insulation.
3. Higher moisture content of the batt insulation in the SIF assembly slightly affected the thermal conductivity of the wall, and this assembly had slightly higher heat flux values compared to the ISF assembly constructed with same insulation thickness.
4. The study showed that the hygrothermal performance of the wall highly depends on the level of indoor relative humidity and air exfiltration rate. The minimum ratio of outboard-to-inboard thermal resistance necessary to prevent the mould growth and

excessive moisture accumulation was recommended for eight locations in Canada, three indoor humidity levels and three air leakage rates. Two wall assemblies, where an exterior insulation was placed either outboard or inboard to the structural sheathing, that have the same ratio of outboard-to-inboard thermal resistance showed the same wetting and drying potentials. Therefore, the same outboard-to-inboard thermal resistance ratio can be applied to both wall assemblies to prevent the mould growth and excessive moisture accumulation within the wall. It was shown that putting insulation between the sheathing and framing (SIF), instead of outboard to the sheathing (ISF), could increase this ratio by approximately 0.07 and 0.04 for 38 mm × 89 mm and 38 mm × 140 mm wood frame walls, respectively. Consequently, the SIF wall assemblies could potentially meet the proposed minimum requirement for the outboard-to-inboard thermal resistance ratio using a thinner exterior insulation when compared to the ISF wall assemblies.

Structural and hygrothermal performance of wood-frame walls with exterior insulation

Inserting a continuous insulation layer between the sheathing and framing markedly reduces the lateral resistance of the shear wall, however, this wall configuration has a higher ratio of outboard-to-inboard thermal resistance when compared to the wall assembly where that same exterior insulation is placed outboard to the structural sheathing. Therefore, a wall assembly with intermediate insulation may allow for a thinner exterior insulation, in some climate conditions, and meet the requirement for the minimum outboard-to-inboard insulation ratio.

5.3 Recommendations for future research

Further research is recommended to expand the understanding of the structural and hygrothermal performance of exterior wall systems with insulated sheathing. Some areas that would benefit from further study include:

1. Predicting the stiffness of light wood-frame walls with insulated sheathing based on nail joint properties.
2. Testing and further investigation of nail joints and shear walls constructed with power-driven nails.
3. Investigation of required minimum nail penetration length into lumber for walls that include a layer of intermediate insulation.
4. Hygrothermal modeling considering different air leakage paths, different interior vapour barrier and vapour permeance of exterior insulation.
5. Field testing and monitoring of hygrothermal performance in cold climates should be done to increase confidence in the modeling results.

REFERENCES

- ANSI/ASHRAE. 1989. *62-1989 Ventilation for Acceptable Indoor Air Quality*. Atlanta: American Society of Heating, Refrigeration and Air-Conditioning Engineers.
- APA & USDA. 2014. *Wood structural panel and foam insulation system: Hygrothermal behavior and lateral load resistance - experimental studies*. USDA Joint Venture Agreement 11-JV-11111136-070.
- ASHRAE. 2009. *Heat, air, and moisture control in building assemblies-Fundamentals*. In: *2009 ASHRAE Handbook-Fundamentals*. Atlanta: American Society of Heating, Refrigerating and Air-Conditioning Engineers, Inc. Chapter 25.
- ASHRAE. 2016. *Criteria for moisture-control design analysis in buildings*. *ANSI/ASHRAE Standard 160-2016*. Atlanta: American Society of Heating, Refrigerating and Air-Conditioning Engineers.
- ASTM. 2008. *ASTM F1575 Standard Test Method for Determining Bending Yield Moment of Nails*, ASTM International, West Conshohocken, PA, 2008, DOI: 10.1520/F1575, www.astm.org.
- ASTM. 2011. *Standard test methods for cyclic (reversed) load test for shear resistance of vertical elements of the lateral force resisting systems for buildings*. West Conshohocken, PA: E2126-11.
- ASTM. 2012. *D1761 Standard Test Methods for Mechanical Fasteners in Wood*. ASTM International, West Conshohocken, PA, 2012, DOI: 10.1520/D1761-12, www.astm.org.
- ASTM. 2015. *Standard Test Methods of Conducting Strength Tests of Panels for Building Construction*. West Conshohocken, PA, US: STM E72-15, American Society for Testing and Materials.
- Aune, P., & Patton-Mallory, M. 1986. *Lateral Load-Bearing Capacity of Nailed Joints Based on the Yield Theory*. Washington, DC.: No. FPL-469, Forest Products Laboratory, US Dept. of Agriculture.
- Bomberg, M. and Onysko, D. 2002. *Heat, Air and Moisture Control in Walls of Canadian Houses: A Review of the Historic Basis for Current Practices*. *Journal of Thermal Environmental & Building Science*, Vol. 26(1), pp. 3-29.
- Brown C. W., Roppel P., Lawton M.,. 2007. *Developing a Design Protocol for Low Air and Vapour Permeance Insulating Sheathing in Cold Climates*. Proceedings of the Tenth International Conference on the Performance of Whole Buildings, Clearwater, FL, 2007, ASHRAE, Atlanta, GA.
- Building Science Corporation. 2015. *Thermal Metric Summary Report*. Westford, MA: Building Science Corporation (www.buildingscience.com).

- Chown, G. A. and P. Mukhopadhyaya. 2005. *BC 9.25. 1.2.: The on-going development of building code requirements to address low air and vapour permeance materials. Conference on Building Science and Technology: Building Science and integrated Design Process, Ottawa ON, May 12-13, 2005, v. 1, pp. 48-58.* (10th Canadian Conference on Building Science and Technology: Building Science and integrated Design Process,).
- CSA. 2005. *Engineering Design in Wood CSA O86-01.* Etobicoke, Canada: Canadian Standards Association.
- CSA. 2014. *Engineering Design in Wood.* Mississauga, Canada: Canadian Standards Association.
- CWC. 2014. *Engineering Guide for Wood Frame Construction.* Ottawa, ON: Canadian Wood Council.
- Glass, S.V. 2013. *Hygrothermal Analysis of Wood-Frame Wall Assemblies in a Mixed-Humid Climate.* United States Department of Agriculture, Forest Service, Forest Products Laboratory, Research Paper FPL–RP–675, pp. 1-25, April 2013.
- Health Canada. 2016. *Relative humidity indoors: Fact sheet.* Ottawa. Cat.: H144-33/2016E-PDF: Government of Canada.
- Huber. 2012. *Zip-R Sheathing Overview.* Accessed July 10, 2019. <https://www.huberwood.com/assets/pdfs/ZIP-R-Sheathing-Overview.pdf>.
- IBP, Fraunhofer. 2018. *WUFI® Pro v. 6.2.* Holzkirchen, Germany: Fraunhofer Institute for Building Physics.
- ICC. 2012. *International Residential Code.* Country Club Hills, Illinois: International Code Council.
- Johansen, K., W. 1949. *Theory of timber connections.* International Association of Bridge and Structural Engineering (Vol. 9, pp. 249-262).
- Karagiozis, A. N. and Kumaran, M. K. 1993. *Computer model calculations on the performance of vapor barriers in Canadian residential buildings.* ASHRAE Transactions, Volume 99(2), pp. 991-1003.
- Kumaran, M. K. and Haysom, J. C. 2000. *Low Permeance Materials in Building Envelopes.* Institute for Research in Construction, National Research Council of Canada; Construction Technology Update #41.
- Kumaran, M.K. 2002. *A Thermal and Moisture Transport Database for Common Building and Insulating Materials. ASHRAE Research Project RP-1018, sponsored by TC 4.4 Building Materials and Building Envelope Performance .* National Research Council Canada.
- Kumaran, M.K., J.C. Lackey, N. Normandin, D. Van Reenen, and F. Tariku. 2002. *Summary Report From Task 3 of MEWS Project at the Institute for Research in Construction -*

- Hygrothermal Properties of Several Building Materials*. Research Report 110, National Research Council Canada, Research Report 110.
- Latta, K.,. 1976. *Vapor barriers: What are they? Are they effective?* Canadian Building Digest, Division of Building Research, National Research Council Canada, CBD 175.
- Lstiburek, Joseph. 2011. *BSD-106: Understanding Vapor Barriers*. Building Science Corporation.
- Maref, W., Kumaran, M.K., Lacasse, M.A., Swinton, M.C., and van Reenen, D. 2002. "Laboratory measurements and benchmarking of an advanced hygrothermal model." *Proc. 12th International Heat Transfer Conference*. Grenoble, France: NRCC-43054. pp. 117-122.
- Mi, H. 2004. *Behavior of Unblocked Wood Shear Walls*. MSc thesis, Fredericton, NB: University of New Brunswick.
- Newport Partners Report, LLC. 2004. *Building moisture and durability - Past, Present and Future work*. Maryland: Prepared for: U.S. Department of Housing and Urban Development.
- Ni, C., Chui, Y. H., Karacabeyli, E. 2012. *Mechanics-based approach for determining the shear resistances of shearwalls and diaphragms*. Auckland, New Zealand: Proceedings of 2012 World Conference on Timber Engineering.
- NRC. 1995. *National Building Code of Canada*. Ottawa: National Research Council Canada.
- NRC. 2015a. *National Building Code of Canada*. Ottawa: National Research Council of Canada.
- NRC. 2015b. *National Energy Code of Canada for Buildings*. Ottawa: National Research Council of Canada.
- NRC. 2017. *ZIP System® R-sheathing*. Ottawa, ON: The National Research Council of Canada.
- Ojanen T. and Kumaran, M.K.,. 1992. *Air Exfiltration and Moisture Accumulation in Residential*. Clearwater, FL: Thermal Performance of Exterior Envelopes of Buildings V.
- Ojanen, T. & M. K. Kumaran. 1996. *Effect of Exfiltration on the Hygrothermal Behaviour of a Residential Wall Assembly*. *Journal of Thermal Insulation and Building Envelopes*, Volume 19, pp.215-227.
- Ojanen, T., Viitanen, H. A., Peuhkuri, R., Lähdesmäki, K., Vinha, J., and Salminen, K. 2010. "Mold Growth Modeling of Building Structures Using Sensitivity Classes of Materials." *11th International Conference on Thermal Performance of the Exterior Envelopes of Whole Buildings XI*. Clearwater, FL, USA.

- Phillips, Ross Johnson. 2015. *Investigation of Shear Capacity for Light-Frame Wood Walls Constructed with Insulated Oriented Strand Board Panels*. MSc thesis, Clemson University.
- Plesnik, Tomas. 2014. *Effect of an Intermediate Material Layer on the Lateral Load-Slip Characteristics of Nailed Joints*. Ottawa, Ontario: Carleton University.
- Plesnik, T., Erochko, J., Doudak, G. 2016. "Nailed connection behaviour in light-frame wood shear walls with an intermediate layer of insulation." *ASCE J. Struct. Eng.* 142(7): 04016045.
- Roppel, P. J., M. D. Lawton & W. C. Brown. 2007. *Modelling of Uncontrolled Interior Humidity for HAM Simulations of Residential Buildings*. Clearwater Beach, FL: Thermal Performance of Exterior Envelopes of Whole Buildings X, Proceedings of ASHRAE/DOE/BTECC Conference.
- Saber, H. H., Maref, W., Abdulghani K.,. 2014. *Report on Properties and Position of Materials in the Building Envelope for Housing and Small Buildings*. National Research Council Canada.
- Straube and Burnett. 2001. *Overview of hygrothermal (HAM) analysis methods*. In: Trechsel, H.R., ed., *Moisture analysis and condensation control in building envelopes*. West Conshohocken, PA: American Society for Testing and Materials: 81–89. Chapter 5.
- Straube, J.,. 2006. *Thermal Control in Buildings (BSD-011)*. Building Science Corporation. <http://www.buildingscience.com/documents/digests/bsd-011-thermal-control-in-buildings/>.
- Tsongas G. 2000. "Case Studies of Moisture Problems in Residences." Madison, Wisconsin: Proceeding of the 2nd Annual Conference on Durability and Disaster Mitigation in Wood-Frame Housing.
- Viitanen, H., Salonvaara, M. 2001. *Failure criteria*. In: Trechsel, H.R., ed., *Moisture analysis and condensation control in building envelopes*. ASTM MNL40. West Conshohocken, PA: American Society for Testing and Materials: 66–80. Chapter 4.
- VTT. 1994. *TCC2D - Simulations on the Performance of Air*. An Interim Report.
- Wang, Qing. 2009. *Relationship between fastening properties and load-deflection response of wood shear walls*. MSc Thesis, Canada: University of New Brunswick (UNB).

APPENDIX A – Density and moisture content of framing members

Table A.1: Density and MC of framing members used in fabricating nail joints with 10d nails

Nail Type	Insulation thickness [mm]	Specimen number	Specimen size [mm]			Mass [g]	Density [g/cm ³]	MC [%]
			Length	Width	Depth			
10d	0	1	51.51	51.55	37.74	43.1	0.43	9.8
		2	51.83	51.82	38.39	46.7	0.45	10.7
		3	51.47	51.66	38.27	46.3	0.46	10.7
	12.7	1	51.54	51.68	38.57	46.9	0.46	9.7
		2	51.59	51.22	38.43	46.4	0.46	10.2
		3	51.56	51.6	38.21	46.4	0.46	10.2
	25.4	1	51.91	51.83	37.59	43.1	0.43	9.5
		2	51.46	52.47	37.92	44.4	0.43	9.6
		3	51.7	51.68	38.25	46.1	0.45	9.6
						Mean	0.45	10.0
						SD	0.01	0.47
						COV	0.03	0.05

Table A.2: Density and MC of framing members used in fabricating nail joints with PD nails

Nail Type	Insulation thickness [mm]	Specimen number	Specimen size [mm]			Mass [g]	Density [g/cm ³]	MC [%]
			Length	Width	Depth			
PD	38.1	1	51.76	51.71	37.73	38.1	0.38	9.7
		2	51.7	51.88	37.74	39.9	0.39	10.6
		3	51.55	51.81	37.6	38.2	0.38	10.5
	50.8	1	52.01	51.22	37.77	41.4	0.41	10.7
		2	51.97	51.44	37.7	38.4	0.38	9.5
		3	51.47	51.48	37.61	41.1	0.41	10.4
						Mean	0.39	10.2
						SD	0.02	0.50
						COV	0.04	0.05

Table A.3: Density and MC of framing members used in fabricating nail joints with 16d nails

Nail Type	Insulation thickness [mm]	Specimen number	Specimen size [mm]			Mass [g]	Density [g/cm ³]	MC [%]	
			Length	Width	Depth				
16d	0	1	51.92	51.9	37.77	38.8	0.38	10.6	
		2	51.66	51.55	37.76	39.1	0.39	11.4	
		3	52.03	51.9	37.6	38.4	0.38	10.3	
	12.7	1	51.94	51.9	37.77	39.1	0.38	11.1	
		2	51.97	51.95	37.7	38.8	0.38	10.4	
		3	51.57	51.48	37.61	39.8	0.40	12.5	
	25.4	1	51.61	51.56	37.51	36.9	0.37	9.7	
		2	55.61	55.63	37.48	37.5	0.38	10.1	
		3	52.1	51.62	37.93	42.5	0.42	11.2	
	38.1	1	51.76	51.71	37.73	38.2	0.38	11.0	
		2	51.7	51.88	37.74	39.8	0.39	10.2	
		3	52.31	51.71	37.77	37.2	0.36	9.9	
	50.8	1	51.46	51.55	38.01	38.5	0.38	11.6	
		2	51.97	51.41	37.55	39.1	0.39	10.2	
		3	53.12	51.21	37.63	40.1	0.39	11.3	
							Mean	0.39	10.8
							SD	0.02	0.70
							COV	0.04	0.06

Table A.4: Density and MC of framing members used in fabricating shear walls

Specimen number	Specimen size [mm]			Mass [g]	Density [g/cm ³]	MC [%]
	Length	Width	Depth			
1	77.59	38.43	23.47	31.19	0.45	11.2
2	77.93	37.94	25.72	32.38	0.43	10.5
3	78.35	38.91	24.3	34.3	0.46	12.1
4	77.28	37.43	25.21	31.33	0.43	11.6
5	78.98	37.62	24.5	35.5	0.49	13.1
6	77.14	37.93	23.91	35.1	0.50	15.6
7	79.49	38.09	24.23	35.22	0.48	14.8
8	79.17	38.05	24.38	36.34	0.49	15.1
9	77.56	38.05	23.99	35.53	0.50	15.3
10	78.12	38.01	24.22	34.33	0.48	14.6
11	78.21	37.87	23.94	31.12	0.44	11.4
12	77.93	37.33	25.33	35.21	0.48	15.2
13	77.43	37.97	25.01	31.11	0.42	10.4
14	77.21	38.43	24.25	31.69	0.44	13.2
15	78.54	39.03	23.76	31.4	0.43	13.1
16	79.01	38.44	25.11	36.62	0.48	13.6
17	77.44	37.88	24.67	36.4	0.50	14.1
18	79.26	37.77	24.29	35.5	0.49	12.2
19	78.13	39.01	25.31	35.2	0.46	11.1
20	78.43	38.41	23.92	31.14	0.43	10.1
				Mean	0.46	12.9
				SD	0.03	1.82
				COV	0.07	0.14

APPENDIX B – Nail joint load-slip response curves

Nail Joints constructed with 10d nails

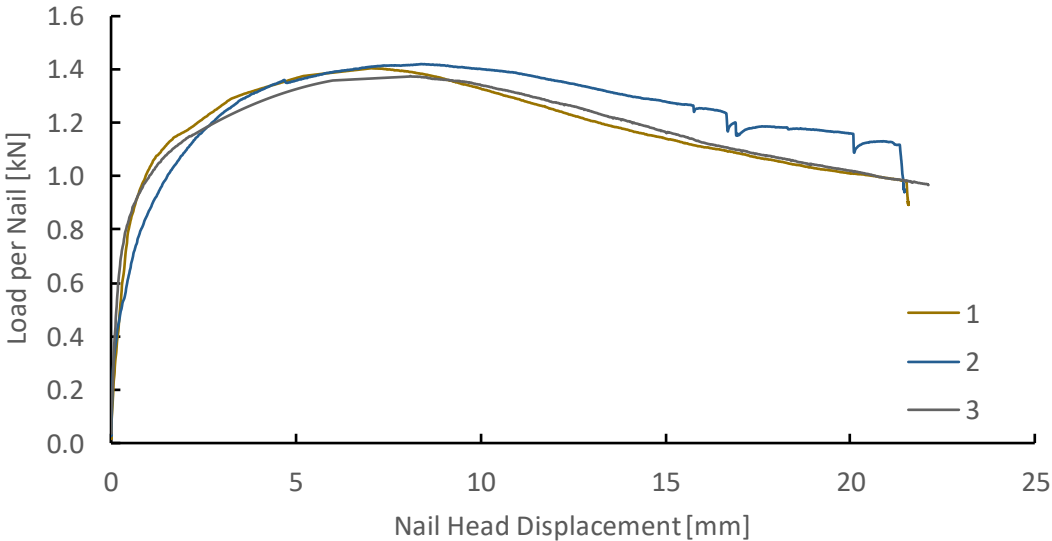


Figure B.1: Nail joints constructed with 10d nails and 0 mm of intermediate insulation

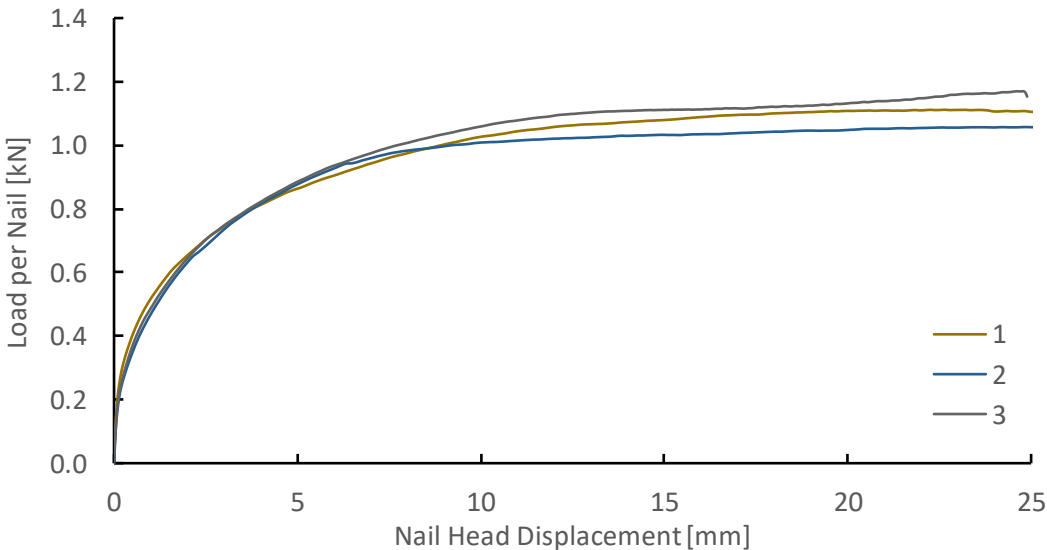


Figure B.2: Nail joints constructed with 10d nails and 12.7 mm of intermediate insulation

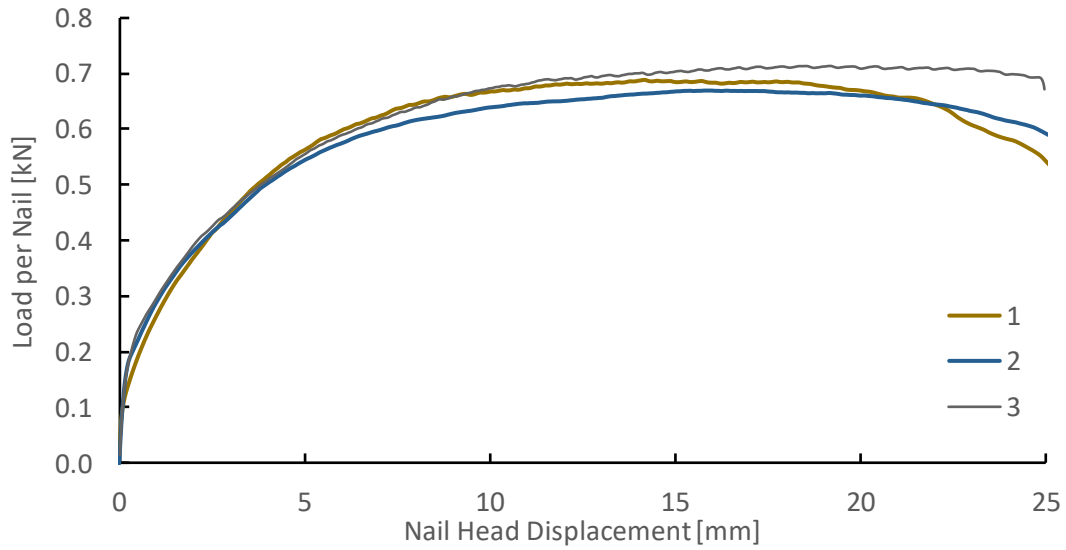


Figure B.3: Nail joints constructed with 10d nails and 25.4 mm of intermediate insulation

Nail Joints constructed with 16d nails

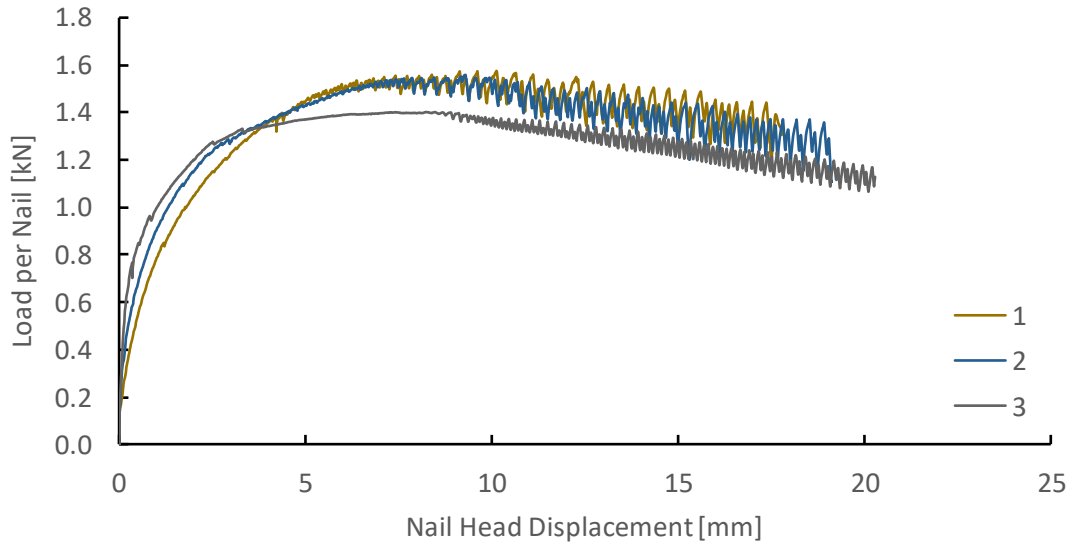


Figure B.4: Nail joints constructed with 16d nails and 0 mm of intermediate insulation

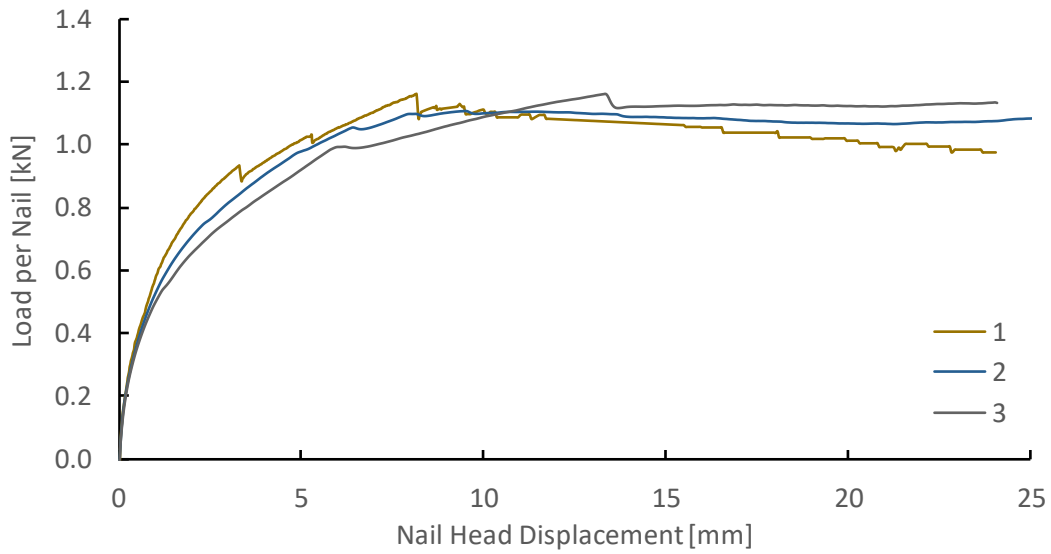


Figure B.5: Nail joints constructed with 16d nails and 12.7 mm of intermediate insulation

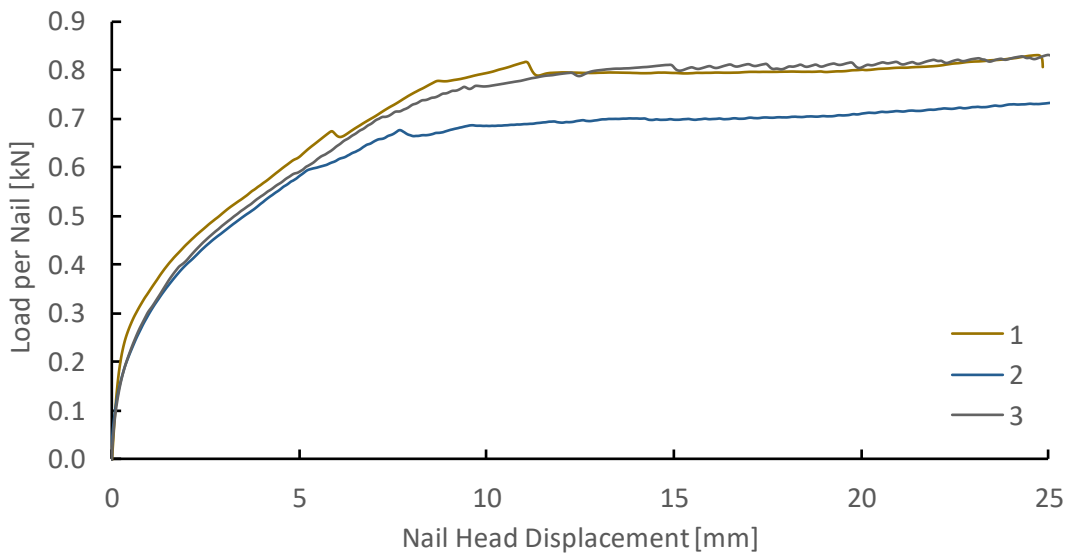


Figure B.6: Nail joints constructed with 16d nails and 25.4 mm of intermediate insulation

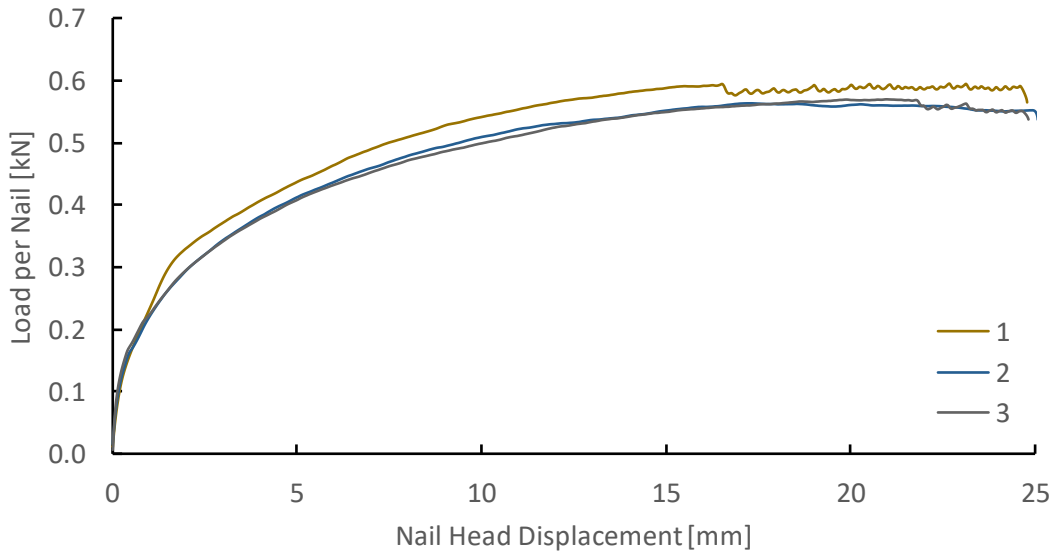


Figure B.7: Nail joints constructed with 16d nails and 38.1 mm of intermediate insulation

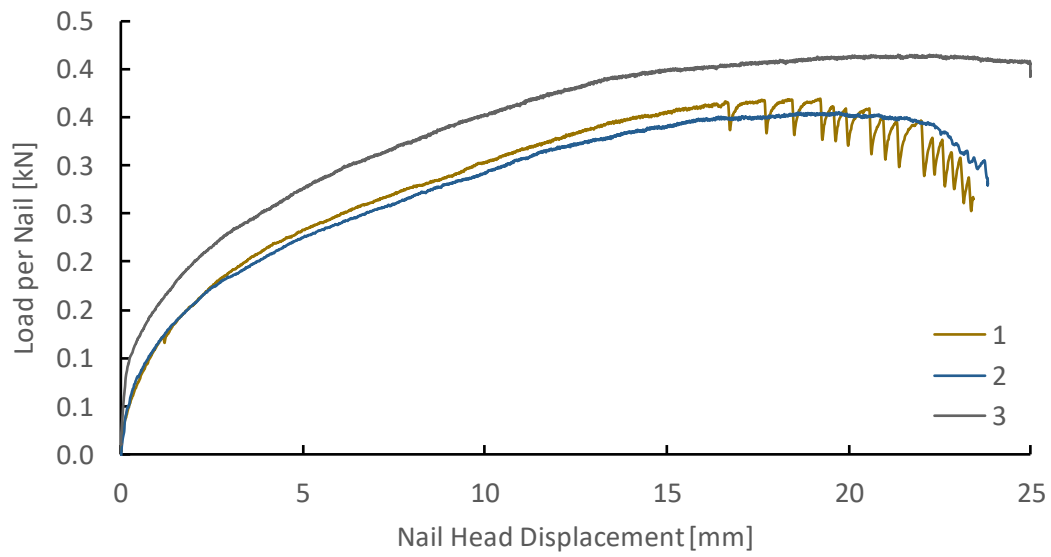


Figure B.8: Nail joints constructed with 16d nails and 50.8 mm of intermediate insulation

Nail Joints constructed with PD nails

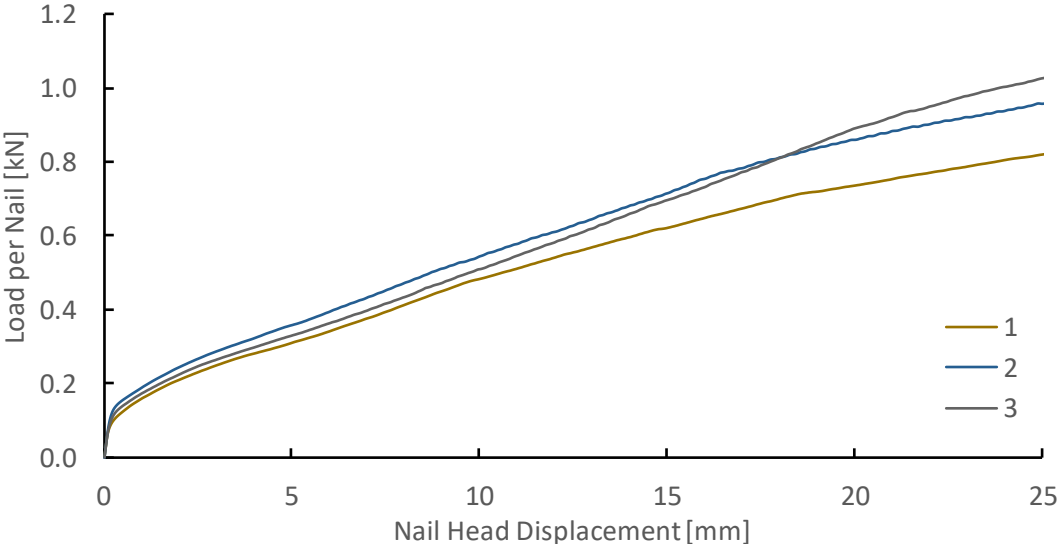


Figure B.9: Nail joints constructed with PD nails and 38.1 mm of intermediate insulation

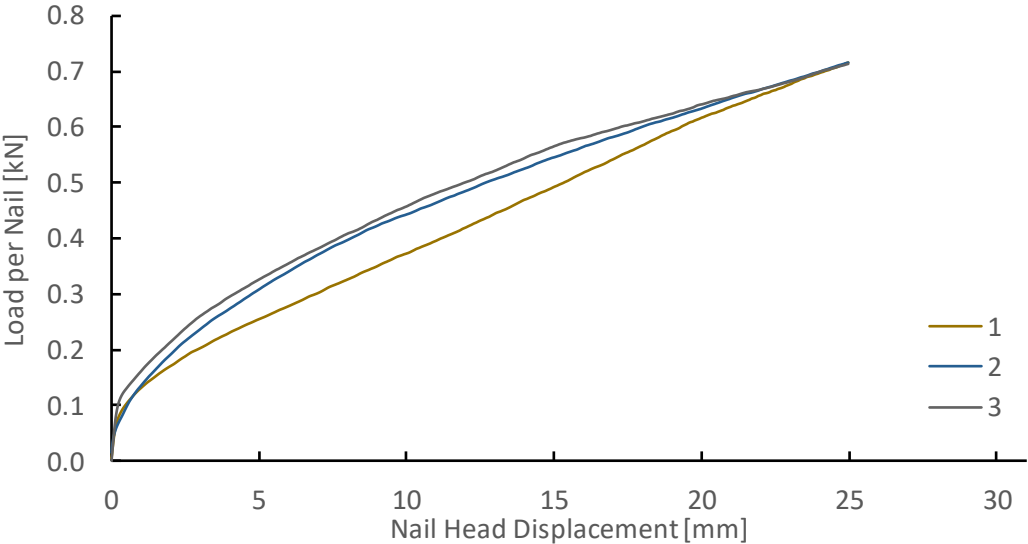


Figure B.10: Nail joints constructed with PD nails and 50.8 mm of intermediate insulation

APPENDIX C – Nail Joint failure modes



Figure C.2: Nails after the testing of nail joints

APPENDIX D – Shear wall failure modes



Figure D.1: Failure mode of S1 Shear wall: nail bending, splitting of the bottom plate, sheathing tearing, nail head pull through



Figure D.2: Failure mode of S2, S3, and S4 Shear wall: nail bending



Figure D.3: Failure mode of S5 and S6 Shear wall: nail bending and nail pullout (splitting of the bottom plate occurred during nailing of the framing)



Figure D.4: Failure mode of S7 Shear wall: S7 wall did not fail; the OSB was squashing the insulation as the displacement was increasing

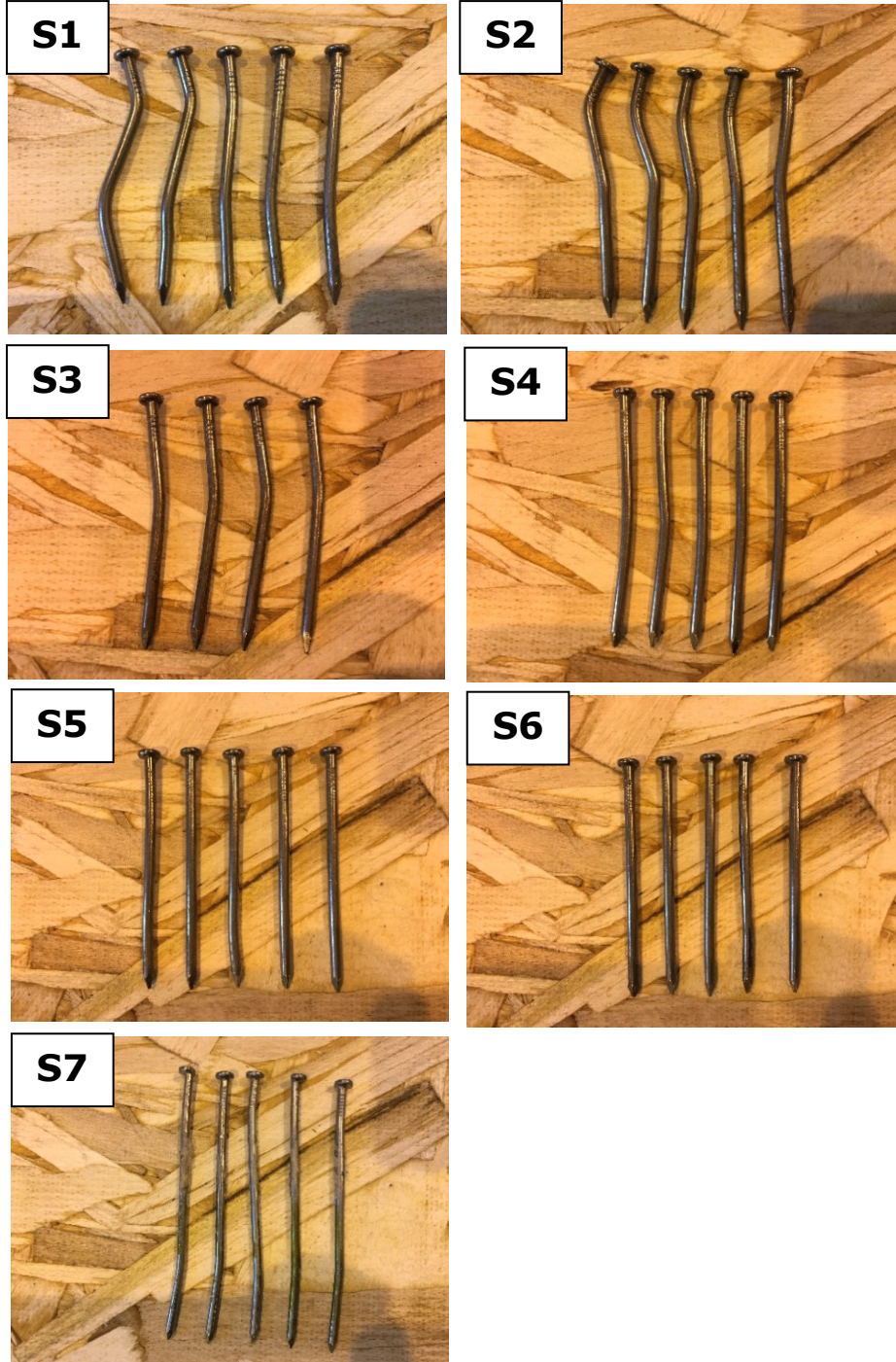


Figure D.5: Nails after the shear wall testing

APPENDIX E – Nail bending tests

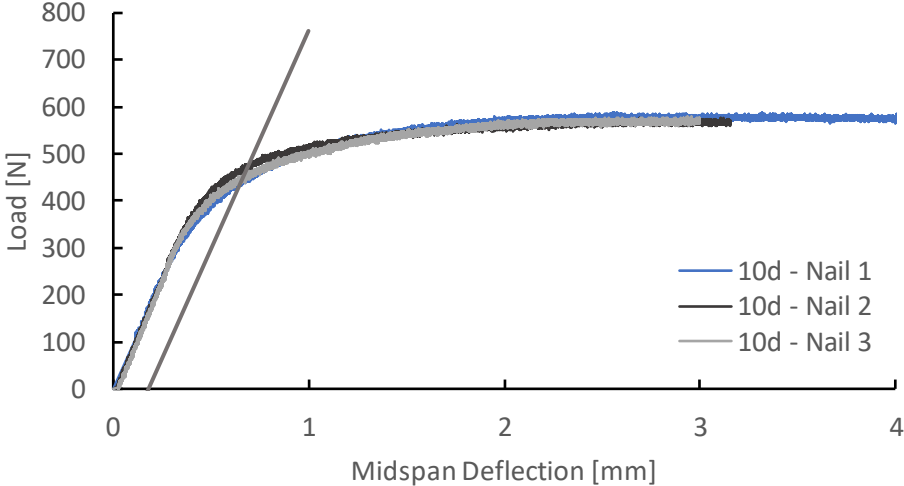


Figure E.1: Center-point nail bending results of 10d nails

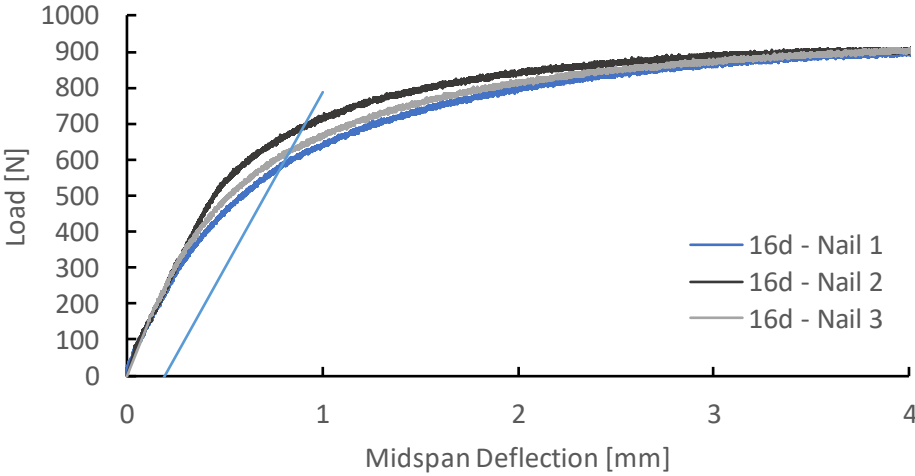


Figure E.2: Center-point nail bending results of 16d nails

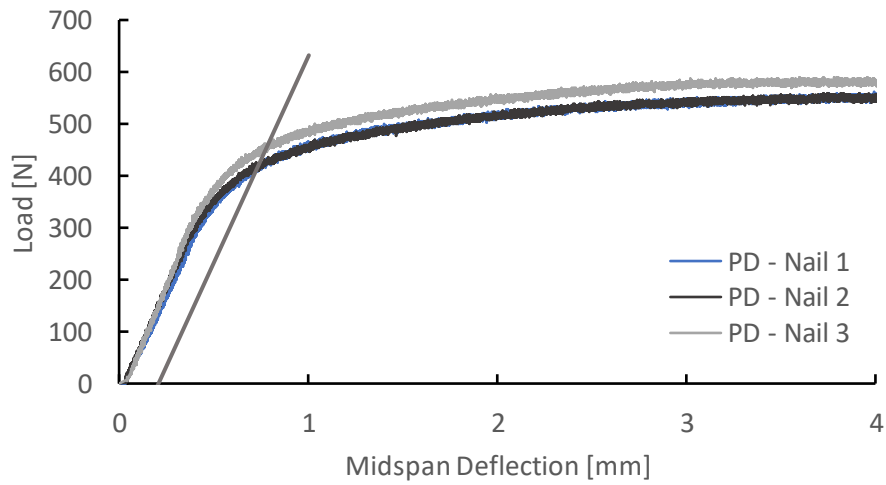


Figure E.3: Center-point nail bending results of PD nails

Table E.1: Center-point nail bending results

Nail Type	Specimen	Mean Nail Diameter [mm]	Bearing Span [mm]	Plastic Section Modulus [mm ³]	Yield Load [N]	Moment [Nmm]	Yield Strength [MPa]
10d	Nail 1	3.79	43.18	9.07	445	4804	530
	Nail 2	3.79		9.07	460	4966	548
	Nail 3	3.79		9.07	475	5128	565
	Mean	3.79		9.07	460	4966	548
16d	Nail 1	4.12	48.26	11.66	560	6756	579
	Nail 2	4.12		11.66	620	7480	642
	Nail 3	4.12		11.66	680	8204	704
	Mean	4.12		11.66	620	7480	642
PD	Nail 1	3.23	38.1	5.62	435	4143	737
	Nail 2	3.25		5.72	435	4143	724
	Nail 3	3.25		5.72	460	4382	766
	Mean	3.24		5.69	443	4223	742

APPENDIX F – Hygrothermal material properties

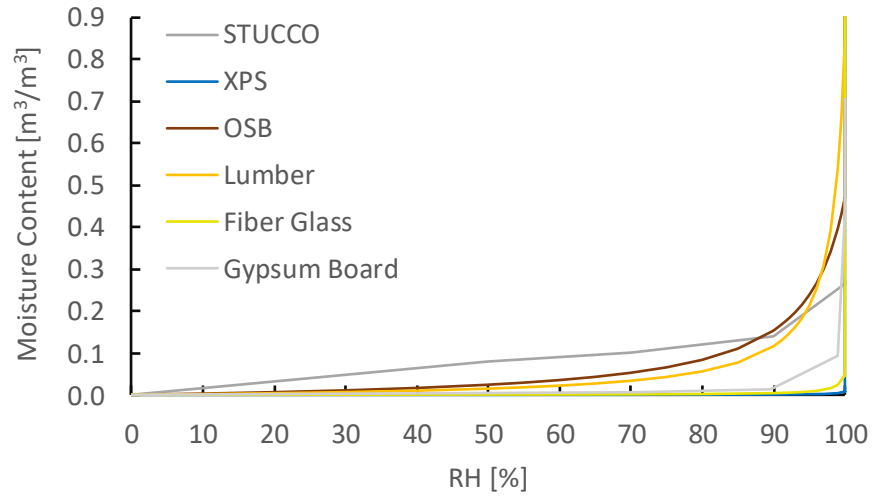


Figure F.1: Moisture Storage Functions

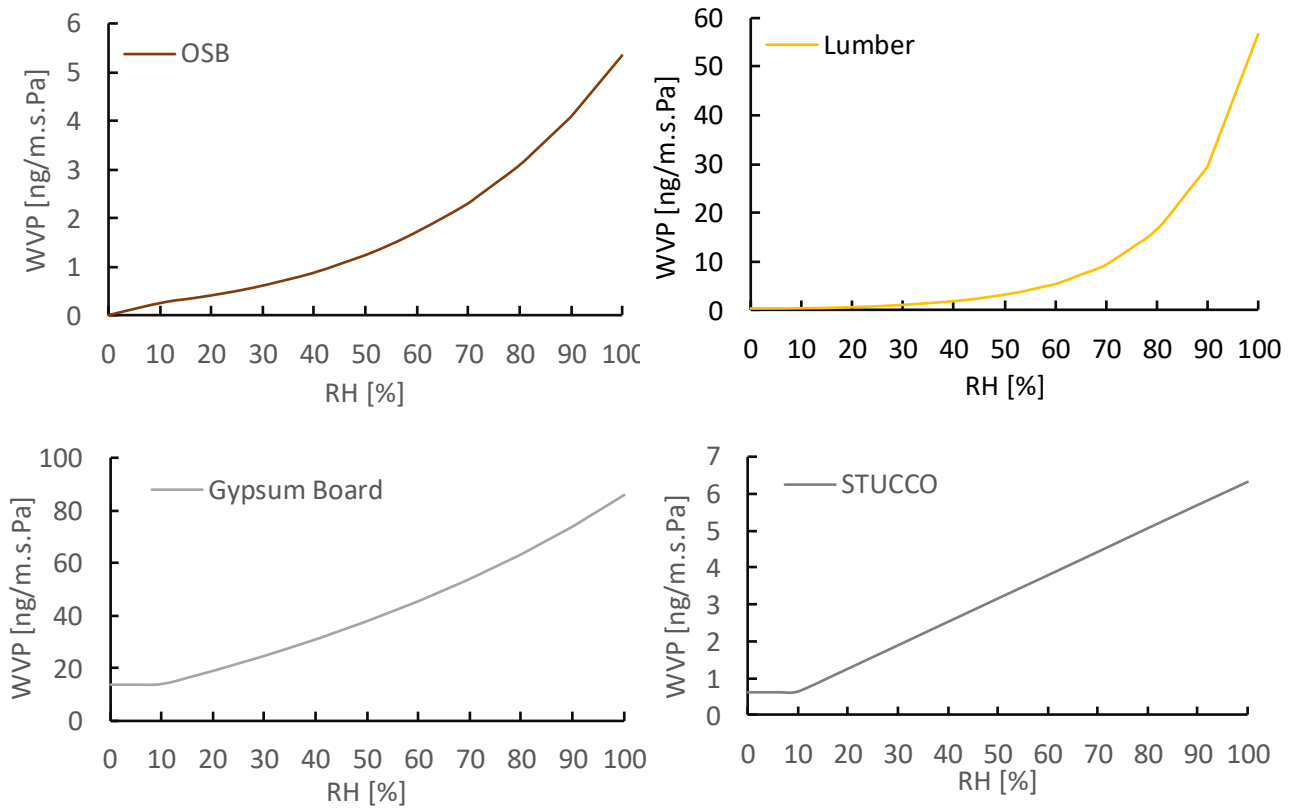


Figure F.2: Water Vapour Permeability

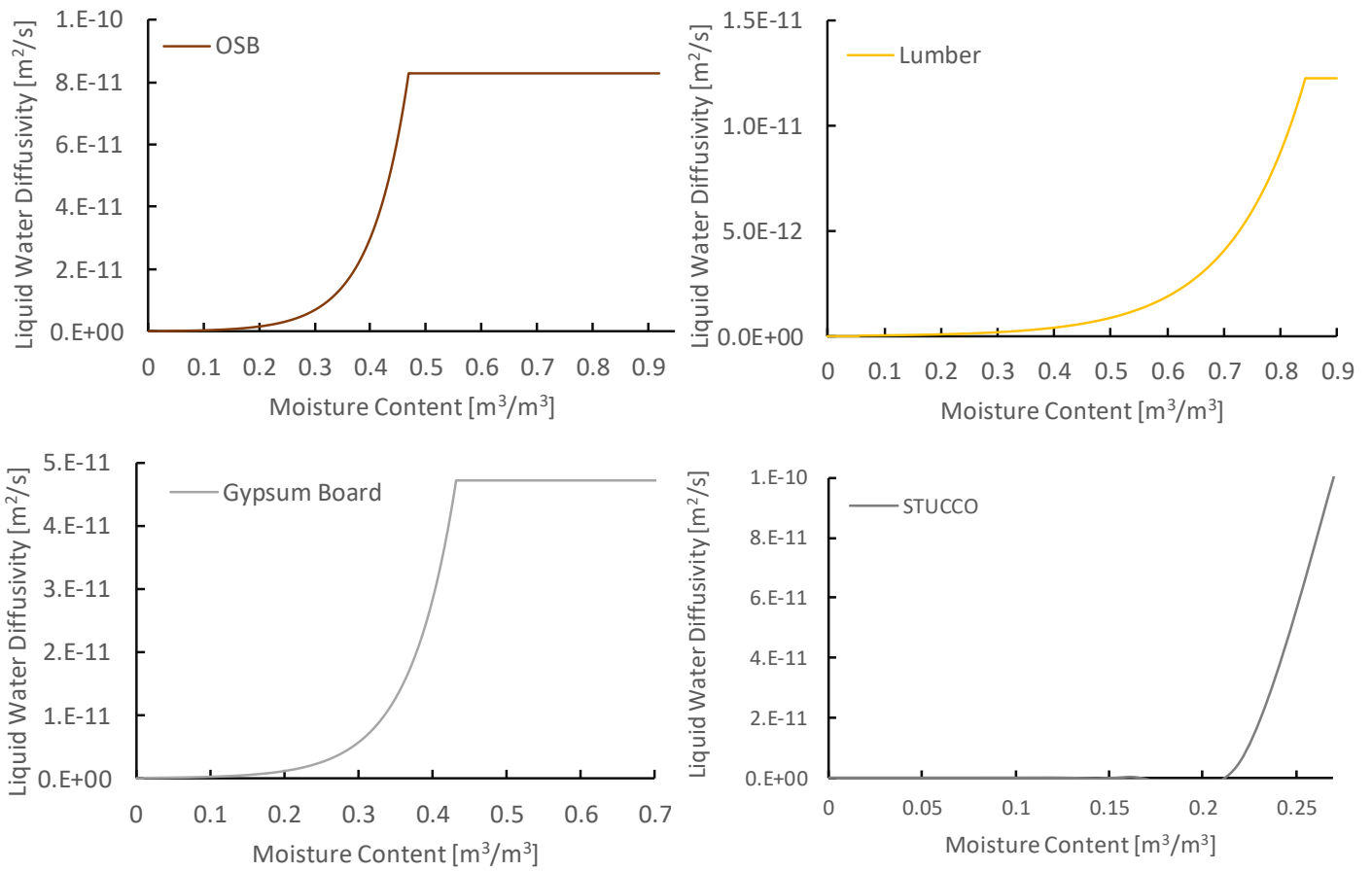


Figure F.3: Liquid Diffusivity

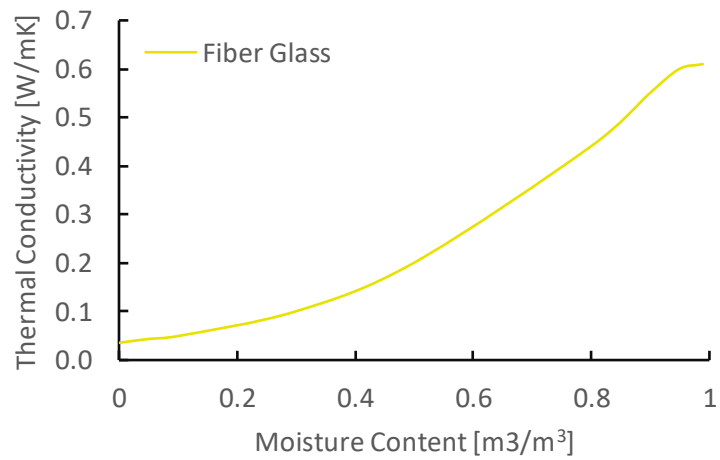


Figure F.4: Fiber Glass Moisture Dependant Thermal Conductivity